

SEISMIC ANALYSIS OF AN OLDER REINFORCED CONCRETE FRAME
STRUCTURE

Chaitanya Paspuleti

A thesis submitted in partial fulfillment of the
requirements for the degree of

Master of Science in Civil Engineering

University of Washington

2002

Program Authorized to Offer Degree:
Department of Civil and Environmental Engineering

University of Washington

Graduate School

This is to certify that I have examined this copy of a master's thesis by

Chaitanya Paspuleti

and have found that it is complete and satisfactory in all respects,
and that any and all revisions required by the final
examining committee have been made.

Committee Members:

Laura N. Lowes

John. F. Stanton

Dawn Lehman

Date: _____

In presenting this thesis in partial fulfillment of the requirements for a Master's degree at the University of Washington, I agree that the Library shall make its copies freely available for inspection. I further agree that extensive copying of this thesis is allowable only for scholarly purposes, consistent with "fair use" as prescribed in the U.S. Copyright Law. Any other reproduction for any purposes or by means shall not be allowed without my written permission

Signature _____

Date _____

University of Washington

Abstract

SEISMIC ANALYSIS OF AN OLDER REINFORCED CONCRETE FRAME
STRUCTURE

Chaitanya Paspuleti

Chairperson of Supervisory Committee: Assistant Professor Laura N. Lowes
Department of Civil and Environmental Engineering

Reinforced concrete frame buildings constructed in the 1950s and 1960s typically have design details that today are considered to be inadequate for regions of high seismicity. Many of these structures have suffered significant structural damage during recent earthquakes (EERI, special earthquake report 1999). Significant research effort has been devoted to the development of behavioral models and modeling techniques to predict the behavior of these buildings. However there are no models that have been shown to predict observed response with a high level of accuracy and precision. Further, there is a wide variation in the modeling techniques adopted by researchers and practitioners.

The study presented here investigates modeling of the earthquake response of an existing, instrumented, reinforced concrete building located in Southern California. The building is a seven-story reinforced concrete frame, that suffered significant structural and non-structural damage during the Northridge earthquake (EERI, special earthquake report 1999). This study focusses on the effectiveness of the applied inelastic modeling procedure to predict building response including the observed failure modes of the building. A model was developed that simulated the primary damage mechanisms

observed after the earthquakes, however this model failed to simulate the observed displacement histories with a high level of accuracy.

Additionally, the results of nonlinear static and dynamic analyses were evaluated to identify the modeling parameters and modeling assumptions that have the most significant impact on variability in simulated response. It was found that variability in response due to ground motion input had a greater impact on variability in building response than modeling assumptions.

TABLE OF CONTENTS

| | |
|----------------------------------------------------------------|-----|
| LIST OF FIGURES | iv |
| LIST OF TABLES | vii |
| CHAPTER 1: INTRODUCTION | 1 |
| 1.1: Objectives of the Current Research | 2 |
| 1.2: Scope | 2 |
| 1.3: Organization | 3 |
| CHAPTER 2: CASE STUDY BUILDING – DESCRIPTION AND DETAILS | 4 |
| 2.1: Case Study Building | 4 |
| 2.2: Building Description | 4 |
| 2.2.1: Structural System Design Details | 7 |
| 2.3: Inadequacies in Detailing | 12 |
| 2.3.1: Transverse Reinforcement of Frame Members | 12 |
| 2.3.2: Column Lap Splices | 13 |
| 2.3.3: Beam-Column Joints | 14 |
| 2.4: Observed Damage | 14 |
| CHAPTER 3: MODEL CHARACTERISTICS | 18 |
| 3.1: Global Characteristics | 18 |
| 3.2: Element Formulations | 19 |
| 3.3: Discretization of Beam and Column Sections | 23 |
| 3.4: Material Properties | 23 |
| 3.4.1: Concrete | 24 |
| 3.4.2: Steel | 26 |
| 3.5: Column Failure Modes..... | 27 |

| | |
|--------------------------------------------------------------------------|----|
| 3.5.1: Splice Failure Model | 27 |
| 3.5.2: Shear Failure Model | 29 |
| 3.6: Gravity Load | 33 |
| 3.7: Damping | 33 |
| 3.8: Effective Slab Width | 35 |
| 3.9: Foundation | 37 |
| 3.10: Beam-Column Joints | 38 |
| | |
| CHAPTER 4: OPENSEES IMPLEMENTATION | 39 |
| 4.1: Basic Structure | 39 |
| 4.2: VanNuysAnalysis.tcl | 40 |
| 4.3: Set Analysis Parameters | 41 |
| 4.4: Self Run | 44 |
| | |
| CHAPTER 5: EVALUATION, VERIFICATION AND REFINEMENT OF THE MODEL | 45 |
| 5.1: Eigenvalue Analysis | 45 |
| 5.1.1 Effective Stiffness Factors | 46 |
| 5.2: Pushover Analysis | 49 |
| 5.2.1: Lateral Load Patterns | 49 |
| 5.2.2: Results of Pushover Analyses | 50 |
| 5.2.3: Curvature Demand under Pushover Loading | 52 |
| 5.3: Nonlinear Dynamic Analysis | 55 |
| 5.3.1: Response Calculated using Nonlinear Dynamic Analysis | 55 |
| 5.3.2: Damping Induced Spurious Forces | 62 |
| 5.3.3: Equivalent Viscous Damping | 64 |
| | |
| CHAPTER 6: INFLUENCE OF MODELING PARAMETERS | 65 |
| 6.1: Global Level Parameters | 68 |
| 6.2: Element Level Parameters | 70 |

| | |
|--------------------------------------------------------------------|-----|
| 6.3: Failure Models | 74 |
| 6.4: Material Level Parameters | 76 |
| 6.5: Statistics of Preliminary Parameter Study | 78 |
| 6.6: Parameter Study | 81 |
| 6.6.1: Variability in Maximum Inter-Story Drifts | 84 |
| 6.7: Impact of Ground Motion Variability | 86 |
| 6.8: Impact of Shear Strength Variation on Building Response | 89 |
| | |
| CHAPTER 7: SUMMARY AND CONCLUSIONS | 94 |
| 7.1 Summary | 94 |
| 7.2 Conclusions | 95 |
| 7.3 Recommendations for Future Research | 96 |
| | |
| REFERENCES | 98 |
| | |
| APPENDIX A: DETAILS OF THE TCL SCRIPTS | 102 |
| | |
| APPENDIX B: GROUND MOTIONS FOR THE VANNUYS BUILDING | 122 |

LIST OF FIGURES

| | |
|-----------------------------------------------------------------------------------------------------------------------|----|
| Figure 2.1: Typical Floor Plan and Column Schedule (Rissman, 1965) | 5 |
| Figure 2.2: Elevation View (Rissman, 1965) | 6 |
| Figure 2.3: Typical Longitudinal Spandrel Beam Elevation (NOAA report, 1973) | 9 |
| Figure 2.4: Typical Column Detail (NOAA report, 1973) | 9 |
| Figure 2.5: Typical Longitudinal Spandrel Beam Cross-Section (NOAA report, 1973) | 10 |
| Figure 2.6: Horizontal Motion Sensor Locations in the Building | 15 |
| Figure 2.7: Observed Damage Pattern for the Northridge Earthquake (Trifunac, 2001).. | 17 |
| Figure 3.1: P-delta Relation for the Different Element Formulations | 22 |
| Figure 3.2: Behavior of Concrete Material Being Used in the Model | 25 |
| Figure 3.3: Simulated Stress-Strain Responses for Column Longitudinal Reinforcement | 28 |
| Figure 3.4: P-delta Relations for a Typical Column Section | 32 |
| Figure 3.5: Viscous Damping as a Percentage of Critical Damping for 8 Modes | 34 |
| Figure 3.6: Typical Nomenclature for Dimensions of Flat-Slab Structures (adapted from Luo and Durrani, 1995) | 36 |
| Figure 4.1: Basic Structure of Model Building Process | 40 |
| Figure 5.1: Fundamental Period – Northridge Earthquake (Base model) | 48 |
| Figure 5.2: Load Distributions used in Pushover Analysis | 50 |
| Figure 5.3: Base Shear versus roof Displacement | 51 |
| Figure 5.4: Failure Sequence | 51 |
| Figure 5.5: Plot of Moment vs. Curvature Showing the Yield Moment and Yield Curvature | 52 |
| Figure 5.6: Frame Member Curvature Ductility Demands at 2% Roof Drift for the Base model | 54 |
| Figure 5.7: Northridge Groundmotion | 56 |
| Figure 5.8: Response spectrum ($\xi=5\%$) | 56 |

| | |
|-------------------------------------------------------------------------------------------------------------------------------------------|----|
| Figure 5.9: Observed and Calculated Roof Displacement Time History using the Base model | 56 |
| Figure 5.10: Plot of Story Displacements for Base model at Maximum Roof Displacement | 58 |
| Figure 5.11: Frame Member Curvature Ductility Demands under Northridge Earthquake | 59 |
| Figure 5.12: Moment Curvature Response of a Typical Non-Yielding Column in the Ground Floor under Northridge Earthquake | 60 |
| Figure 5.13a: Moment Curvature Response of a Typical Column on the Fifth Story just before Yielding under the Northridge Earthquake | 61 |
| Figure 5.13b: Moment Curvature Response of a Typical Column on the Fifth Story just after Yielding under the Northridge Earthquake | 61 |
| Figure 5.14: Typical Spurious Moments in Rotational Degrees of Freedom due to Damping | 63 |
| Figure 6.1a: Dynamic Analysis - Effect of Global Level Parameters | 69 |
| Figure 6.1b: Pushover Analysis - Effect of Global Level Parameters | 70 |
| Figure 6.2a: Dynamic Analysis - Effect of Element Level Parameters | 73 |
| Figure 6.2b: Pushover Analysis - Effect of Element Level Parameters | 73 |
| Figure 6.3a: Dynamic Analysis - Effect of Failure Models | 75 |
| Figure 6.3b: Pushover Analysis - Effect of Failure Models .. | 75 |
| Figure 6.4a: Dynamic Analysis - Effect of Material Level Parameters | 77 |
| Figure 6.4b: Pushover Analysis - Effect of Material Level Parameters | 77 |
| Figure 6.5: Plot of Story Drifts for 50in50_SF_vnuy for Different Parameters | 81 |
| Figure 6.6: Plot of Story Drifts for 50in50_SF_466 for Different Parameters | 81 |
| Figure 6.7: Plot of Story Drifts for 10in50_NR_vnsc for Different Parameters | 82 |
| Figure 6.8: Plot of Story Drifts for 10in50_SF_461 for Different Parameters | 82 |
| Figure 6.9: Plot of Story Drifts for 02in50_NR_vnuy for Different Parameters | 83 |
| Figure 6.10: Plot of Story Drifts for 02in50_NR_ros for Different Parameters | 83 |
| Figure 6.11: Effect of Ground motion Variability on Building response (02% in 50 years) | 86 |

| | |
|---------------------------------------------------------------------------------------------------------------------------------------------------------------------------------------------------------------|-----|
| Figure 6.12: Effect of Ground motion Variability on Building response (10% in 50 years) | 86 |
| Figure 6.13: Effect of Ground motion Variability on Building response (50% in 50 years) | 87 |
| Figure 6.14: Shear Strength Capacity Variability - 2% in 50 years | 90 |
| Figure 6.15: Shear Strength Capacity Variability - 10% in 50 years | 90 |
| Figure 6.16: Shear Strength Capacity Variability - 50% in 50 years | 91 |
| Figure B-1: Variability in the Ground motions of each set of ten Scaled Recordings for the Longitudinal and Transverse Components for each of Three Ground motion Levels (Somerville and Collins, 2002) | 125 |

LIST OF TABLES

| | |
|--------------------------------------------------------------------------------------------------------------------------------------|-----|
| Table 2.1: Reinforcement Details in Columns (Rissman, 1965) | 11 |
| Table 3.1: Concrete Compressive Strengths used in Simulating Building Response | 25 |
| Table 3.2: Longitudinal Reinforcing Steel Yield Strength used in Simulating Building Response | 26 |
| Table 3.3: Shear Strength Capacities defined by the Shear models | 31 |
| Table 3.4: Gravity Loads Applied to Van Nuys Building Model | 33 |
| Table 5.1: Results of Eigenvalue Analysis of the Van Nuys Building | 48 |
| Table 5.2: Error Estimation for Different Models | 57 |
| Table 6.1: Properties of the Base Model | 66 |
| Table 6.2: Properties of the different Parameter models Considered | 67 |
| Table 6.3: Parameter Study – Pushover Analysis | 78 |
| Table 6.4: Parameter Study – Dynamic Analysis (Northridge Earthquake) | 79 |
| Table 6.5: Brittle model – Variation of Maximum Inter-Story Drift (%) | 84 |
| Table 6.6: Flexure model – Variation of Maximum Inter-Story Drift (%) | 85 |
| Table 6.7: Effect of Variability in Ground motion on Maximum Inter Story Drift | 88 |
| Table 6.8: Maximum Inter-Story Drift for three Models with Varying Shear Strengths | 93 |
| Table B-1: Time Histories Representing 50% in 50 years hazard level at the Van Nuys Building (Somerville and Collins, 2002) | 123 |
| Table B-2: Time Histories Representing 10% in 50 years hazard level at the Van Nuys Building (Somerville and Collins, 2002) | 124 |
| Table B-3: Time Histories Representing 02% in 50 years hazard level at the Van Nuys Building (Somerville and Collins, 2002) | 124 |

ACKNOWLEDGEMENTS

The author would like to express his deepest gratitude to Professor Laura Lowes for her continued guidance and support throughout this research project. The author would also like to thank Professor John Stanton and Professor Dawn Lehman for their invaluable comments and for serving on the examination committee.

The author would also like to acknowledge Jubum Kim, Hiroyuki Tagawa, Catherine, Mike, Tomas, Jaewook park and Nilanjan Mitra, who inconvenienced themselves, on several occasions, in order to facilitate my research.

CHAPTER 1

INTRODUCTION

Earthquakes pose an important challenge for the art and science of structural engineering. Damage to buildings, bridges and lifelines during the 1989 Loma Prieta and the 1994 Northridge earthquakes resulted in estimated economic losses exceeding \$50 billion and over 100 deaths were attributed to the two events (EERI, 1995). The reduction of earthquake risk will require improved understanding of structural earthquake behavior, advancement of the methods used to simulating structural response, and the development of new seismic design procedures.

The building stock on the west coast of the United States, an area with relatively high seismic hazard, includes many older reinforced concrete buildings. These buildings represent a particularly significant earthquake risk as most are designed prior to modern seismic design codes and include design details that could be expected to result in inadequate earthquake performance. In order to assess the risk associated with these buildings and evaluate retrofit strategies that will reduce this risk it is necessary to predict the response of these buildings under variable levels of earthquake loading and to quantify the uncertainty with which response quantities are predicted. The research presented here seeks to improve the numerical simulation of earthquake response of older reinforced concrete frame buildings.

1.1 Objectives of the Current Research

The current research effort seeks to develop and apply nonlinear analysis modeling procedures to simulate the earthquake response of an older reinforced concrete frame building. This building is referred to subsequently as the case study building. The primary objectives of the research follow:

1. To develop tools to improve and facilitate simulation of earthquake response.

2. To evaluate the accuracy with which nonlinear modeling procedures predict building response, including inelastic failure modes.
3. To investigate the influence of model parameters and modeling assumptions on the simulated response.
4. To quantify the uncertainty in demand prediction resulting from variability in modeling assumptions

1.2 Scope

1. Develop a series of two-dimensional models of the case study building using the OpenSees analysis platform.
2. Evaluate the accuracy of the different models by comparing the simulated and the observed response of the building to the 1994 Northridge earthquake and identify a baseline model that best simulates the observed response.
3. Use OpenSees analysis platform, with its scripting language input format that facilitates parametric investigation, to accomplish a series of analysis using multiple ground motion records that represent earthquake hazard levels.
4. Quantify the uncertainty in predicted response resulting from modeling assumption and variability in the predicted ground motion record for a specific hazard level.

1.3 Organization

Presentation of the research effort is organized as follows:

- Chapter 2 describes the case study building, including the choice of this building as the case study building, details of the structural system and design details that

are considered inadequate by current codes, the layout of instrumentation within the building and damage observed following recent earthquakes.

- Chapter 3 describes the series of models implemented initially in OpenSees, evaluation of these models and selection of the baseline model which best simulates observed response during the Northridge earthquake.
- Chapter 4 provides a brief overview of the OpenSees implementation, including an introduction to *tcl*, the scripting language used with OpenSees and the organization of the *tcl* scripts used to generate the OpenSees model of the building and perform the parametric study.
- Chapter 5 presents results of eigenvalue, pushover and dynamic analyses using the baseline model.
- Chapter 6 discusses the results of three parametric studies: one which includes a large number of model parameters and assumptions and considers simulated response under Northridge earthquake ground motion, one which includes a subset of model parameters and considers simulated response for a series of six ground motion records that represent three earthquake hazard levels, and one which includes a subset of model parameters and considers simulated response for a series of 30 ground motion records that represent three earthquake hazard levels.
- Chapter 7 summarizes the research effort, presents conclusion and suggests topics to be addresses in the future.
- Appendices provide additional information about the *tcl* scripts used to define and analyze the model and about the ground motions used in the parameter study.

CHAPTER 2

CASE STUDY BUILDING – DESCRIPTION AND DETAILS

This chapter presents the case study building, including choice of the building, details of the structural system, and damage observed as a result of recent earthquakes.

2.1 Case Study Building

The building selected for study is the Holiday Inn hotel located at 8244 Orion Avenue, Van Nuys, California. The building was chosen for study primarily because this building was instrumented with accelerometers for the 1971 San Fernando, 1987 Whittier Narrows and the 1994 Northridge earthquakes, and acceleration data are available at multiple locations within the building for the three earthquakes (this is discussed in Section 2.5). Additionally, because the building was instrumented, damage resulting from these earthquakes was documented. The fact that the response of the building to these earthquakes was measured and that the structural failure modes were known, provided a significant opportunity to validate analytical models for the simulation of the response of building with non-confirming reinforcing details which was one of the main reasons behind choosing the building as the case study building.

2.2 Building Description

The site of the case study building is near the center of the San Fernando Valley, approximately 4.5 miles from the epicenter of the 1994 Northridge earthquake. The building was designed in 1965 as per the 1965 building code.

Figure 2.1 shows the plan view of a typical floor and Figures 2.2a and 2.2b show the north and east elevation views of the building. The building is seven stories with mechanical equipment located on the roof, the roof of the building is at an elevation of 788.5 in. The first story of the building is 162 in. in height and all other stories are approximately 104 in. in height. The plan dimensions of the structure are 62 feet (north-south dimension) by 150 feet (east-west dimension).

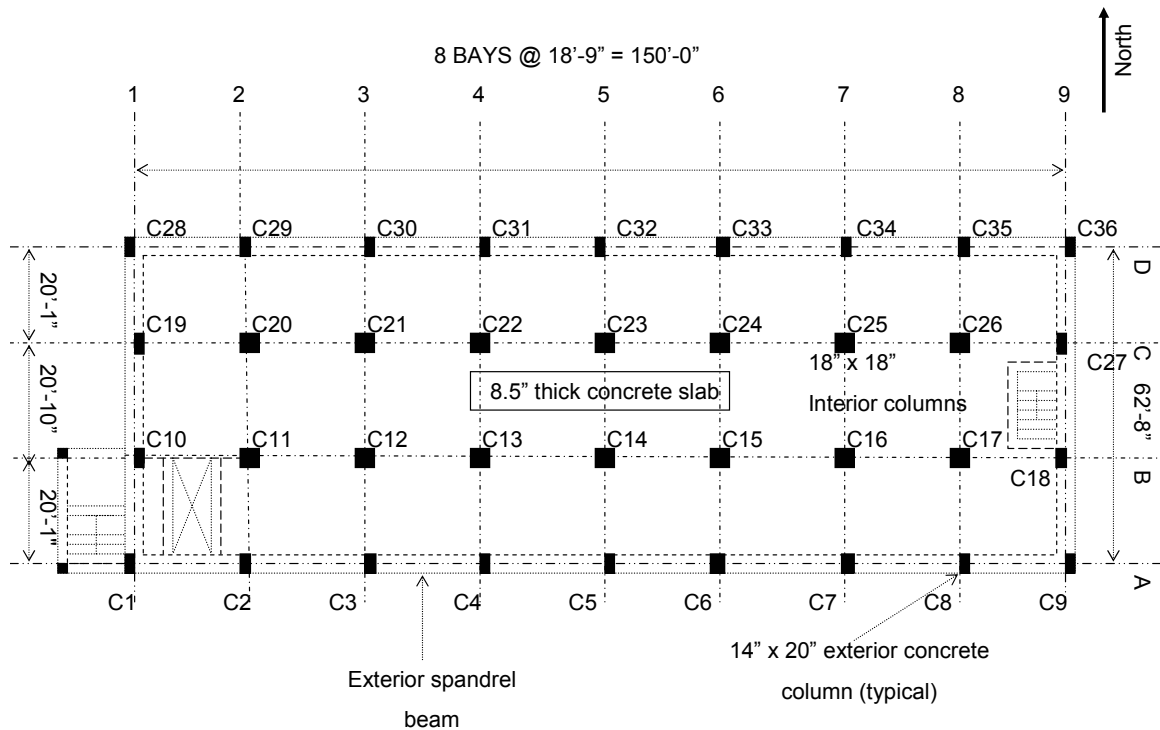
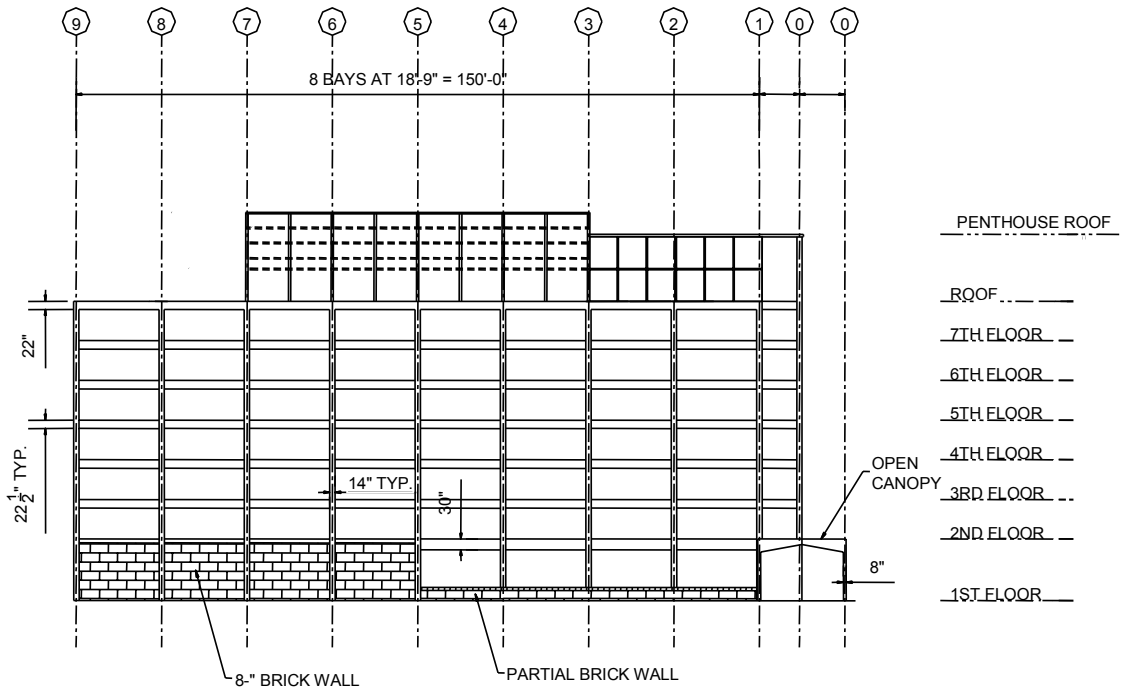
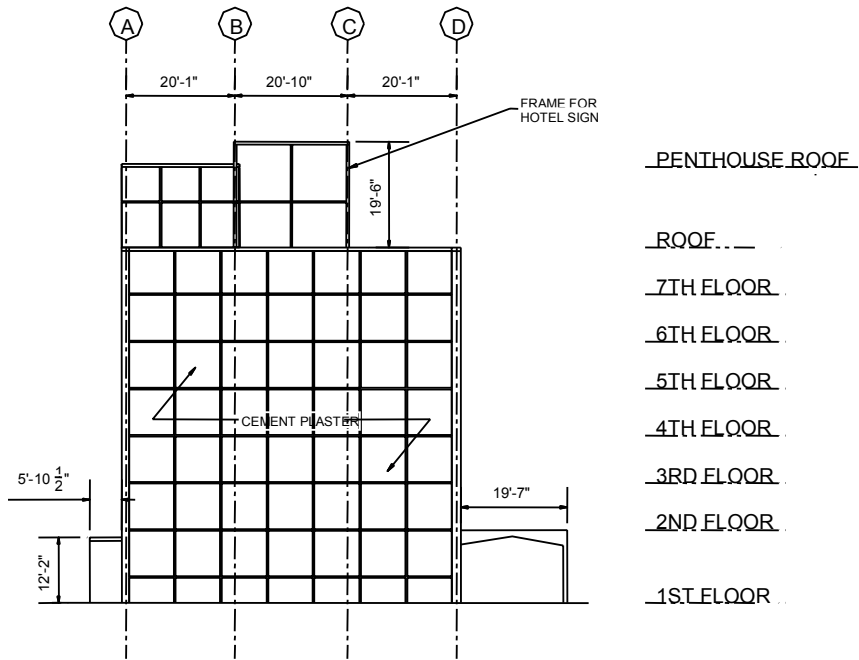


Figure 2.1 Typical Floor Plan and Column Schedule (Rissman, 1965)



(a) North Perimeter Elevation



(b) East Perimeter Elevation

Figure 2.2 Elevation View (Rissman, 1965)

2.2.1 Structural System Design Details

The case study building was designed in accordance with the 1963 building code. The structural system consists of perimeter moment-resisting frames and interior column-slab frames. There are seven frame bays in EW direction; each bay is approximately 20 feet in length (Figure 2.1). There are three frame bays in the NS direction; each bay is approximately 19 feet in length (Figure 2.1).

Perimeter Frames

The perimeter frames were designed to resist the lateral loads specified in the 1965 code. Table 2.1 lists column reinforcement details, and Figure 2.4 shows reinforcement details for a typical column.

Design details for the perimeter frame column that are of interest to the current study include the following:

- Columns are 14 inch by 2 inch, oriented such that activation of the perimeter frame to resist lateral loading results in bending of the columns about the weak axis.
- Column longitudinal reinforcement ratios range from 0.029 at the first story to 0.013 at the seventh story.
- Column transverse reinforcement ranges from No. 3 grade, 40 hoops spaced at 12 inch at the first story to No.2, Grade 40 hoops spaced at 12 inch at the seventh story.
- Column longitudinal reinforcement is spliced above each floor, splice are 36 inches in length.

Design details for the perimeter frame beams that are of interest to the current study include the following:

- Perimeter frame beams on the second floor are 30 inch deep, giving them an aspect ratio (length divided by depth) of 8. Perimeter frame beams on the third through seventh floors are 22.5 in., giving them an aspect ratio of 11.
- Typical beam longitudinal reinforcement above the third floor consisted of 2 No. 6 bars at the bottom of the section and 3 No. 9 bars at the top. The top reinforcement is continuous through the beam-column joint region and it is spliced in the mid-span with a lap length of 36 in. (32 bar diameters for a No. 9 reinforcing bar).
- The transverse reinforcement of the beams consists of No. 3 stirrups spaced at 3 inch near the beam ends; the spacing increases to between 10 inch and 13 inch at mid-span.
- Typical reinforcement and cross sectional details of the spandrel beams are shown in Figure 2.3 and 2.5

Interior Frames

The interior column-slab frames were designed to resist the gravity loads specified in the 1963 code. Table 2.1 lists column reinforcement details for exterior and interior column. Design details for the interior frame columns that are of interest to the current study include the following:

- The first story interior columns are 20 inch by 20 inch; second through seventh story columns are 18 inch by 18 inch.
- Column longitudinal reinforcement ratios range from 0.037 at the first story to 0.011 at the seventh story.
- Column transverse reinforcement ranges from No. 3, Grade 40 hoops spaced at 1 inch at the first story to No. 2, Grade 40 hoops spaced at 12 inch at the seventh story.
- Floor slabs are 10inch thick on the second floor, 8-1/2 inch thick on the second through the seventh floors, and 8 inch thick at the roof (Rissman, 1965).

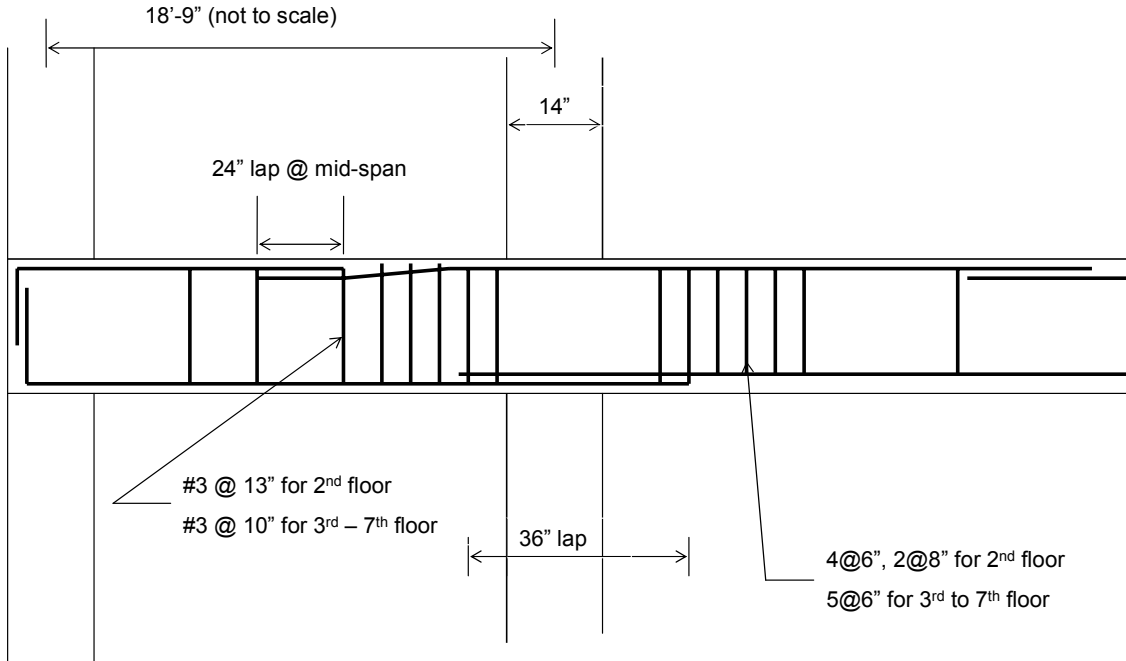


Figure 2.3 Typical Longitudinal Spandrel Beam Elevation (NOAA report, 1973)

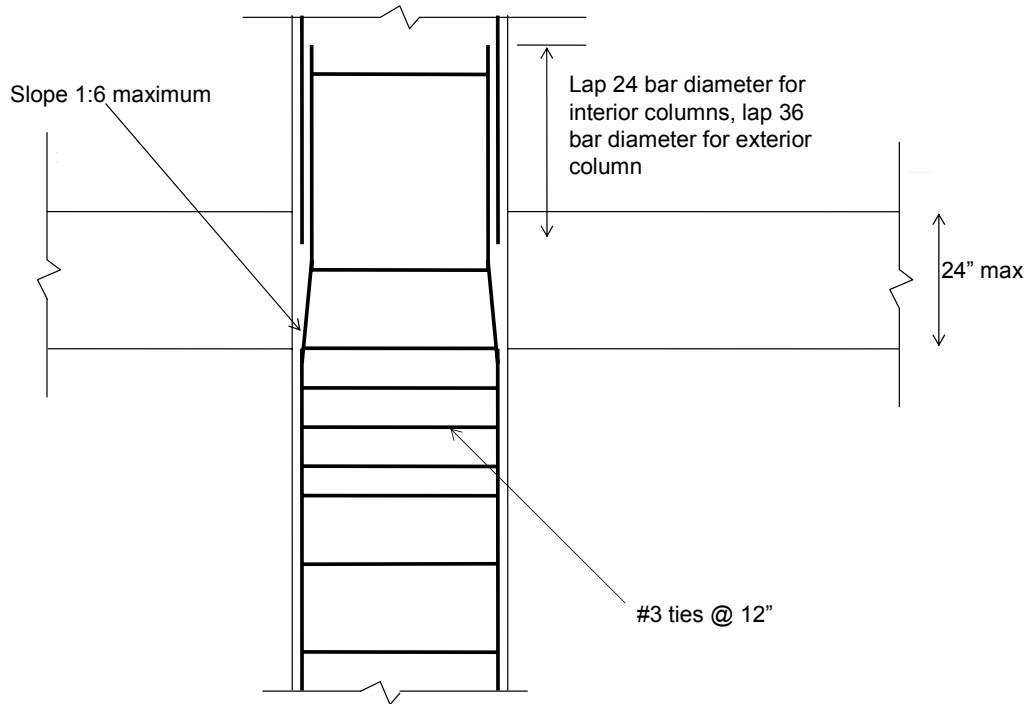


Figure 2.4 Typical Column Detail (NOAA report, 1973)

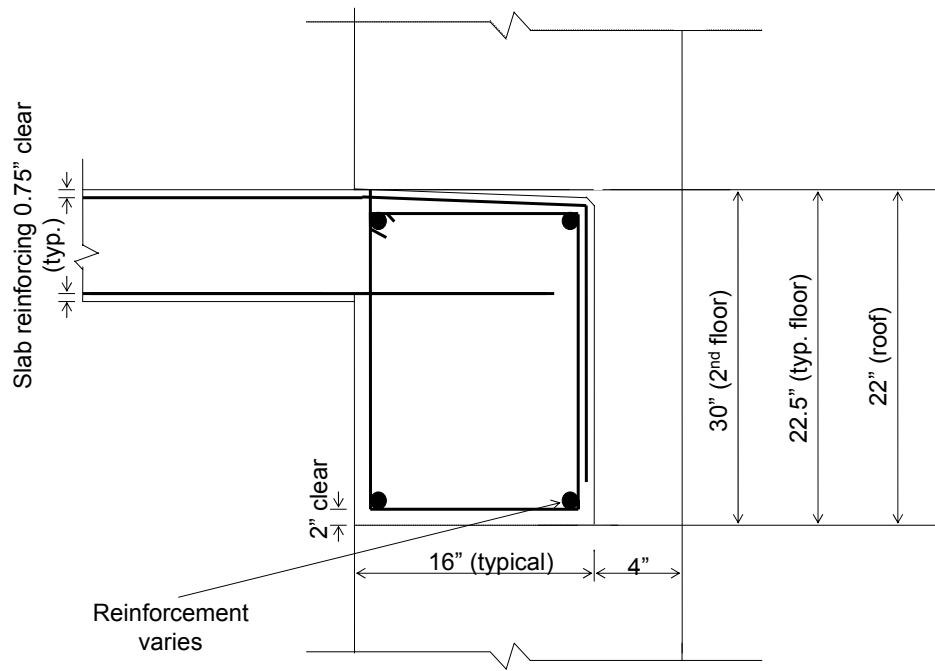


Figure 2.5 Typical Longitudinal Spandrel Beam Cross-Section (NOAA report, 1973)

Table 2.1 Reinforcement Details in Columns (Rissman, 1965)

| Story | concrete design strength (psi) | Reinf. and Group ID. | Column ID | | | | | |
|-------|--------------------------------|----------------------|----------------|-------------------|----------------|------------------|---------------|------------------|
| | | | C1,C9, C28,C36 | C2,C3,C8 ,C29,C35 | C4-C7, C30-C34 | C10,C18, C19,C27 | C11, C12 ,C20 | C13-C17, C21-C26 |
| 1 | 5000 | Long. Bars | 8 - #9 | 10 - #9 | 10 - #9 | 12 - #9 | 12 - #9 | 10 - #9 |
| | | Ties | #3@12" | #3@12" | #3@12" | #3@12" | #3@12" | #3@12" |
| | | Group ID | 11 | 9 | 9 | 10 | 2 | 1 |
| 2 | 4000 | Long. Bars | 6 - #7 | 8 - #9 | 6 - #9 | 8 - #9 | 12 - #9 | 10 - #9 |
| | | Ties | #2@12" | #3@12" | #3@12" | #3@12" | #3@12" | #3@12" |
| | | Group ID | 14 | 13 | 12 | 13 | 4 | 3 |
| 3 | 3000 | Long. Bars | 6 - #7 | 8 - #9 | 6 - #9 | 8 - #9 | 12 - #9 | 8 - #9 |
| | | Ties | #2@12" | #3@12" | #3@12" | #3@12" | #3@12" | #3@12" |
| | | Group ID | 17 | 16 | 15 | 16 | 6 | 5 |
| 4 | 3000 | Long. Bars | 6 - #7 | 6 - #7 | 6 - #7 | 6 - #9 | 8 - #9 | 6 - #8 |
| | | Ties | #2@12" | #2@12" | #2@12" | #3@12" | #3@12" | #3@12" |
| | | Group ID | 27 | 23 | 18 | 15 | 19 | 8 |
| 5 | 3000 | Long. Bars | 6 - #7 | 6 - #7 | 6 - #7 | 6 - #7 | 6 - #8 | 6 - #7 |
| | | Ties | #2@12" | #2@12" | #2@12" | #2@12" | #2@12" | #2@12" |
| | | Group ID | 28 | 24 | 24 | 24 | 20 | 7 |
| 6 | 3000 | Long. Bars | 6 - #7 | 6 - #7 | 6 - #7 | 6 - #7 | 6 - #7 | 6 - #7 |
| | | Ties | #2@12" | #2@12" | #2@12" | #2@12" | #2@12" | #2@12" |
| | | Group ID | 29 | 25 | 25 | 25 | 21 | 21 |
| 7 | 3000 | Long. Bars | 6 - #7 | 6 - #7 | 6 - #7 | 6 - #7 | 6 - #7 | 6 - #7 |
| | | Ties | #2@12" | #2@12" | #2@12" | #2@12" | #2@12" | #2@12" |
| | | Group ID | 30 | 26 | 26 | 26 | 22 | 22 |

Irregularities in Exterior and Interior framing

The interior and exterior framing system is very regular. Beam and column dimensions and reinforcement patterns are approximately the same and are approximately symmetric on each floor. Irregularities in the system occur to accommodate stairs located in the south east corner of the building.

The two perimeter frames and the two interior frames in the longitudinal direction (east-west direction) were identical in terms of the general geometry and member sizes. There were, however, certain differences in the reinforcement between the columns on column line 3 (refer to Figure 2.2). The reinforcement of columns C3 was slightly different from the reinforcement of columns C30 (see Table 2.1). Similarly, the reinforcement in columns C12 and C21 were different. These differences were believed to make a negligible difference between the lateral responses of the frames on the north and south of the building (Barin and Pincheria, 2002).

2.3 Inadequacies in Detailing

This section provides a brief summary of the deficiencies which are typical in older reinforced concrete frame building.

2.3.1 Transverse Reinforcement of Frame Members

The transverse reinforcement in column and beam members in older reinforced concrete buildings was designed typically for shear forces obtained from linear analyses under design lateral forces. This practice often resulted in widely spaced ties or stirrups along the length of the member. It is now understood that the maximum shear forces induced in a frame member are related to the flexural capacity at the ends rather than to the forces indicated by elastic analyses. For this reason, current design provisions require frame members be designed for the forces associated with maximum moment strengths at

the member ends to avoid shear failures and to ensure the development of full flexural strength of the member. The transverse reinforcement of the columns in the case study building consists of No. 3, Grade 40 ties spaced at 12 in. Current code provisions (ACI, 2002). require that the maximum spacing that the code allows is given by the formula:

$$s = \frac{\phi A_v d f_y}{(V_u - \phi V_c)} \quad (\text{Eq. 2.1})$$

For the columns of the case study building is a maximum of 4 inches for the No. 3 ties.

ACI Committee 318 (2002) recommends for members carrying a factored axial force exceeding $0.1A_g f_c'$ (A_g is the gross section area of the frame member and f_c' is the compressive strength of concrete), transverse reinforcement be spaced at a distance of not more than (a) one-quarter of the minimum member dimension (which in the case study building is $14/4 = 3.5$ in for the ground story columns), (b) six times the diameter of the longitudinal reinforcement (which in the case study building is 6 in.), and (c) S_x , where S_x is defined by

$$S_x = 4 + \left(\frac{14 - h_x}{3} \right) \leq 6 \text{ in.} \quad (\text{Eq. 2.2})$$

with h_x equal to the maximum horizontal dimension of the hoop. Following these recommendations, the required hoop spacing is 3.5 in., rather than the 12 in. provided.

2.3.2 Column Lap Splices

The design of the older buildings was governed primarily by gravity loading since the 1950's and 1960's codes were relatively low. Consequently, columns were considered as 'compression members' and lap splices were designed to transmit compressive forces. The length of lap splices specified in older codes was typically 24 bar diameters (ACI-1963). Today the ACI suggests a lap length of 30 bar diameters and not less than 12 inches (ACI, 2000).

Additionally there was no restriction placed on splice location and there were no requirements for additional transverse steel reinforcement along the splice length. The splices in the columns in the case study building are located just above the slab at each

floor level. Thus, the columns spliced would be deemed inadequate by today's standards. One would expect limited tensile capacity and limited ductility. This was observed during the Northridge earthquake.

2.3.3 Beam-Column Joints

The role of the beam-column joint is to transfer the forces between columns and beams. Therefore, adequate strength of the joint is essential to develop the full capacity of the frame members. Joint provisions for seismic loading in which transverse reinforcement is required throughout the connection were first introduced in the 1971 edition of the ACI code (2002). The case study building, built prior to 1971, had essentially no transverse joint reinforcement (Figure 2.4). Under severe ground motion, one would expect loss of bond capacity within the joint for column and beam steel and shear failure of the joint. Such damage has been observed in laboratory test of joints with no transverse reinforcement (Walker, 2001)

2.4 Observed Damage

The building was instrumented by the California Strong Motion Instrumentation Program (CSMIP) before the Northridge earthquake event. Strong motion data is also available for the 1971 San Fernando and 1987 Whittier Narrows earthquakes. Nine channels of data were obtained from the accelerometers located at the roof, 4th and ground floors during the San Fernando earthquake. Following the 1971 event, building instrumentation was enhanced by seven additional channels increasing the total number of sensors to sixteen. The location of the sensors over the height of the building is shown in Figure 2.6. Ten of these sensors recorded the north-south (transverse) response, five recorded the east-west (longitudinal) response and one recorded the vertical acceleration. All sensors were triggered simultaneously at nominal 1%g vertical acceleration. Digitized response records for approximately 60 seconds are available for each of the 16 sensors.

Peak ground accelerations in the east-west, north-south and vertical directions were 0.45g, 0.42g and 0.27g, respectively. The measured peak accelerations at the roof level were 0.58g at 9.22 sec in the east-west direction and 0.57g at 7.36 sec in the north-south direction (Somerville, 2002).

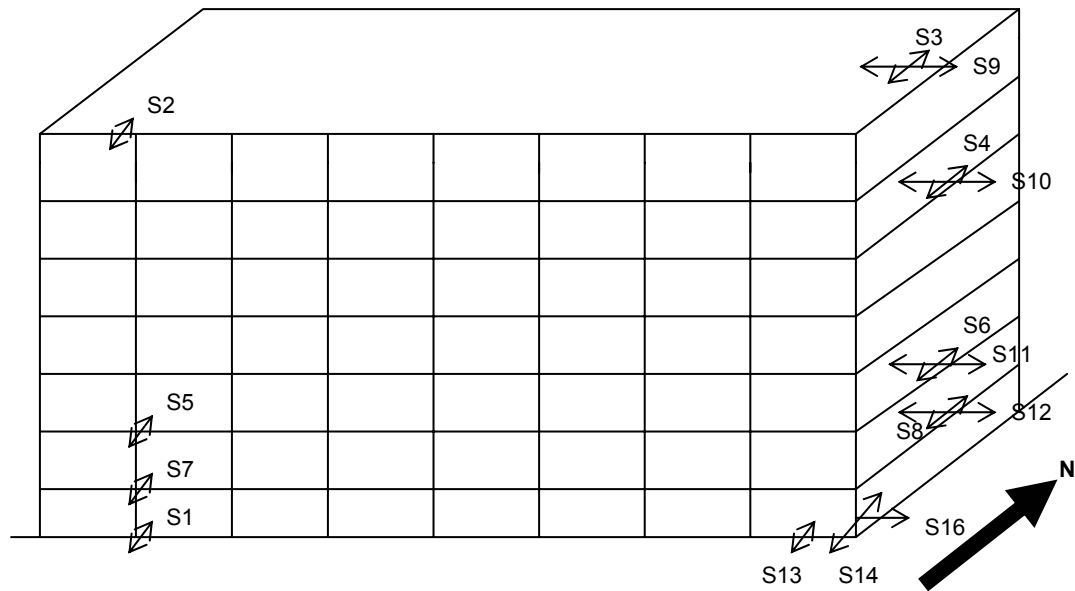


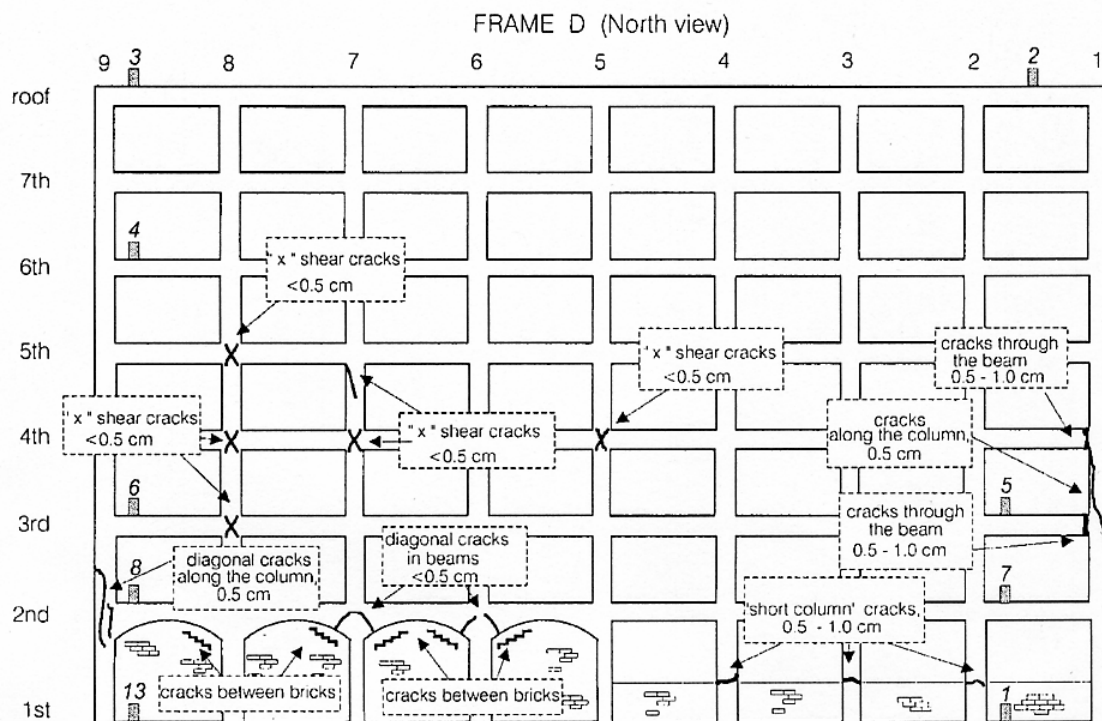
Figure 2.6 Horizontal Motion Sensor Locations in the Building

The building suffered minor structural damage and extensive nonstructural damage during the 1971 San Fernando earthquake. This damage was repaired subsequently. Repair of the structural damage was limited to a single beam-column joint at the northeast corner of the building. Nonstructural damage was most severe on the 2nd and 3rd floors. About 80% of the total repairs costs were allocated for the damaged gypsum wall partitions, bathroom tile and plumbing fixtures. The cost of the repair for the non-structural damage was approximately 10% of the initial construction cost of the building at that time.

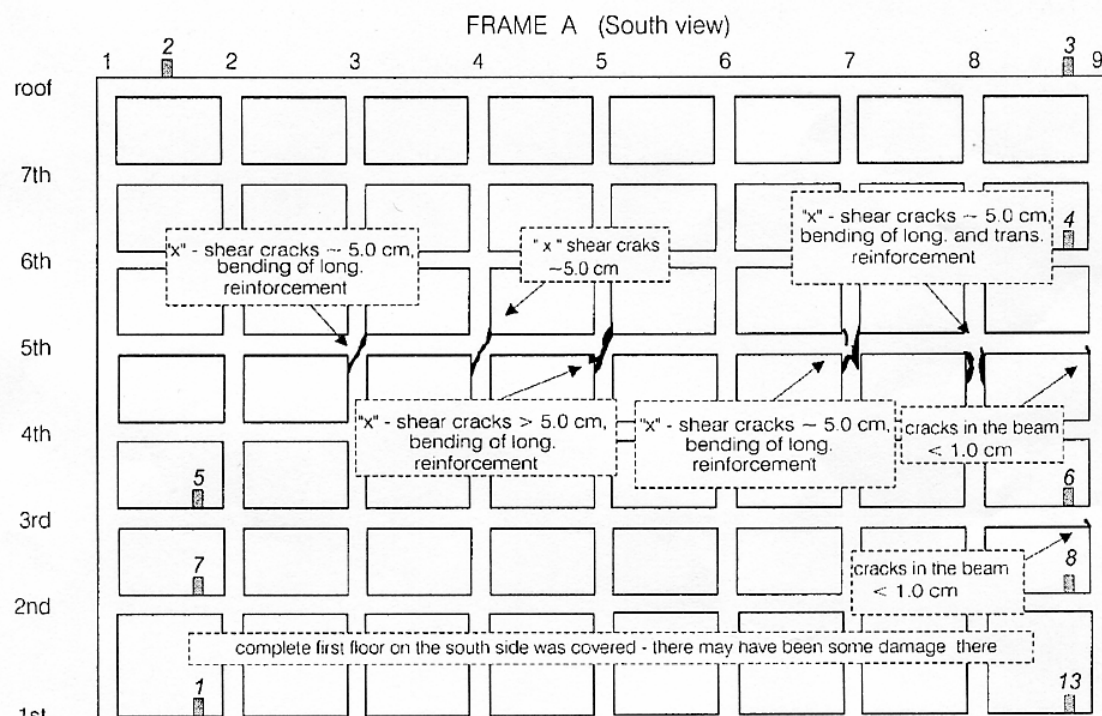
The hotel building suffered extensive structural damage during the 1994 Northridge earthquake. The damage was most severe in the south longitudinal perimeter frame, where five of the nine columns between the 4th and 5th floors failed in shear (Trifunac, 2001). Figure 2.7 shows the damage pattern observed on the exterior frame. The development of cracks and eventually shear failure in the columns might be

attributed to the poor transverse reinforcement in the columns as discussed in the previous section. As a result of the shear failures, the vertical reinforcement between the widely spaced ties buckled due to loss of concrete cover. The south perimeter frame was supported with temporary shoring after the earthquake. Some beam-column joints on the 3rd, 4th and 5th story in the north perimeter frame and on the 3rd story in the south perimeter frame experienced minor to moderate cracking

Non structural damage during the 1994 Northridge earthquake was not very extensive and was mostly confined to the 4th story. Doors, windows and drywall partitions in the east-west direction suffered severe damage between the 4th and 5th floor levels. This is attributed to the large deformation of this story during the earthquake.



(a)



(b)

Figure 2.7 Observed Damage Pattern after the Northridge Earthquake (Trifunac, 2001)

CHAPTER 3

MODEL CHARACTERISTICS

There are numerous approaches to modeling the earthquake response of reinforced concrete structures. In this study, as in most cases, the primary objective was to provide accurate prediction of 1) the load and deformation demands imposed on structural components, and 2) the displacement, velocity and acceleration of the structure. Structural component demands may be used to estimate component performance, while displacement, velocity and acceleration data may be used to predict nonstructural damage. In this study, as in most cases, the need for accurate prediction of building response was balanced against limited time for model development and limited computing time. This chapter discusses the fundamental characteristics of the model used in this study, the model parameters and modeling assumptions that are incorporated into the model, and the decisions that were made during the model development process to balance accuracy and efficiency.

3.1 Global Characteristics

A two dimensional model of the east-west frames of the case study building was developed for this project. Two-dimensional, rather than three-dimensional modeling of the structure was chosen for several reasons. First, the data from two-dimensional modeling are sufficient to accomplish the project objectives of investigating and quantifying the variability in predicted response resulting from modeling decisions. Second, given that scope of the project included a parametric investigation, minimizing computational time and maximizing model robustness was critical. It was found that the two-dimensional model greatly out-performed the three-dimensional model in these areas. Third, as this investigation constituted one of the first large-scale applications of

the OpenSees platform, beginning with a two-dimensional model and progressing to a three-dimensional model was considered to be appropriate.

To accurately predict response and to facilitate three-dimensional modeling in the future, a two dimensional model of the case study building was generated by modeling one exterior frame and one interior frame of the structure and constraining joints on the same floor and on the same north-south column line to have equal displacements. This is equivalent to assuming that the concrete slabs do not exhibit in-plane shear deformation.

The two-dimensional model uses the northern most exterior and interior frames. As discussed previously, the structural system is regular and approximately symmetric about the north-south and east-west axes, so these two frames are approximately identical to the southern most exterior and interior frames. The northern frames were chosen because the stairs and elevators located on the southwest corner of the building do introduce some irregularity in the structural system and do impact the design of beams and columns in the vicinity.

3.2 Element Formulations

In the past researchers have used a variety of element formulations to model beam-columns. The earliest element formulations modeled only flexural deformation and included the assumptions of small displacements and elastic material response. Recently beam-column element formulations have been developed that account for large displacements (Crisfield, 1986) and inelastic material response. Additionally, recent implementations of force-based elements (beam-column element formulation in which a linear moment distribution rather and a quadratic curvature distribution is assumed) with fiber-discretization of the cross-section have been shown to provide accurate and efficient simulation of the inelastic response of reinforced concrete beam-columns.

In the current study several different element formulations have been used to model the beam-columns that comprise the structure. The effect on the predicted building response of element formulation is discussed in Chapter 6. The four different approaches

to modeling the response of the building beam-columns, which employ three different element formulations (Scott, 2001), are as follows:

- 1) Elastic model: The beams, slabs and columns are modeled using an elastic beam-column element formulation. Member stiffness is defined by the dimensions of the gross section and by the concrete modulus of elasticity
- 2) Effective stiffness model: Beams, slabs and columns are modeled using an elastic beam-column element. Member stiffness is defined by the dimensions of the gross section, the concrete elastic modulus and a stiffness reduction factor. The stiffness reduction factor is intended represent the reduction in stiffness due to damage that accumulates during the earthquake. Independent stiffness reduction factors are used to reduce flexural, shear, axial and torsional stiffness; independent stiffness reduction factors are used for columns, beams and interior slabs. These factors are discussed in more detail in Chapter 5.
- 3) Lumped plasticity model: Beams, slabs and columns are modeled using a force-based element formulation in which material inelasticity is assumed to occur only in “plastic-hinge” regions at the ends of the element. An inelastic moment-curvature response is defined at each end of the element. In the models considered for this study, the moment-curvature response of the cross-section is defined using a fiber discretization of the member cross section and one-dimensional concrete and steel material models. The deformation of the beam-column element is determined by the inelastic deformation of the hinges and by the deformation of the elastic length of the element between the hinges. The hinges that are present at both ends of the element are of finite length and the length of the elastic part in between the two plastic hinges at the end depends on the lengths of the plastic hinges. Parameters that must be defined for this model include 1) the plastic hinge length, 2) the fiber discretization of the each of the sections at the ends of the element and 3) the stiffness properties of the elastic portion of the element
- 4) Nonlinear beam-column model: Beams, slabs and columns are modeled using a force-based element formulation in which inelasticity is allowed to spread along the length of the element. As with the lumped-plasticity model, a linear moment

distribution is assumed along the length of the element. However, in this element formulation, the element deformation is defined by the curvatures that develop at multiple locations along the length of the element. A Gauss-Labotto integration scheme, rather than a classical Gaussian integration scheme is used so that the curvature at the ends of the element is included in the computations. As with the lumped-plasticity element, the moment-curvature response is defined using a fiber discretization of the member cross section. Parameters that must be defined for this model include 1) the section – fiber discretization of the section to determine the section response, and 2) the number of integration points along the length of the element.

Since both the lumped-plasticity model and the non linear beam column use a force-based formulation, a linear moment distribution is assumed along the length of the element and element end rotations are computed to satisfy compatibility requirements. A single element can be used to represent exactly the moment distribution along a column. It is assumed that earthquake load dominates gravity loads and the use of a single force-based element provides accurate results.

Figure 3.1 shows the typical load versus displacement for a cantilever column that is modeled using each of the modeling approaches discussed above. This figure shows the effective stiffness, lumped-plasticity, and nonlinear beam-column models all to have approximately the same initial stiffness. This similarity is due to the fact that the moment-curvature response of a member section, which determines response for the lumped-plasticity and nonlinear beam-column element formulations, is defined assuming that concrete has zero tensile strength. Thus, at approximately zero load, the nonlinear elements provide cracked section stiffnesses, which are comparable to the effective elastic stiffness for this particular element. Additionally, the lumped-plasticity and nonlinear beam-column models are found to have approximately the same load-displacement response. These similarities are due to the fact that stiffness reduction factors are applied to the elastic stiffness parameters that define the response of the “elastic” region of the lumped-plasticity model.

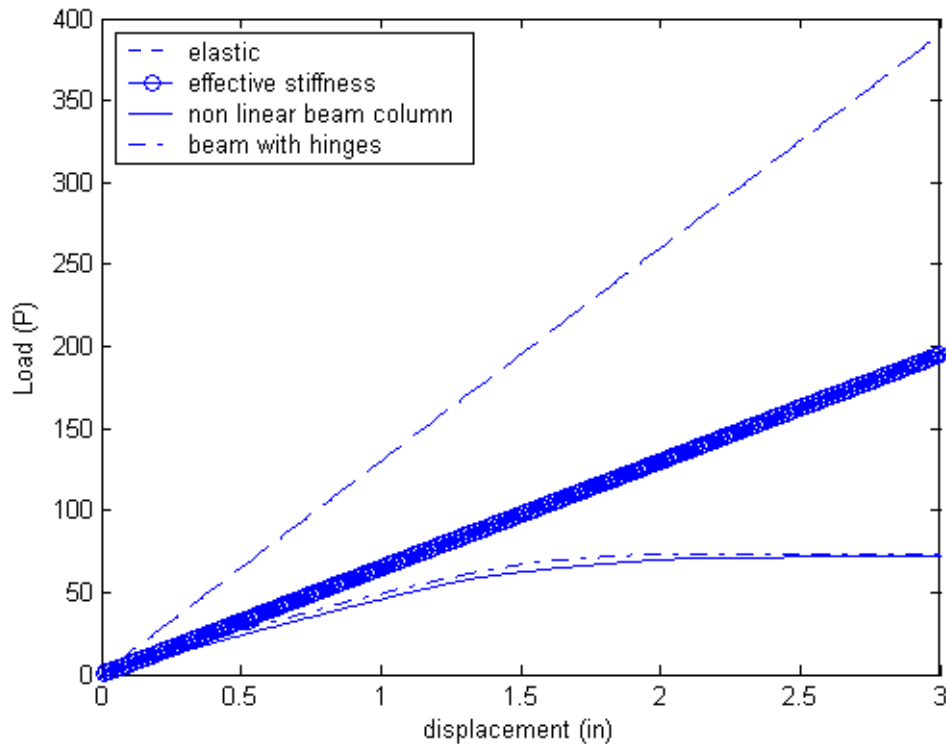


Figure 3.1 P-delta Relation for the Different Element Formulations

The lumped plasticity element formulation is used in the baseline model of the case study building. The elastic and effective stiffness models could not be expected to predict the observed nonlinear response of the structure. While the nonlinear beam-column element formulation could be expected to provide a better prediction of the curvature distribution along the length of the element, the nonlinear and lumped plasticity models show similar load-displacement response for the cantilever column (Figure 3.1). Thus, both elements could be expected to provide similarly accurate prediction of component load and deformation demand as well as similarly accurate prediction of global structural response. Additionally, the nonlinear beam column, because it includes multiple fiber sections, requires significant computational time in comparison with the lumped plasticity model. Quantitative comparison of the lumped-plasticity and nonlinear beam-column models and the other is presented in Chapter 5.

3.3 Discretization of Beam and Column Sections

The lumped-plasticity and nonlinear beam-column elements require a section model to define the moment-curvature response at points along the length of the member. Two approaches can be employed to define the moment-curvature response for a section: use a one-dimension material model to define the moment-curvature relationship or use a fiber discretization of the section and one-dimensional material models to represent the stress-strain response of the plain concrete and reinforcing steel that compose the section. The use of a one-dimensional moment-curvature response has the advantage of reducing computational time and reducing the memory required to run the model. However, a one-dimensional moment-curvature response model cannot represent variability in flexural response due to variation in axial load, which may be significant for columns. Additionally, accurate calibration of a one-dimensional moment-curvature response model for reversed cyclic loading is difficult and requires the analyst to introduce multiple assumptions about response. A fiber discretization model has the advantage that model is defined entirely by the geometry of the gross concrete section, the location and size of longitudinal bars, a one-dimensional concrete stress-strain model and a one-dimensional steel stress-strain model. One-dimensional concrete and steel material models are well defined by experimental data.

3.4 Material Properties

Standard one-dimensional concrete and steel stress-strain response models are used to define section response. These material models are discussed in the following sub-sections.

3.4.1 Concrete

OpenSees provides three models that can be used to simulate concrete stress-strain response. These models are named *Concrete01*, *Concrete02*, and *Concrete03*. All of these models define the same response under compressive loading: parabolic stress-strain response to the point of maximum compressive strength, linear post-peak response to a residual compressive strength. This response curve is shown in Figure 3.2. *Concrete01* defines zero tensile strength. *Concrete02* defines a brittle response under tensile loading with complete loss of tensile strength once peak tensile strength is exceeded. *Concrete03* defines a brittle response under tensile loading with an exponential decay in tensile strength once peak tensile strength is exceeded. In the current study, *Concrete01* (concrete without tensile strength) is used, as previous earthquake loading of the structure is assumed have resulted in substantial concrete cracking and thus loss of concrete tensile strength.

Concrete response under compressive loading is defined by 1) the concrete compressive strength, 2) the compressive strain at which compressive strength is developed, 3) the post-peak stiffness and 4) the residual concrete strength. As discussed in Chapter 2, the confinements provided by transverse reinforcement in the beams and columns are minimal, with non-ductile detailing. Thus it is assumed that all concrete behaves as “unconfined” concrete with no increase in strength or deformation capacity due to confinement. The strain at which compressive strength is developed is assumed to be 0.002 and the post-peak stiffness is defined such that a residual strength equal to 80% of the compressive strength is developed at a strain level equal to 0.004. These strain values are consistent with the results of Mander et al. (1971).

The case study building is constructed of nominal-weight concrete of multiple strengths. Previous research (Islam, 1996) showed that the actual concrete strength in the building to be substantially higher than the design strength. Research suggests that increased concrete compressive strength attributable to age and required over-strength at casting (ACI-318, 2002). FEMA 356 recommends factors to account for concrete over-strength. Listed below in Table 3.1 is the design concrete compressive strength for

various groups of structural components, strength values recommended in the FEMA 356 guidelines, and strength values used by previous researchers.

Table 3.1 Concrete Compressive Strengths used in Simulating Building Response

| Concrete | Design strength f'c(psi) (Rissman, 1965) | f'c used in model (psi) – FEMA 356 | f'c used by Islam (1996) and Moehle and Lynn (1997) |
|----------------------|------------------------------------------------|------------------------------------------|-----------------------------------------------------------|
| Columns ground floor | 5000 | 7500 | 6650 |
| Columns second floor | 4000 | 6000 | 5320 |
| Columns other floors | 3000 | 4500 | 4000 |
| Beams Second floor | 4000 | 6000 | 5320 |
| Beams other floor | 3000 | 4500 | 4000 |

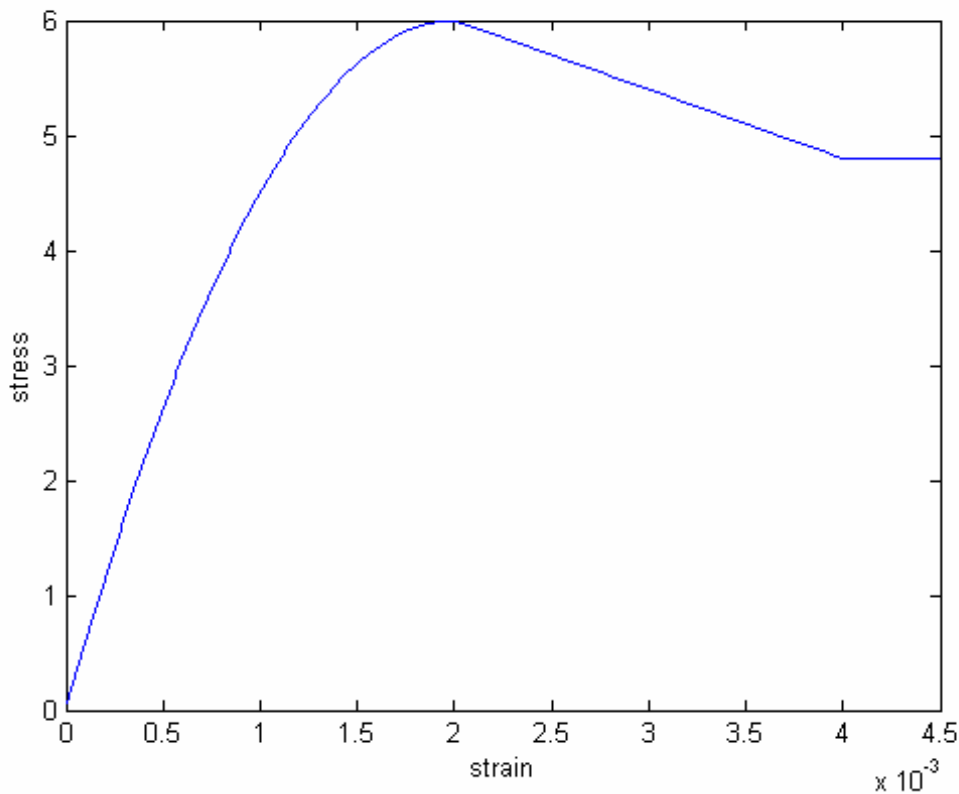


Figure 3.2 Behavior of Concrete Material Being Used in the Model

3.4.2 Steel

OpenSees provides two models for use in simulating the stress-strain response of reinforcing steel. These models are named *Steel01* and *Steel02*. The *Steel01* model is a classical one-dimensional plasticity formulation with linear isotropic hardening. The *Steel02* uses the same envelope as the *Steel01* model, but Menegotto-Pinto (1973) curves are used to describe unload-reload response. Thus, the *Steel02* model provides a better representation of the Bauschinger effect. The stress-strain relation for a Menegotto-Pinto model is given by the following equation.

$$\frac{f}{f_o} = b \frac{\varepsilon}{\varepsilon_o} + \frac{(1-b) \frac{\varepsilon}{\varepsilon_o}}{\left[1 + \left(\frac{\varepsilon}{\varepsilon_o} \right)^R \right]^{1/R}} \quad (\text{Eq. 3.1})$$

where, b is the strain hardening ratio and f_o and ε_o are the yield stress and the yield strain of the steel. R is the parameter that controls the curvilinearity of the stress-strain response. R varies with cyclic loading. Recommendations of Filippou (2000) are used to define the parameters.

Table 3.2 presents the specified steel yield strength, yield strength used in the model and values used by others. Steel yield strength has been increased from nominal strength to account for typically observed over-strength following the recommendations of the FEMA 356 guidelines.

Table 3.2 Longitudinal Reinforcing Steel Yield Strength used in Simulating Model Response

| Steel | Specified minimum yield strength (ksi) | Fy used in model (ksi) * FEMA 356 | fy used by Islam (1996) (ksi) | fy used by Moehle and Lynn (1997) (ksi) |
|-----------------|----------------------------------------|-----------------------------------|-------------------------------|-----------------------------------------|
| Beams and Slabs | 40 | 50 | 50 | 50 |
| Column bars | 60 | 75 | 72 | 75 |

3.5 Column Failure Modes

As discussed in Chapter 2, inadequacies in the column transverse and longitudinal reinforcement detailing would be expected to result in column shear failure or failure of the column longitudinal steel splices. Damage observed following the 1994 Northridge earthquake indicates that one or both of these failure mechanisms developed in several columns on the 1st, 4th and the 5th story columns prior to the columns reaching full flexural capacity (Trifunac, 2001). Simulation of these failure mechanisms is discussed in the following sections.

3.5.1 Splice Failure Model

Splice failure in the columns is simulated by modifying the stress-strain history used for the column longitudinal steel reinforcement at the column section nearest the column splice. The modified steel stress-strain history includes reduced yield strength and a negative post-yield stiffness. The recommendations of FEMA 356 are used as a basis for calculating the spliced steel. The reduced yield strength of the steel is given by the following equation

$$f_{y,splice} = f_{y,actual} * \left(\frac{l_b}{l_d}\right) \quad (\text{Eq. 3.2})$$

where, l_b is the provided lap-splice length ($24d_b$ for interior columns and $36d_b$ for exterior columns) and l_d is the design lap-splice length calculated using the recommendations of ACI Committee 318 (2002)

$$l_d = \left[\frac{3}{40} \frac{f_y}{\sqrt{f'_c}} \frac{1}{\left(\frac{c + K_{tr}}{d_b}\right)} \right] d_b \quad (\text{Eq. 3.3})$$

In Eq. 3.3, c is the smaller of the distance from the center of bar being developed to the nearest concrete surface, and of (2) one-half the center-to-center spacing of bars being developed, the term $\left(\frac{c + K_{tr}}{d_b}\right)$ cannot exceed 2.5, and

$$K_{tr} = \frac{A_{tr} f_{yt}}{1500sn} \quad (\text{Eq. 3.4})$$

where, A_{tr} is the area of the transverse reinforcement in plane of splitting, f_{yt} is the yield strength of longitudinal reinforcement, s is the spacing of transverse reinforcement (within l_d) and n is the number of bars being developed. Figure 3.3 shows the simulated stress-strain response for column longitudinal reinforcement with and without splice failure.

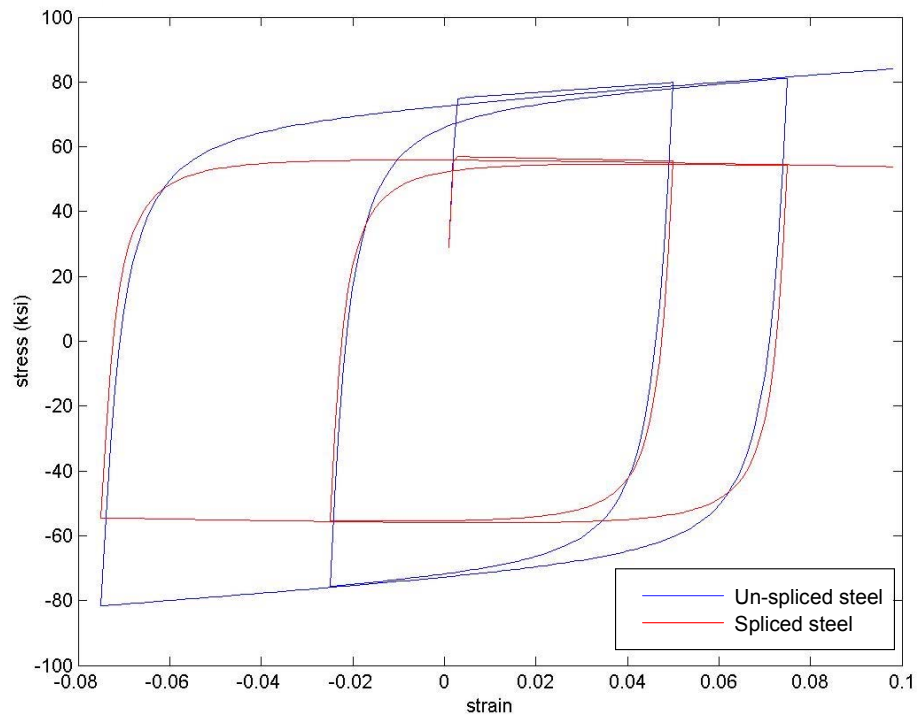


Figure 3.3 Simulated Stress-Strain Responses for Column Longitudinal Reinforcement

3.5.2 Shear Failure Model

Three models have been developed for use in simulating shear failure of the columns. These models are named the FEMA356 model, the UCSD model and the ACI model and are based loosely on the recommendations of FEMA 356, Kowalsky and Priestley (2000) and the ACI 318 (2002) respectively. The FEMA356 model is the most conservative and the ACI model is the least conservative model. For all the models, if a column is shear critical, column response is controlled by flexure until the shear demand exceeds the shear capacity. At this point, the column exhibits a brittle shear failure characterized by essentially no lateral stiffness. A column that has failed in shear maintains axial load carrying capacity. Details about the models follow:

1. The FEMA356 model defines the shear strength of the column according to the recommendations of ACI Committee 318 (2002), with one exception. Here the full strength of the transverse steel is used. FEMA 356 recommends using half the strength if the ties are spaced greater than 50% of the section depth. Also, in the OpenSees model, columns are defined to have a brittle response with essentially no ductility; FEMA356 recommends limited ductility capacity. The FEMA356 model is the most conservative with shear strengths ranging from 28% to 115% of the maximum shear demand assuming that the column develops nominal flexural strength at both ends.
2. The UCSD model is developed on the basis of the recommendations of Kowalsky and Priestley (2000). In the Kowalsky and Priestley model, the contributions of three mechanisms define shear capacity: a transverse steel contribution, an axial load contribution and a concrete contribution with the magnitude of the concrete contribution defined as a function of ductility demand. At the current time it is not possible to define shear strength be a function of ductility demand within OpenSees. Thus, the “UCSD shear model” is implemented using the minimum concrete shear strength factor; this corresponds to the shear capacity that would be developed at a large ductility demand. The UCSD model is moderately conservative with shear

strengths ranging from 55% to 194% of the maximum demand. The equations used to calculate the shear strength for the UCSD model are as below

$$V_n = V_c + V_s + V_p \quad (\text{Eq. 3.5})$$

$$\text{where, } V_c = \alpha\beta\gamma\sqrt{f'_c} (0.8A_g) \quad (\text{Eq. 3.6})$$

$$V_p = P\left(\frac{D-C}{2L}\right) \quad (\text{Eq. 3.7})$$

$$V_s = A_v f_y \left(\frac{D'}{s}\right) \cot \theta \quad (\text{Eq. 3.8})$$

Here, V_p represents the strength attributed to the axial load, P is the axial load, D is the column width and D' is the confined core diameter. θ represents the assumed angle of inclination between the shear cracks and the vertical column axis and is assumed to be 30 degrees. The γ factor is a measure of the allowable shear stress and is a function of curvature ductility. α accounts for the column aspect ratio and is given by the equation $1 \leq \alpha = 3 - \frac{M}{VD} \leq 1.5$. The factor β is a modifier that accounts

for the longitudinal steel ratio, and is given by the equation

$$\beta = 0.5 + 20\rho_l \leq 1 \quad (\text{Eq. 3.9})$$

where, ρ_l is the longitudinal steel ratio.

3. The ACI model is developed on the basis of the recommendations of ACI Committee 318 (2002), with the exception that concrete is assumed to contribute to shear strength in the plastic-hinge region (ACI 318 recommends that the concrete contribution to shear capacity be ignored for members that will experience flexural yielding). The ACI model is least conservative of all the models with shear strengths ranging from 96% to 254% of the maximum demand. The equations used to calculate the shear strength capacity for the ACI model are as below.

$$V_n = V_c + V_s \quad (\text{Eq. 3.10})$$

$$\text{where, } V_s = \frac{A_v f_y d}{s} \quad (\text{Eq. 3.11})$$

$$\text{and, } V_c = 2 \left[1 + \frac{N_u}{2000 A_g} \right] \sqrt{f_c'} b_w d \quad (\text{Eq. 3.12})$$

where, V_s is the strength provided in terms of the area A_v , yield strength f_y , spacing s of the shear reinforcement and d is the effective depth. N_u is the factored axial load and b_w is the width of the section. Table 3.3 shows the shear demand of the columns and the shear strengths of the columns calculated for the three shear models described above. Columns have been divided into 30 groups depending upon their properties (refer Table 2.3 for column Group ID).

Table 3.3 Shear Strength Capacities defined by the Shear models.

| Group ID | V_demand (ksi) | V_ACI/ V_demand | V_FEMA/ V_demand | V_UCSD/ V_demand |
|----------|-------------------|--------------------|---------------------|---------------------|
| 1 | 40.21 | 2.54 | 0.32 | 1.5 |
| 2 | 50.81 | 2.26 | 0.38 | 1.4 |
| 3 | 36.93 | 2.1 | 0.31 | 1.56 |
| 4 | 36.93 | 2.41 | 0.46 | 1.82 |
| 5 | 31.65 | 2.14 | 0.36 | 1.63 |
| 6 | 31.65 | 2.5 | 0.54 | 1.94 |
| 7 | 24.67 | 2.07 | 0.21 | 1.28 |
| 8 | 31.65 | 2.07 | 0.36 | 1.48 |
| 9 | 40.21 | 1.67 | 0.21 | 0.92 |
| 10 | 75.23 | 1.25 | 0.21 | 0.61 |
| 11 | 54.23 | 1.24 | 0.15 | 0.68 |
| 12 | 36.93 | 1.62 | 0.23 | 1.08 |
| 13 | 62.33 | 0.96 | 0.13 | 0.64 |
| 14 | 36.93 | 1.29 | 0.1 | 0.72 |
| 15 | 24.67 | 2.05 | 0.34 | 1.34 |
| 16 | 31.65 | 1.65 | 0.26 | 1.13 |
| 17 | 31.65 | 1.33 | 0.12 | 0.8 |
| 18 | 24.67 | 1.68 | 0.15 | 1.02 |
| 19 | 31.65 | 1.68 | 0.26 | 1.17 |
| 20 | 24.67 | 2.07 | 0.34 | 1.35 |
| 21 | 19.10 | 2.08 | 0.2 | 1.14 |
| 22 | 19.10 | 1.96 | 0.2 | 0.94 |
| 23 | 31.65 | 1.33 | 0.12 | 0.79 |
| 24 | 31.65 | 1.27 | 0.12 | 0.71 |
| 25 | 19.10 | 2.02 | 0.2 | 1.04 |
| 26 | 19.10 | 1.93 | 0.2 | 0.9 |
| 27 | 31.65 | 1.26 | 0.12 | 0.69 |
| 28 | 31.65 | 1.22 | 0.12 | 0.63 |
| 29 | 19.10 | 1.97 | 0.2 | 0.95 |
| 30 | 19.10 | 1.91 | 0.2 | 0.86 |

Five models of the structure were developed using the different splice and shear failure models. These models are named no-splice-no-shear, splice-no-shear, splice-UCSD, splice-ACI, splice-FEMA356 depending upon the type of splice and shear failure exhibited by the model. These models may be evaluated by comparing the load-displacement response of a cantilevered column subjected to monotonic loading predicted using the different models. Column response is simulated using the beam-with-hinges element formulation, which preliminary analysis indicated would be best suited to the current modeling needs and combination of the splice and shear failure models. Numerical data are presented in Figure 3.4 with data identified on the basis of the splice and shear failure models employed:

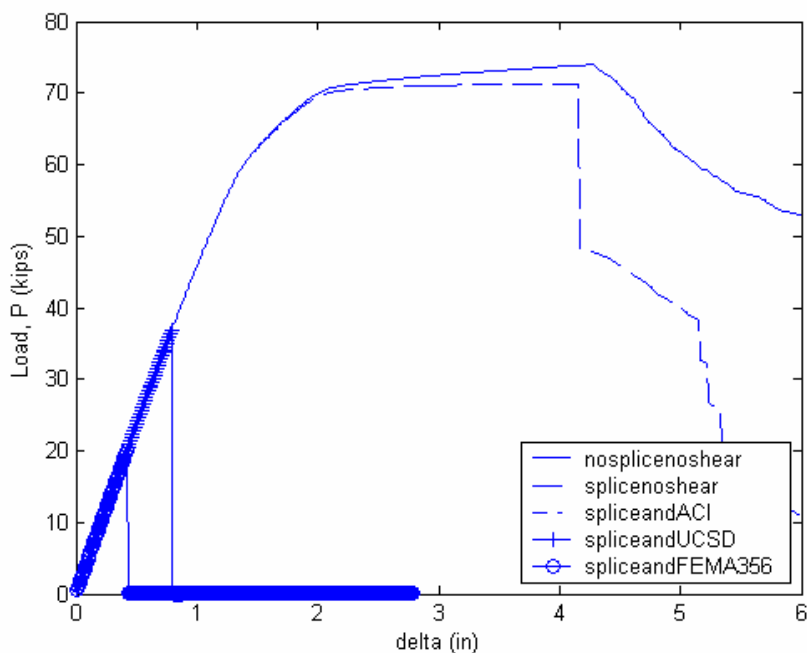


Figure 3.4 P- Δ Relations for a Typical Column Section

The UCSD failure model was chosen as the shear failure model to be incorporated into the baseline model as it represented a middle ground between the two other models. Comparison of the different failure models is discussed in more detail in Chapter 5. The impact of shear capacity on predicted response was investigated as part of the parameter study presented in Chapter 6.

3.6 Gravity Load

Gravity load is computed as dead load plus live load, with live load assumed to be 10 psf (UBC 2000). Gravity load is applied as a distributed load along the length of the beams. Total gravity loads applied at the top of each column is listed below in Table 3.4.

Table 3.4 Gravity Loads Applied to Van Nuys Building Model

| Floor | Interior column loads (kip) | Exterior column loads (kip) | Corner column loads (kip) |
|-------|--------------------------------|--------------------------------|------------------------------|
| 7 | 47.0 | 29.8 | 20.2 |
| 6 | 41.0 | 34.0 | 23.0 |
| 5 | 41.0 | 34.0 | 23.0 |
| 4 | 41.0 | 34.0 | 23.0 |
| 3 | 41.0 | 34.0 | 23.0 |
| 2 | 41.0 | 34.0 | 23.0 |
| 1 | 56.4 | 37.5 | 25.9 |

3.7 Damping

The introduction of viscous damping (ξ) in dynamic analysis is intended to represent energy dissipation mechanisms that cannot be represented through the load-deformation response of structural components. If a hysteretic structural model is used, such as the beam with hinges model, then a relatively low level of viscous damping is appropriate since viscous damping accounts only for damping provided by non-structural elements.

A previous investigation of the case study building by Hart (1975) used building acceleration records from the San Fernando earthquake to compute equivalent viscous damping levels. Hart concluded that during the San Fernando earthquake equivalent viscous damping was equal to 9.7% and 16.4% of critical damping for 1st mode response in the EW and the NS directions of the building. Hart found that there was no noticeable difference between viscous damping levels for different modes. These values are

appropriate for use with the effective stiffness model of the case study building for a moderate earthquake demand.

For the models of the case study building that do not employ elastic element formulations, the viscous damping levels reported by Hart (1975) represent an upper-bound. Few investigations have addressed appropriate viscous damping levels for hysteretic structural models; commonly used values range from 2% to 5% of critical damping in the 1st mode (Islam 1996, Browning et al. 2000, Barin and Pincheria 2000). Additionally, the results of previous research suggest that viscous damping should be increased as the magnitude of earthquake demand increases (Chopra, 2000), to account for additional energy dissipation. For the current study, a viscous damping level equal to 5% of critical is assumed. Chapter 5 discusses the procedure used to estimate the total effective damping due to viscous and hysteretic damping; estimated values suggest that this is a reasonable assumption. The impact of viscous damping on predicted response was investigated as part of this study and is discussed in Chapter 6.

OpenSees supports stiffness-dependent, mass-dependent and Rayleigh damping, thereby enabling a user to define damping for at most two response modes. Figure 3.5 shows viscous damping levels in the first eight response modes for the beam with hinges model for the case of Rayleigh damping with damping defined to be 5% of critical in modes one and two. Typically, it is assumed that the use of higher levels of damping in higher modes (as shown in Figure 3.5) is appropriate.

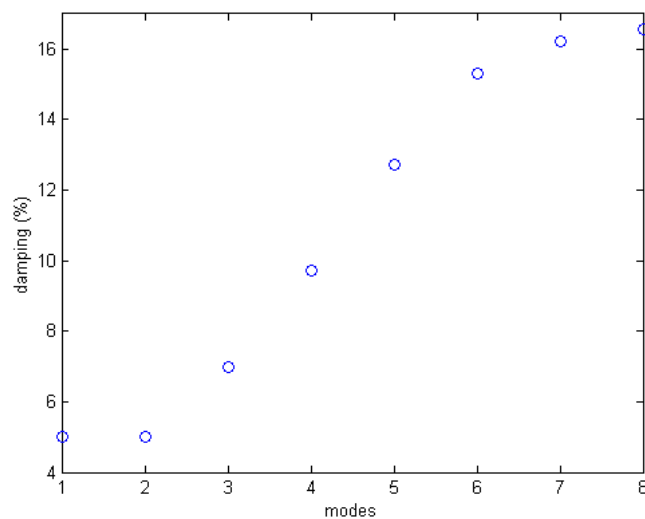


Figure 3.5 Viscous Damping as a Percentage of Critical Damping for 8 Modes

3.8 Effective Slab Width

Modeling of the slabs in slab-column frames is often done by using an equivalent beam that represents the portion of the flat slab contributing to the flexural response. This approach is adopted in the current study. Previous experimental and analytical investigations (Pan and Moehle 1988, Luo and Durrani 1995) have shown that lateral loading of a column of a slab-column frame causes a variable rotation pattern across the slab, with the maximum value near the column and minimum values near the slab centerlines. The equivalent slab width is defined as the width of the slab that provides the same column displacement as the true slab, if a uniform rotation is assumed across slab width. Accordingly, the effective width factor is defined as the ratio of the width of the equivalent slab to the distance between the columns in the direction perpendicular to modeling direction.

Researchers have developed recommendations for the effective width of slab on the basis of analytical and experimental studies. Pecknold (1975) conducted one of the earliest analytical studies for elastic modeling of flat slabs. The results of this investigation include a recommended method for computing effective slab width for use in linear finite element analysis results. Applying the method recommended by Pecknold, the effective width factor for the case study building is 0.66.

More recently, Luo and Durrani (1995) developed a method for computing the effective slab width using experimental data from forty interior RC beam-column connection tests. The Luo and Durrani model consists of a modification factor, χ , that is applied to a simplified version of Pecknold's formula. This modification factor was introduced to account for cracking due to gravity loads in an elastic analysis. The simplified version of Pecknold's formula for computing the effective slab width ratio, α , is given by Eq. 3.13. The terms in the expression are illustrated in Figure 3.6.

$$\alpha_i = \frac{1.02\left(\frac{c_1}{c_2}\right)}{0.05 + 0.002\left(\frac{l_1}{l_2}\right)^4 - 2\left(\frac{c_1}{l_1}\right)^3 - 2.8\left(\frac{c_1}{l_1}\right)^2 + 1.1\left(\frac{c_1}{l_1}\right)} \quad (\text{Eq. 3.13})$$

to account for slab cracking. Pan and Moehle noted that this factor is intended for elastic analysis and underestimates slab stiffness at low drifts and overestimate the slab stiffness at high drifts. Using the ACI 318 (2002) and the reduced factor by Pan and Moehle, the effective width factor was calculated to be 0.22 for the case study building.

The recently published guidelines on seismic rehabilitation of buildings (ATC 33, 1997) suggests the following formula for the calculation of the effective width factor:

$$\alpha = \beta(5c_1 + 0.25l_1) \quad (\text{Eq .3.15})$$

where, α is the effective width factor, β is a factor representing cracking effects (0.33 to 0.5), c_1 and l_1 (in inches) are as defined in Fig. 3.7. This recommendation is valid for elastic analyses and inelastic analyses where the initial stiffness is based on cracked properties. The resulting effective width factor for the study building is 0.2 to 0.5 depending on the value of β used. ATC 33 recommends limiting the effective width to column strip as a lower bound representation to expected flexural strength.

For the baseline model, the effective slab width has been chosen as 0.5. Also, a parameter model with effective slab width equal to 0.11 has been chosen to study the effect that slab width has on the building response and has been discussed in Chapter 6.

3.9 Foundation

The foundation system of the structure consisted of 38 inch deep pile caps, supported by groups of two to four poured-in-place 24 inch diameter reinforced concrete friction piles. All pile caps are connected by a grid of tie beams and grade beams. Each pile is approximately 40 ft long and has a design capacity of 100 kips vertical load and up to 20 kips lateral load. The soil in the site was reported to be primarily fine sandy silts and silty fine sands. For the baseline model the foundation is assumed to be rigid and the columns in the 1st story are assumed to be fixed to the ground.

3.10 Beam-Column Joints

The beam-column joints have been assumed to be rigid in both shear and flexure. A rigid offset equal to the frame member depth has been provided at each beam-column connection. Tests for model with flexible joints (considering the center line dimensions of the beam-column elements without any rigid offset) have also been done and are discussed in Chapter 6.

CHAPTER 4

OPENSEES IMPLEMENTATION

OpenSees is a software framework for simulating the inelastic response of structural and geotechnical systems subjected to static and dynamic loads. The scripting language *tcl* is the basic user interface to OpenSees. Models are created through a series of *tcl* commands. One of the primary advantages of using a scripting language as a user interface is the facility with which multiple analyses can be run and output stored to investigate the impact of variation in model parameters and earthquake ground motion. In this chapter the basic structure of the model building process is discussed. The OpenSees input file for the analysis of the case study building comprises a series of *tcl* scripts. For analysis using a single model, analysis is initiated by “sourcing in” the file *VanNuysAnalysis.tcl*. For multiple analyses using multiple parameter models and multiple ground motions, analyses is initiated by “sourcing in” the file *Selfrun.tcl*. The *tcl* scripts used in this investigation are discussed in detail in Appendix A. The files *Selfrun.tcl* and *setAnalysisParameters.tcl* are the most important files from the user’s perspective and are discussed in this chapter.

4.1 Basic Structure

Figure 4.1 shows the basic structure of the model-building process using the scripting language. A series of *tcl* scripts store data defining the building geometry and material properties. Lists and arrays are the simplest data structures. An array is a *tcl* variable with a string-valued index. The array elements are defined using the *set* command in *tcl*. A *list* on the other hand is simply a string with list elements separated by a space. Once the data has been stored into the *lists* and the *arrays*, OpenSees commands are called upon to use this data to define the model. Model defining progresses through, definition of the nodes (using the command *Node* in OpenSees), definition of the material

models (using the command *UniaxialMaterial* in OpenSees), definition of the sections (using the *patch and layer* commands in OpenSees) and definition of the elements (using the *element* command in OpenSees). Once the whole model has been set up the *analyze.tcl* sets up the various analysis tools in OpenSees and performs the required analysis specified in *setAnalysisParameters.tcl*. Figure 4.1 shows the model building process, data transfer and tasks required to accomplish the analysis of the model.

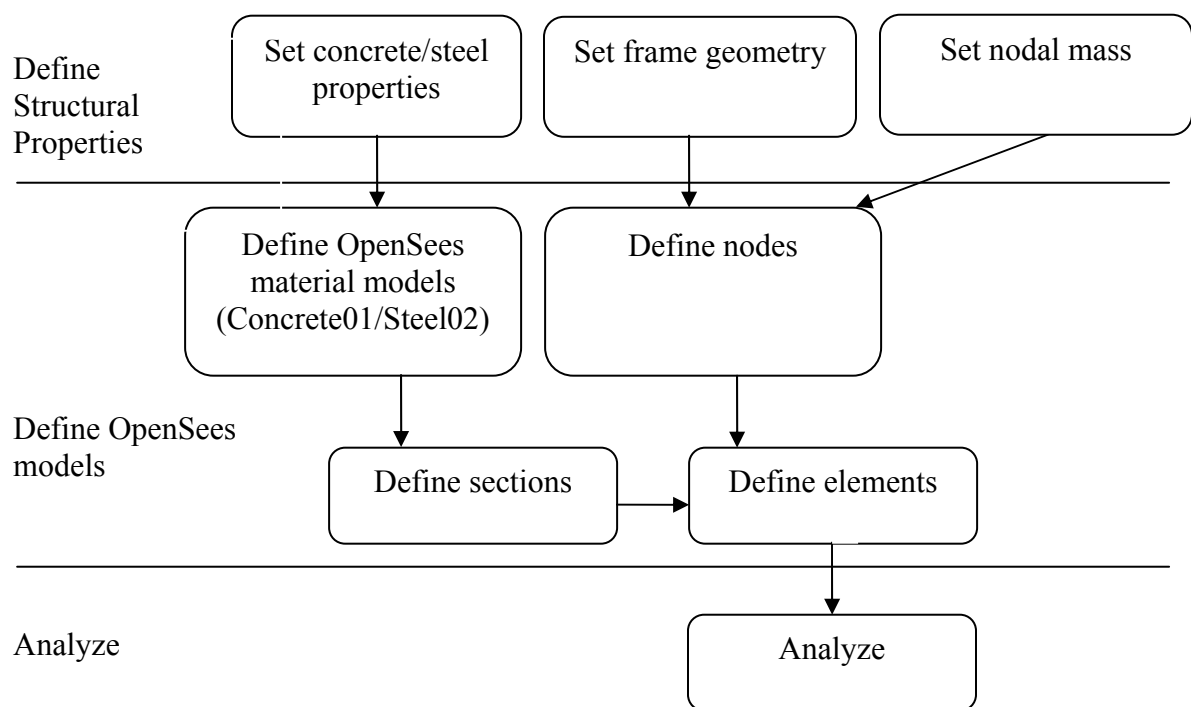


Figure 4.1 Basic Structure of Model Building Process

4.2 *VanNuysAnalysis.tcl*

The integration of the various files is done in the *VanNuysAnalysis.tcl* file which includes the following lines:

```
Source Selfrun.tcl
```

Source setAnalysisParameters.tcl
 Source setFrameGeometry.tcl
 Source serFrameMemberProperties.tcl
 Source setMaterialProperties.tcl
 Source setElasticElementPropeties.tcl
 Source setNodalMass.tcl
 Source defineStructuralMaterials.tcl
 Source defineSections.tcl
 Source defineNodes.tcl
 Source defineElements.tcl
 Source defineBoundaryConditions.tcl
 Source analyze.tcl

As suggested by this *tcl* script, additional *tcl* scripts are used to perform various tasks required to define the model and are ‘sourced in’ in ‘*VanNuysAnalysis.tcl*’. The *tcl* scripts titles *set*.tcl* defines lists and arrays of data for use in generating nodes, materials, sections and elements within the OpenSees model. The *tcl* script titles *define*.tcl* execute the OpenSees commands to generate the nodes, materials, sections, elements, boundary conditions that constitute the OpenSees model. Each of the *tcl* files listed above needs to “source in” other *tcl* files and procedures in order to perform the desired tasks. The *selfrun.tcl* is the file which provides the user interface for setting up parameters for multiple analyses to investigate the impact of parameter variation and earthquake ground motion variation. The *setAnalysisParameters.tcl* and *Selfrun.tcl* which are the most important files from the user’s perspective have been discussed here, the rest of the *tcl* files are discussed in Appendix A.

4.3 Set Analysis Parameters

The *setAnalysisParamters.tcl* file is the most critical file for someone who will be analyzing the building or for someone who wants to know the details of a particular model used to generate a particular set of data. Variables in *setAnalysisParameters.tcl* define the model and allow the analyst to modify the model. These variables include the type of beam-column element used in the model, the level of discretization used with these elements, concrete and steel material type and their over-strength factors, whether

the model simulates shear failure and/or splice failure of the model and if so then the type of model used to simulate the shear failure, etc.

Following is an excerpt from the *setAnalysisParameters.tcl* file:

```
# setAnalysisParameters.tcl
#script to define analysis parameters including element, section and material models
# -----begin setAnalysisParameters

#2D or 3D ANALYSIS
set 2Dvs3DModel "2D";

#ELEMENTS
set ColumnElementType "fiber-hinge";
  # options: "elastic", "elasticEffStiff", "fiber-hinge", "fiber" ,
set BeamElementType "fiber-hinge";
  # options: "elastic", "elasticEffStiff", "fiber-hinge", "fiber",

#if beamElementType or colElementType is "fiber" - Number of Integration Points
set NumColIntPts 5
set NumBeamIntPts 4

set ElementIter "yes"; # forces iteration within the element to satisfy element equilibrium
set NumElementIter 20; # number of iterations within the element
set tol 1e-8; # tolerance for element convergence

# if "fiber-hinge" – set stiffness factors for elastic beam section between hinges
# if "elasticEffStiff" – set effective stiffness factors for beams, columns, slab
set BeamStiffnessReductionFactorFlex 0.5
set BeamStiffnessReductionFactorAxial 1
set BeamStiffnessReductionFactorShear 0.4
set BeamStiffnessReductionFactorTorsion 1
set ColumnStiffnessReductionFactorFlex 0.5
set ColumnStiffnessReductionFactorAxial 1
set ColumnStiffnessReductionFactorShear 0.4
set ColumnStiffnessReductionFactorTorsion 1
set SlabStiffnessReductionFactorFlex 0.5
set SlabStiffnessReductionFactorAxial 1
set SlabStiffnessReductionFactorShear 0.4
set SlabStiffnessReductionFactorTorsion 1

# if beamElementType or colElementType is "fiber-hinge"
set TypicalColumnDepth [expr 18*$in]
set TypicalBeamDepth [expr 24*$in]
set AvgStoryheight [expr 10*$ft]
set AvgBayWidth [expr 225*$in]
set ColumnHingeLengthRatio [expr $TypicalColumnDepth/$AvgStoryheight]
set BeamHingeLengthRatio [expr $TypicalBeamDepth/$AvgBayWidth]
```

```

# if it is simulation of column failure due to inadequate splice length or shear strength is
  required
# Splice failure
set columnSpliceFailure "yes"
set spliceSteelDuctility 2

# Shear failure – note that if disp-based elements are used, one force-based element is
  introduced with the column height
set columnShearFailure "yes"
set shearStrengthModel "FEMA356" # options are "FEMA356", "ACI", "UCSD", "none"

# member dimensions
set ColumnStripWidthFactor 1

#SECTIONS
# set discretization of the section
set MaxFiberDim [expr 0.5*$in]

# set of concrete cover
set CoverBeamColumn [expr 2.0*$in]
set SlabCover [expr 3*$in/4]

#MATERIALS
set ConcreteMaterialType "Concrete01"
#options:"elastic","Kent-Park","tensileStrengthLinearSoftening"
set SteelMaterialType "Steel02" # options: "elastic","bilinear","MP"

# strength factors for concrete
set FcStrengthFactor 1.5 #1.5 suggested by FEMA 356
set ConcreteAgeFactor 1.33 # 1.2 suggested as avg of ACI/CIF
set FcStrengthFactorCasting [expr $FcStrengthFactor/ $ConcreteAgeFactor] #1.25

#ANALYSIS
set AnalysisType "Dynamic"
#options: "Gravity", "Eigen", "Dynamic", "Pushover", "Section"

if {$AnalysisType == "Dynamic"} {
  set groundMotionFileList "groundMotionFileList.tcl"; #name of tcl script that lists
    ground motion files
  set gamma 0.5 #parameters for newmark-beta integration
  set beta 0.25

  #set mass and stiffness proportional damping
  #Rayleigh damping with C = alphaM*M+betaK*K+betaKcomm*(last committed
    K)+betaKinit*(initial K)
  set alphaM 0.3
  set betaK 0.0063

```

```

set betaKcomm 0
set betaKinit 0

} elseif {$AnalysisType == "Pushover"} {
    set PUSHOVER "DispControl"; #pushover under "displacement" or "load" control
}
set loadingType "FEMA356" #options: "FEMA356", "Triangular", "Rectangular"

```

4.4 Self Run

This script automates the analyses process which is very useful for parameter study. Three variables, *controller*, *control* and *groundmotions* are defined. The *controller* is the list of parameters that are to be analyzed and the *control* is a list of values for the parameters that have been defined in *controller*.

```
Set Controller [list "Damping" "Hingelength" "FiberDim" "Slabwidth"];
```

```
Set Control [list "2%" "0.5" "1" "0.22"];
```

```
Set groundmotions [list "50in50_SF_vnuy" "10in50_NR_nord" "02in50_SF_466"];
```

The script has been set up so as to loop through all the parameters with different control values and then loop through all the ground motions defined in the *groundmotions list*. After the analyses has been done the results are saved in separate files named after the type of ground motion used, the parameter being studied and the value of the parameter.

CHAPTER 5

EVALUATION, VERIFICATION AND REFINEMENT OF THE MODEL

The baseline model was subjected to a series of analyses (eigen, pushover and dynamic) and the results obtained from the analyses were compared to the results from some of the previous researchers (Islam 1996, Barin and Pincheria 2002) and with the observed response. Dynamic analyses was also done using the non linear beam column element formulation and other shear failure models in order to verify that the baseline model chosen based on preliminary argument (Chapter 3) was indeed a better model to predict the response of the building.

5.1 Eigenvalue Analysis

The eigenvalue analysis is performed to extract the natural frequencies and mode shapes of a structure. Eigenvalue analysis is important as a predecessor to any dynamic analysis because knowledge of the structure's natural frequencies and modes can help to characterize its dynamic response. In performing an eigenvalue analysis of the structure to determine structural periods and modes of vibration, there are two issues that must be addressed: the components of the structure that are included in the analysis and the load level at which the analysis is done.

1. The two-dimensional model of the case study building includes one exterior and one interior frame with the translational degrees of freedom of the interior frame constrained to move in accordance with the exterior frame. Within the OpenSees environment, an eigenvalue analysis cannot be performed on the constrained structure. Thus, only the exterior frame is used in the eigenvalue analysis of the structure and mass is attributed to the exterior frame in proportion to its relative stiffness of the exterior versus the interior frame. It was found from preliminary pushover analysis that the interior frame was stiffer than the exterior frame and

represented approximately 60% of the total lateral stiffness of the building and the external frame represented approximately 40% of the total stiffness of the building.

2. For the baseline model, under zero loading, the individual concrete and steel fibers that make up a frame-member section carry zero strain and exhibit a tangent stiffness equal to the elastic stiffness. Thus, a section exhibits a tangent stiffness equal to the gross-section, and an eigenvalue analysis of the structure results in periods that are inappropriately small. To compute structural periods and vibration modes that are representative of the structure under gravity plus low-level earthquake loading, the gravity load and a relatively small (1 kip force applied to the roof), static lateral load were applied to the structure before the eigenvalue analysis is done. It was found that with the application of a very small amount of force (1 kip) the time period of the building went up but with the addition of additional force there wasn't any significant variation observed in the fundamental period of vibration of the building.

5.1.1 Effective Stiffness Factors

It was found that for the lumped-plasticity model the eigenvalue analysis after the application of 1 kip static load was found to be much less than 1.5 seconds which was the observed time period of the building under the Northridge earthquake. The reason behind this is that the lumped plasticity model consists of elastic part in between its plastic hinges at the end and the elastic properties being used to define the elastic region were the gross section elastic properties which are not appropriate. Hence it was necessary to define effective elastic properties to define the elastic part of the lumped-plasticity model.

It was found that using the factors specified by FEMA 356 the time period of the model was found to be 1.56 sec, which is close to the observed time period during the Northridge earthquake. Hence, these stiffness reduction factors were used to reduce the gross stiffness properties of the beams and the columns and the reduced stiffness were used to define the effective stiffness model and the lumped-plasticity model. The following are the stiffness reduction factors used:

Element stiffness reduction factor in flexure capacity: 0.5

Element stiffness reduction factor in axial capacity: 1

Element stiffness reduction factor in shear capacity: 0.4

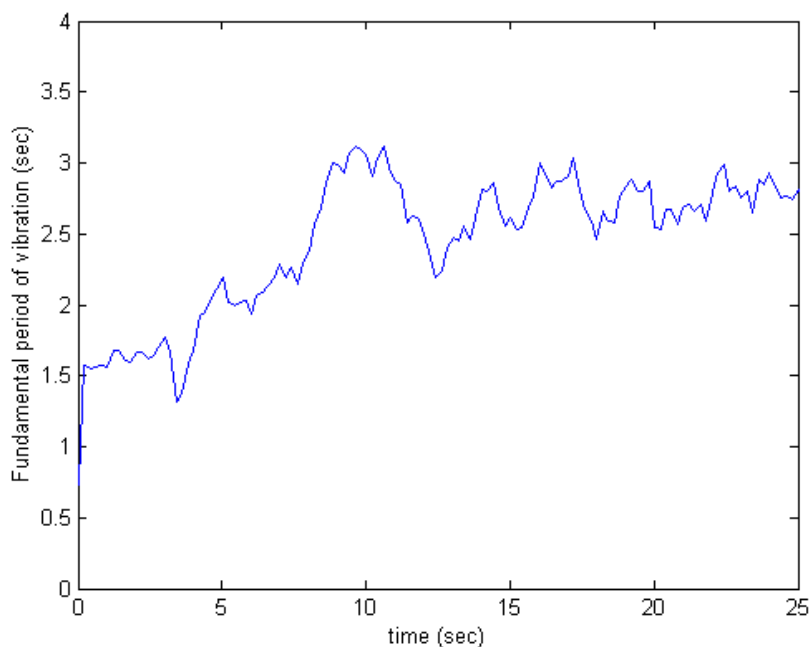
Element stiffness reduction factor in torsion capacity: 1

Eigenvalue analyses were performed for models with elastic, effective stiffness, beam with hinges and the non linear beam column element formulation. For the nonlinear model with fiber-discretization of frame-member sections, gravity and lateral load was applied prior to the eigenvalue analysis as discussed above. First, second and third mode periods for the OpenSees models, first mode periods reported in previous investigations of the Van Nuys building, and fundamental period computed from building acceleration records are listed in Table 5.1. For the baseline model prior to the application of the lateral load of 1 Kip at the roof level it was found that the time period of the building was around 0.9 sec. But for Eigenvalue analyses done with prior lateral load applied to the building it was found that the time period of the building increased from 0.9 sec to 1.56 sec. This is due to the fact that the application of the lateral loads prior to calculating the period of the building opened up cracks in the columns in the ground floor because of which the building became more flexible and hence the increase in time period. The observed time period of the building was 1.5 sec during the early part of the Northridge earthquake and it was found that the baseline model predicts the time period of the building better than the other OpenSees models.

Additionally, for the baseline model of the building, the variation of the fundamental time period was computed during the dynamic analysis for the Northridge ground motion record and is shown in Figure 5.1. Comparison of the values listed in Table 5.1 and the data in Figure 5.1 confirms that the proposed method for computing the period of the structure at the beginning of the earthquake is appropriate. Also the data from Figure 5.1 indicates a fundamental time period of 2.3 sec at 0-10 sec into the earthquake, 2.5 sec at 10-20 sec into the earthquake and 2.7 sec for time more than 20 sec. These values may be compared with the average fundamental structural period computed for these time periods using building acceleration data (last row of Table 5.1)

Table 5.1 Results of Eigenvalue Analysis of the Case Study Building

| Model | 1 st period (sec) | 2 nd period (sec) | 3 rd period (sec) |
|---------------------------------------------------|------------------------------|------------------------------|------------------------------|
| Elastic Model | 0.67 | 0.22 | 0.12 |
| Effective Stiffness model | 0.94 | 0.30 | 0.18 |
| Base model | 1.56 | 0.47 | 0.34 |
| Nonlinear model | 1.93 | 0.64 | 0.36 |
| Model LS2, John A Blume (1997) | 0.79 | 0.26 | 0.15 |
| Islam (1996) | 1.39 | 0.46 | |
| Moehle and Lynn (1997) | 0.73 | | |
| Barin and Pincheira (2000) | 0.81 | | |
| Naeim (1998) | 1.1-1.8 to 2.2 | | |
| UBC 94 Method A | 0.68 | | |
| Pre-1971 San Fernando EQ | 0.52 | | |
| San Fernando EQ, early part, during peak response | 0.70 | | |
| Northridge EQ, Early part (0-10 s) | 1.5 | | |
| Middle part (10-20) | 2.1 | | |
| Towards end (>25) | 2.4 | | |

**Figure 5.1:** Fundamental Period – Northridge Earthquake (Base model)

5.2 Pushover Analysis

Pushover analysis of the case study building was conducted to estimate the lateral strength and deformation capacity and to identify the possible failure mechanisms of the building. Displacement-controlled pushover analyses were conducted on the OpenSees baseline model of the case study building consisting of one interior and one exterior frame. Pushover analysis consists of first applying the distributed gravity load to the structure and then applying an increasing lateral load to the west column line of the structure.

5.2.1 Lateral Load Patterns

Pushover analyses are a common approach for performance evaluation of a structure. Different load patterns can result in different failure mechanisms. The load patterns are intended to represent and bound the distribution of inertia forces in a design earthquake. It is clear that the distribution of inertia forces will vary with the severity of the earthquake (extent of inelastic deformations) and the time within an earthquake. Since no single load pattern can capture the variability in the local demands expected in a design earthquake, the use of at least two load patterns that are expected to bound inertia force distributions is recommended (Krawinkler, 1998).

In this study three load distributions were considered, a uniform distribution (Figure 5.2a), a linear load distribution (Figure 5.2b) and that recommended by the FEMA 356 guidelines (Figure 5.2c) in which the normalized story load is a function of the floor height, h , and the fundamental period of the structure, 1.5 sec. The load pattern suggested by FEMA 356 applies increased lateral forces to the upper levels of the building. This distribution is intended to capture the higher mode effects in the seismic response and is defined by the following exponential equation.

$$F_x = C_{vx} V \quad \text{and} \quad C_{vx} = \frac{w_x h_x^k}{\sum_{i=1}^n w_i h_i^k} \quad (\text{Eq. 5.1})$$

Where, C_{vx} = vertical distribution factor,

V = total base shear,

w_i and w_x = the weight at level i or x ,

h_i or h_x = the height (ft or m) from the base to level i or x , and

k = an exponent related to the structure period ($k = 1.0$ for $T \leq 0.5$, $k = 2.0$ for $T \geq 2.5$, linear interpolation for intermediate values of T)

This equation results in load distributions ranging from a triangular distribution for an exponent value k of 1.0 to a parabolic distribution for a value of 2.0.

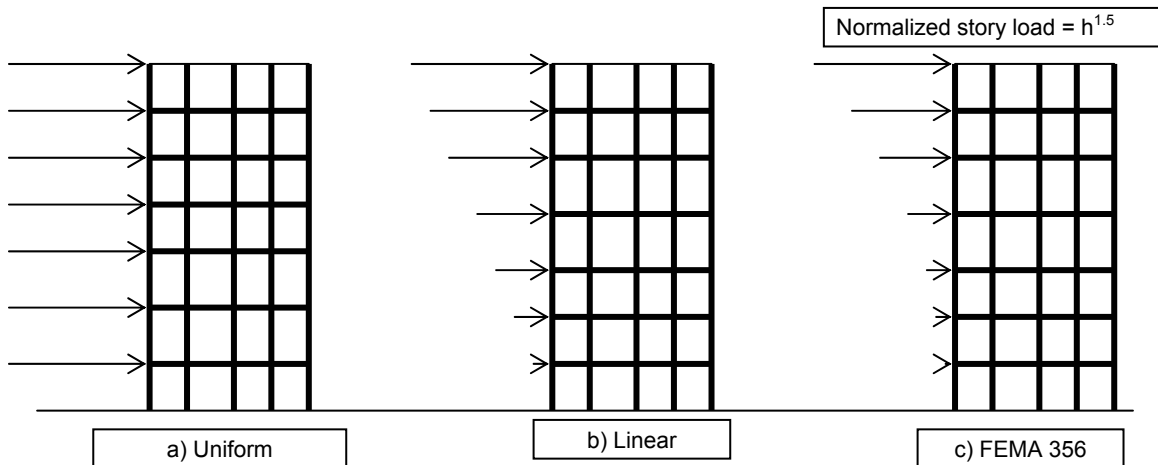


Figure 5.2: Load Distributions used in Pushover Analysis

5.2.2 Results of Pushover Analyses

Figure 5.3 shows the total base shear of the structure versus the corresponding roof displacement for the displacement-controlled pushover analysis with uniform, triangular and FEMA 356 load distributions for the baseline model.

It was observed that the major nonlinear events, their sequence of occurrence and the mechanisms leading to the peak base shear and eventual failure of the building were the same for the analyses with all three different lateral load distributions. The main nonlinear events, common to all the three analyses, were as follows: flexural failure of one of the exterior beams, flexural failure of interior slab, a single column on the first story

failing in shear and eventually the majority of the exterior columns on the fourth and fifth story failing in shear. Shear failures were calculated occurring in several fourth and fifth story columns of the perimeter frame at roof drifts of 8.2, 12.4, 10.2 inches (1.04, 1.57, 1.30% roof drift) for uniform, triangular and FEMA 356 load distributions and the corresponding maximum base shear observed were 640, 510 and 515 kips ($0.12W$, $0.097W$, $0.1W$ respectively, where W is the weight of the building) respectively for the three load distributions.

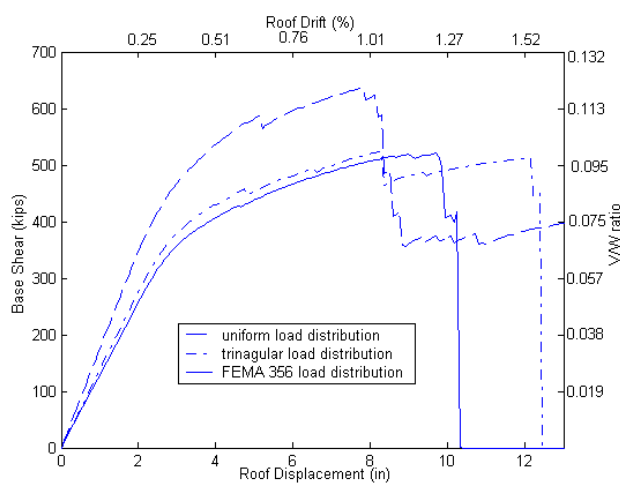


Figure 5.3 Base Shear versus Roof Displacement

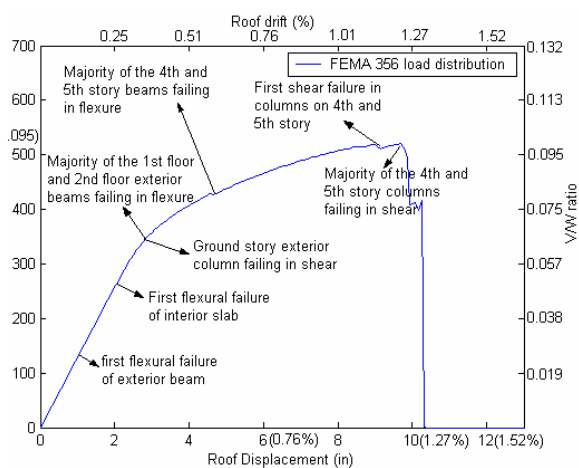


Figure 5.4 Failure Sequence

The main nonlinear events are indicated in sequence as they are observed for the baseline model in Figure 5.4 for the FEMA 356 load distribution. The other load distributions follow a similar trend. As the model was displaced laterally, the structure behaved linearly until a majority of the spandrel beams on the first and second floor began to fail in flexure and the first shear failure was observed in an exterior column on the ground floor at a roof displacement of 2.9 inches as indicated in Figure 5.4 which was followed by the fourth and fifth story beams failing in flexure at a roof displacement of 4.8 inches. Majority of the exterior columns on the fourth and fifth floor started to fail in shear at around 10 inches (1.27% roof drift) at which point the load carrying capacity of the building was brought down drastically and the building failed.

5.2.3 Curvature Demand under Pushover Loading

This section discusses the curvature ductility, μ , at beam and column member ends due to pushover loading to a maximum roof displacement of 15.7 inch which represents 2% roof drift. The baseline model (beam with hinges) element formulation which includes inelastic fiber-sections at both ends of the member is used to simulate the response of beams and columns. Thus, curvature ductility demands are the curvature ductility demands at these sections. Curvature ductility demand is defined as,

$$\mu = \frac{\phi_{\max}}{\phi_{\text{yield}}} \quad (\text{Eq. 5.2})$$

Where, ϕ_{yield} is computed from the moment curvature relations for the sections by drawing a horizontal line at the point of maximum moment and then drawing a line passing through the origin with the initial slope to intersect the horizontal line at ϕ_{yield} and M_{yield} as shown in Figure 5.5.

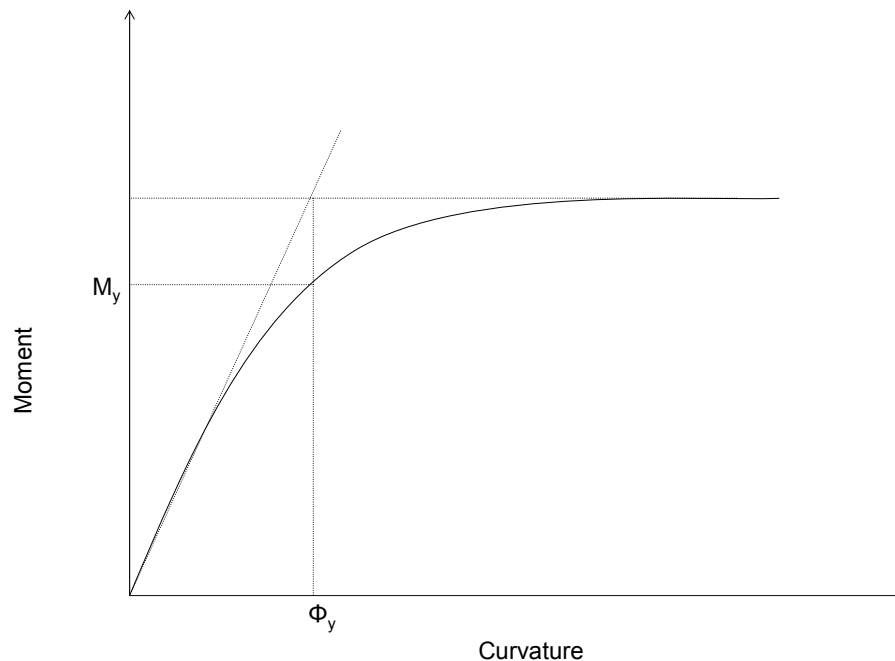
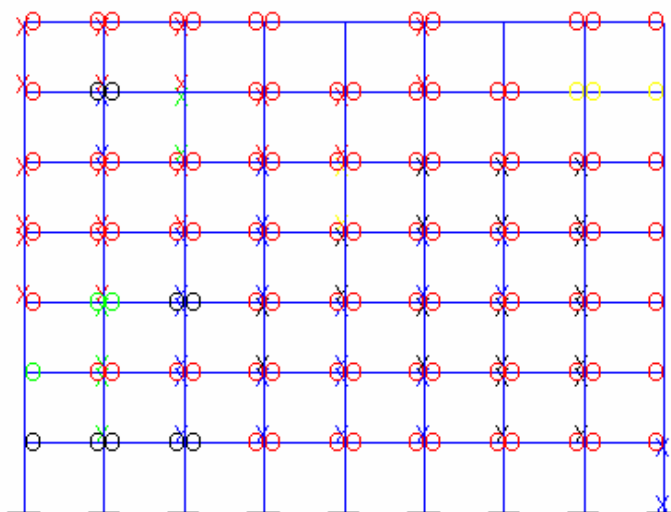
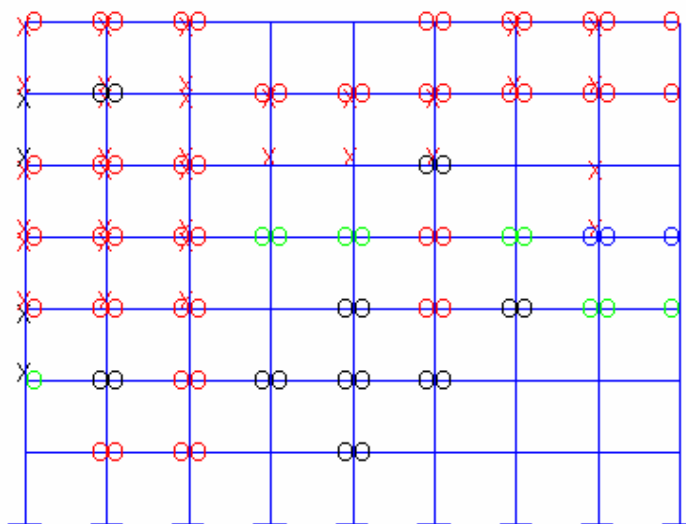
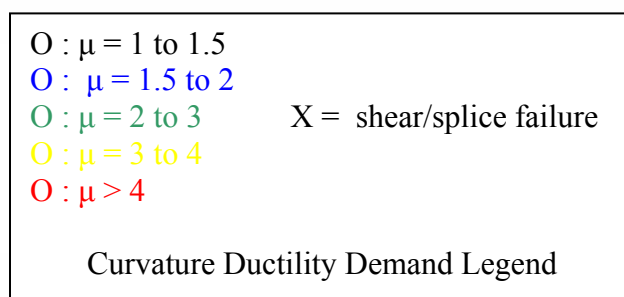


Figure 5.5 Plot of Moment vs. Curvature showing the Yield Moment and Yield Curvature

Curvature ductility demands are presented in a graphical format in Figures 5.6a and Figure 5.6b. Two dimensional representations of the interior and exterior frames are presented which show the curvature ductility demand and the yielding sequence obtained from the pushover analysis of the baseline model for the FEMA 356 load distribution using OpenSees. For the case of a non-ductile column failure (splice or shear failure), curvature ductility is computed as above and the maximum moment compared with the yield moment to check for ductile/non-ductile failure and an “X” is used to indicate a non-ductile failure mode. “O” at member end indicates that a ductile hinge has been formed at that end. It was observed that the exterior frame experienced more damage than the interior frame. Beams exhibited large curvature ductility demands and many columns, especially those on the upper stories, exhibited shear failure with large drift demands.



a) Exterior Frame



b) Interior Frame

Figure 5.6 Frame Member Curvature Ductility Demands at 2% Roof Drift for the Base model

5.3 Nonlinear Dynamic Analysis

The dynamic analysis procedure is the calculation of the building response when subjected to ground excitations. The calculation may be accomplished approximately by direct integration methods which involves the solution of the following equation of dynamic equilibrium by a step-by-step integration procedure

$$M\Delta \ddot{x}(t) + C\dot{x}(t) + K\Delta x(t) = \Delta P(t) \quad (\text{Eq. 5.3})$$

The accuracy of the solution depends on the integration time step, Δt , chosen for analysis. An accurate analysis often requires the use of a very small time step, which increases the computational effort significantly. In addition, the stiffness matrix needs to be updated every time that the stiffness of one or more elements changes. The consequent increase in the computational effort makes inelastic dynamic analysis procedures less attractive for seismic evaluation purposes. However, this procedure provides a better representation of the seismic response than the static procedures. Thus a better assessment of the likely performance of the structures during a probable major seismic event can be made using nonlinear dynamic analysis. In addition, the calculated displacement time histories are invaluable for validation of the models, by comparing the calculated response with the measured response. In this section, the results of time-history analyses performed on the case study for the baseline model using OpenSees are presented. The main objective of these analyses is to evaluate the accuracy of the inelastic modeling procedures used to compute the seismic response and failure modes of the building during the 1994 Northridge earthquake. In the current analyses Newmark integration procedure has been used to solve the above equation with a time step equal to 0.02 seconds. The earthquake record too had a time step of 0.02 seconds.

5.3.1 Responses Calculated using Nonlinear Dynamic Analysis

Dynamic analysis was performed using the baseline model with the acceleration recorded at the base of the case study building during the 1994 Northridge earthquake used as the input ground motion. Figure 5.7 plots the ground motion record used in the

analyses of the 2-D baseline model consisting of both the interior and the exterior frame in the longitudinal (East-West) direction. Significant long-period pulses are not apparent. Responses were calculated at each floor level. Figure 5.8 plots the corresponding spectral accelerations for 5% damping.

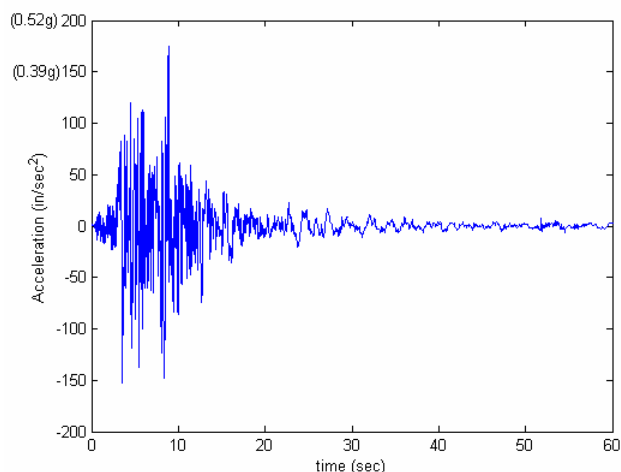


Figure 5.7 Northridge Ground Motion

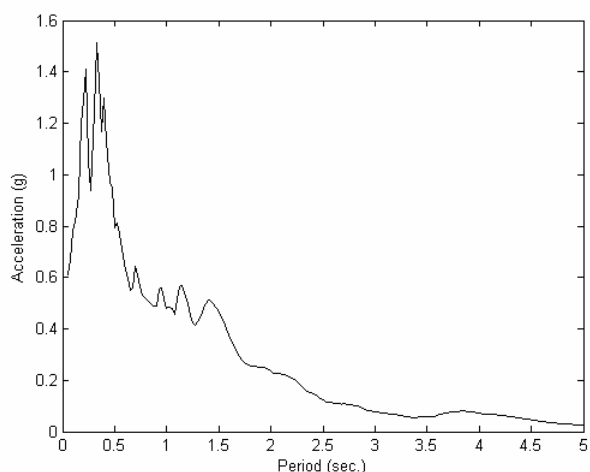


Figure 5.8 Response spectrum ($\xi=5\%$)

The analyses were conducted for the first 60 seconds of the Northridge record and using 5 percent viscous damping as discussed in Chapter 3. The calculated displacement time history is shown in Figure 5.9.

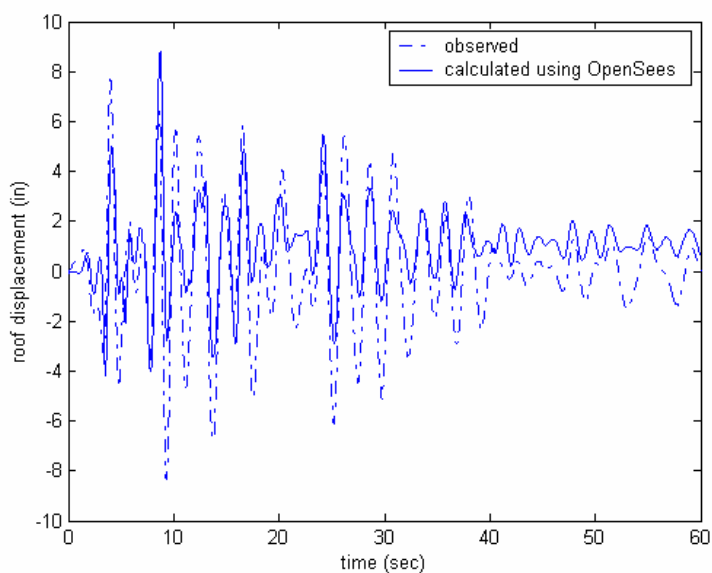


Figure 5.9 Observed and Calculated Roof Displacements using the Base model

The maximum roof displacement observed was around 8.35 inches (<http://www.peertestbeds.net>) and that obtained from the OpenSees baseline model is 8.82 inches. Figure 5.10 shows the story displacements for each story obtained from the dynamic analyses of the baseline model at maximum roof displacement. Dynamic analysis was also done for the non linear beam column element formulation and for different failure models discussed in Chapter 4. The time history results of the roof displacement obtained from each of these analyses have been compared to the observed data and the error between the observed and the simulated data are tabulated in Table 5.2. The error has been defined as

$$\text{Error} = \sqrt{\sum_{\text{time}} \left\{ \frac{[(d_{\text{roof},t})_{\text{obs}} - (d_{\text{roof},t})_{\text{simulated}}]}{\max(d_{\text{roof,observed}})} \right\}^2} \quad (\text{Eq. 5.4})$$

Where, $d_{\text{roof},t}$ is the displacement of the roof at time t .

Table 5.2 Error in Estimation for Different Models

| Model Type | Error |
|--------------------------------------|---------------|
| Beam with hinges/ Splice-UCSD | 13.388 |
| Beam with hinge/ Splice-FEMA 356 | 16.7323 |
| Beam with hinges/ Splice-ACI | 13.7536 |
| Beam with hinges/ Splice-no- Shear | 13.7536 |
| Beam with hinges/ No-Splice-no-Shear | 13.633 |
| Non linear beam column/ Splice- UCSD | 14.2314 |

It was observed that the baseline model showed the least error among all the different models and hence choosing it as the baseline model is appropriate.

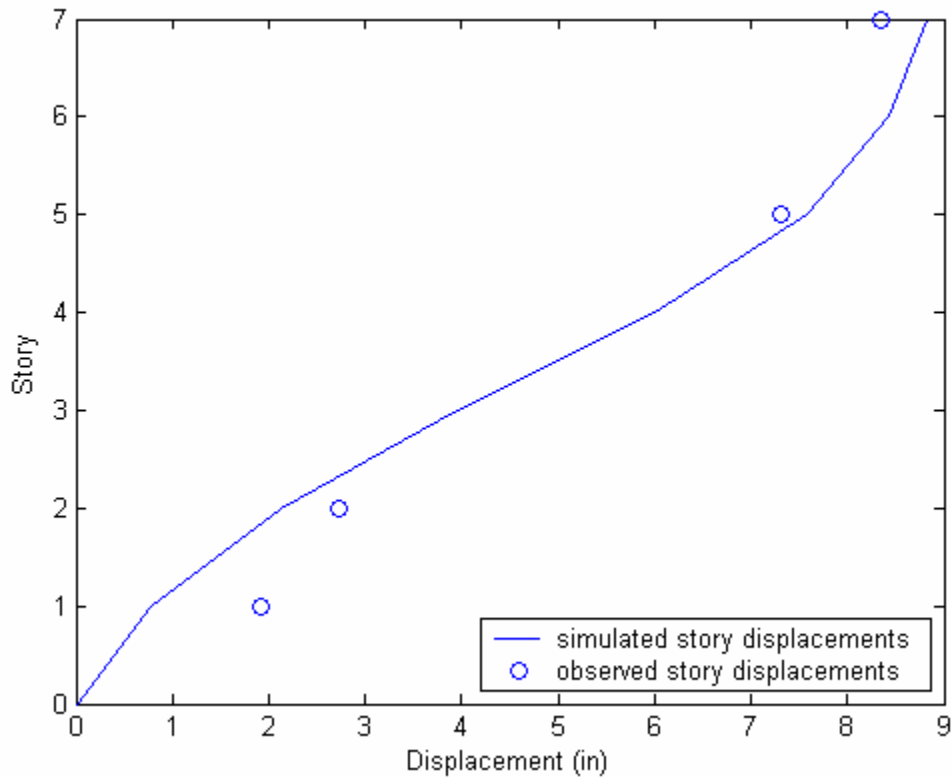
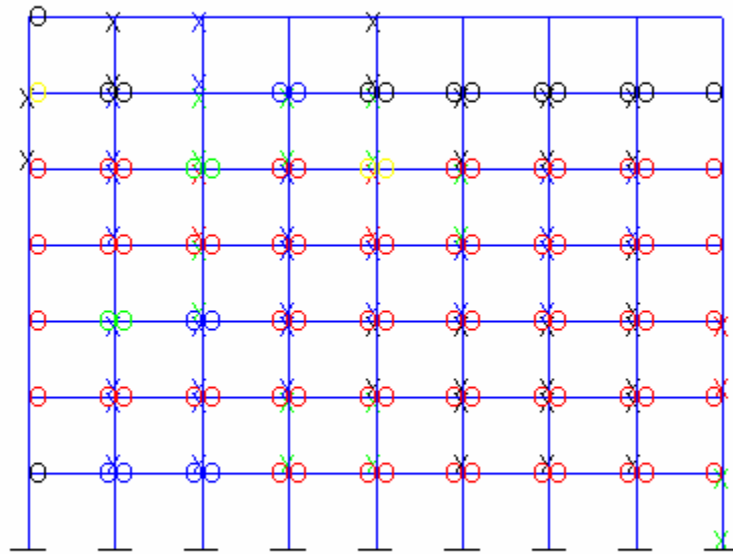
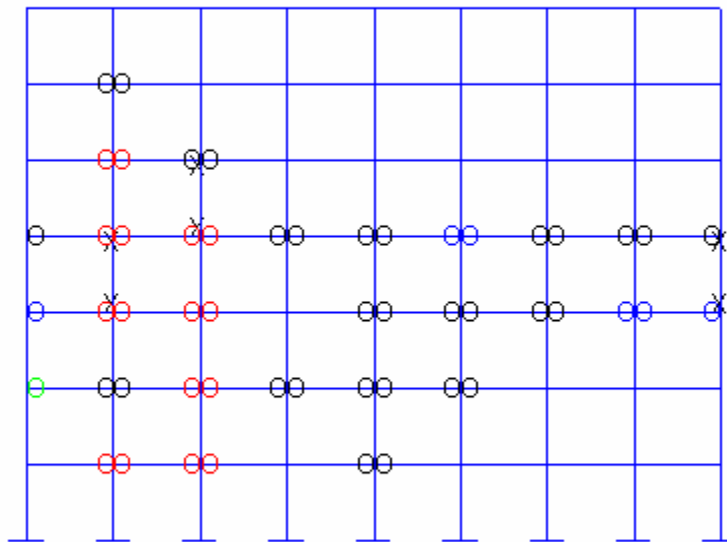


Figure 5.10 Plot of Story displacements for base model at maximum roof displacement

As with the pushover analyses, evaluation of the distribution and magnitude of local ductility demands developed under dynamic loading provides additional understanding of structural behavior. Figure 5.11a and Figure 5.11b show the maximum ductility demands developed under dynamic loading of the interior and the exterior frame for the baseline model. As was observed in pushover analysis the exterior frame experienced more inelastic deformation compared to the interior frame. There wasn't much damage done to the columns except for a few columns failing in shear on the fourth, fifth and upper stories and few on the second story of the exterior frame. The beams however experienced more damage (flexural failure) compared to the column.



a) Exterior Frame



b) Interior Frame

Figure 5.11 Frame Member Curvature Ductility Demands under Northridge Earthquake

Figures 5.12 and 5.13 show the moment curvature diagrams of some of the typical column elements under the Northridge earthquake for the baseline model. Figure 5.12

shows a typical ground story column (column on the first bay, external frame) which is not yielding under the dynamic loading imposed by the Northridge earthquake. The yield moment of the column section was found to be around 4990 kip.in from the preliminary moment curvature analysis that was done to all the column and beam sections of both the interior and the exterior frame.

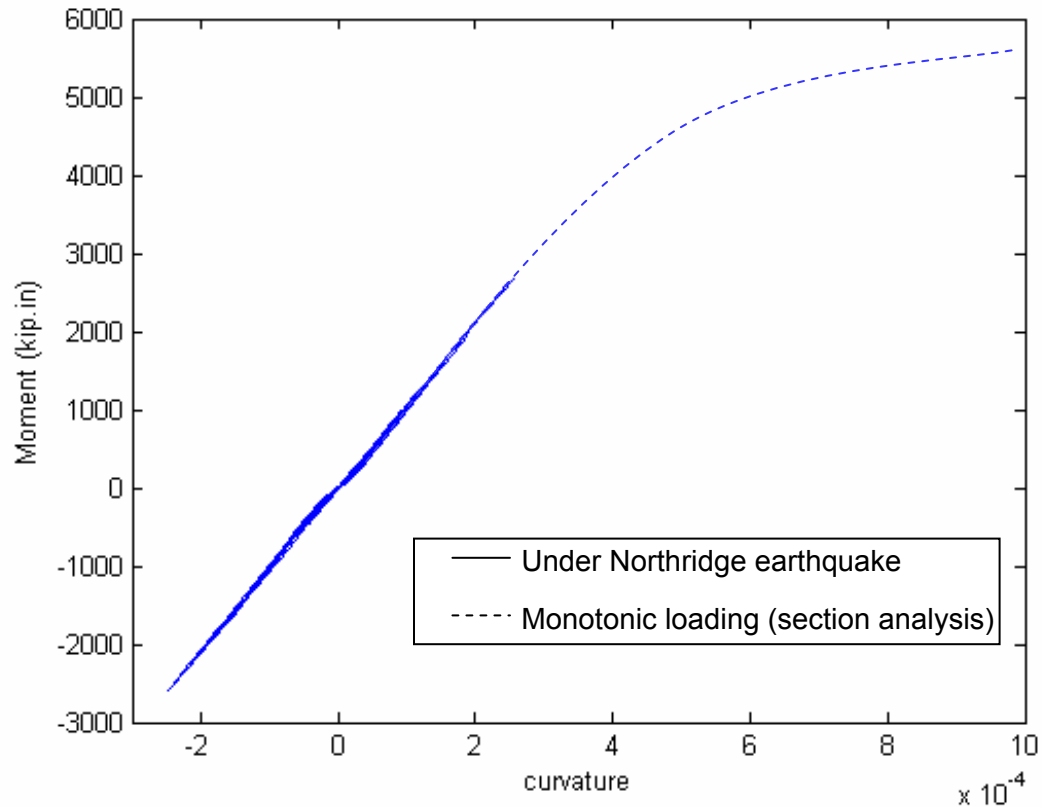


Figure 5.12 Moment Curvature Response of a Typical Non-Yielding Column on the Ground Floor under Northridge Earthquake

Figures 5.13a and 5.13b show the typical moment curvature response of a yielding column on the fifth story just before and just after the column fails. As was noted in Chapter 3 (Figure 3.2) the columns for the baseline model shows a brittle shear failure and hence just after the column reaches the yield curvature there is a very drastic brittle failure occurring in the columns in this story. The yield moment for this column was found to be around 1290 kip.in

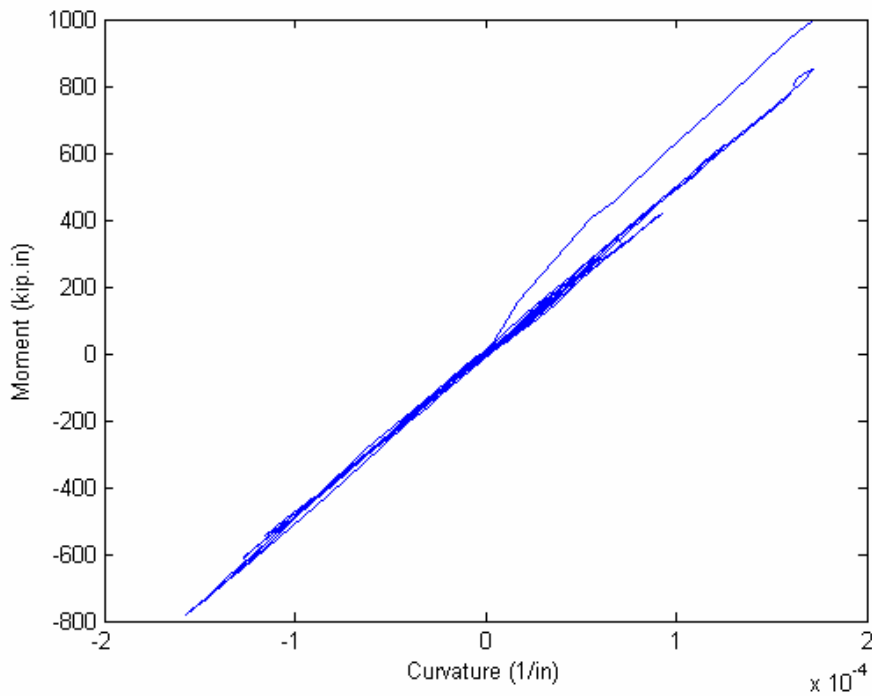


Figure 5.13a Moment Curvature Response of a Typical Column on the Fifth Story just before Yielding under the Northridge Earthquake

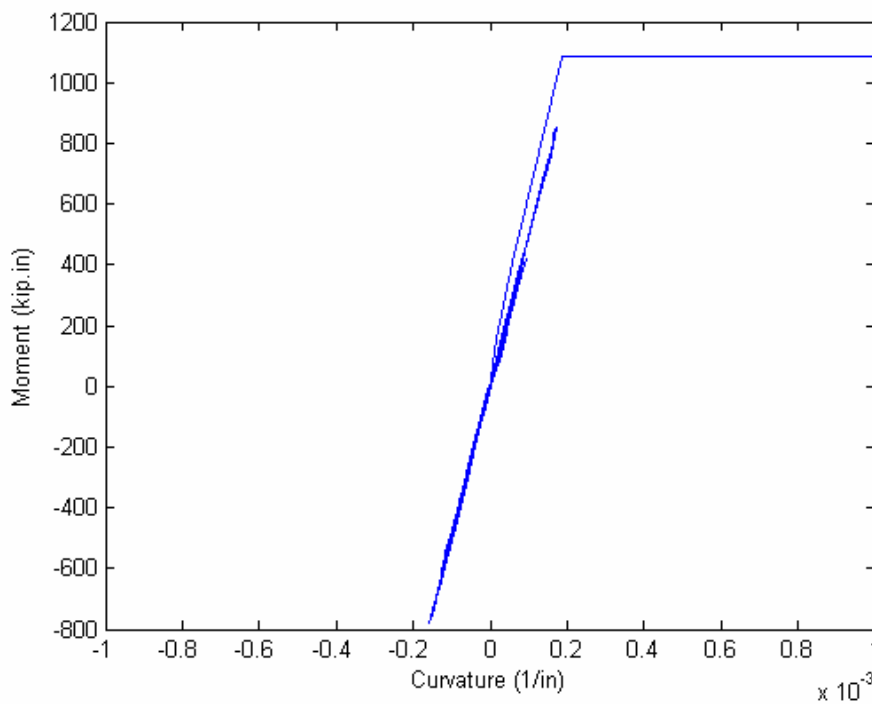


Figure 5.13b Moment Curvature Response of a Typical Column on the Fifth Story just after Yielding under the Northridge Earthquake

5.3.2 Damping Induced Spurious Forces

Recent research by Bernal (1994) suggests that for structural systems that have zero-mass degrees-of-freedom, such as the rotational degrees-of-freedom in typical building and bridge structures, spurious damping forces may be introduced into the system and that the magnitude of these forces increases with the level of viscous damping. In particular the noted behavior derives from the damping mechanism's reaction to the tendency of coordinates with small inertias to undergo abrupt changes in velocity when the tangent stiffness changes. Thus, high levels of viscous damping in higher modes may not be desirable. Checks have been done to ensure that the spurious forces due to the high level of damping in the higher modes are not unreasonable. Figure 5.14 shows spurious moments (ratio of the time difference in the moments in the beam and column to the moment in the beam at the node) introduced at rotational degrees-of-freedom for the baseline model for the damping levels shown in Figure 3.6 for the Northridge earthquake.

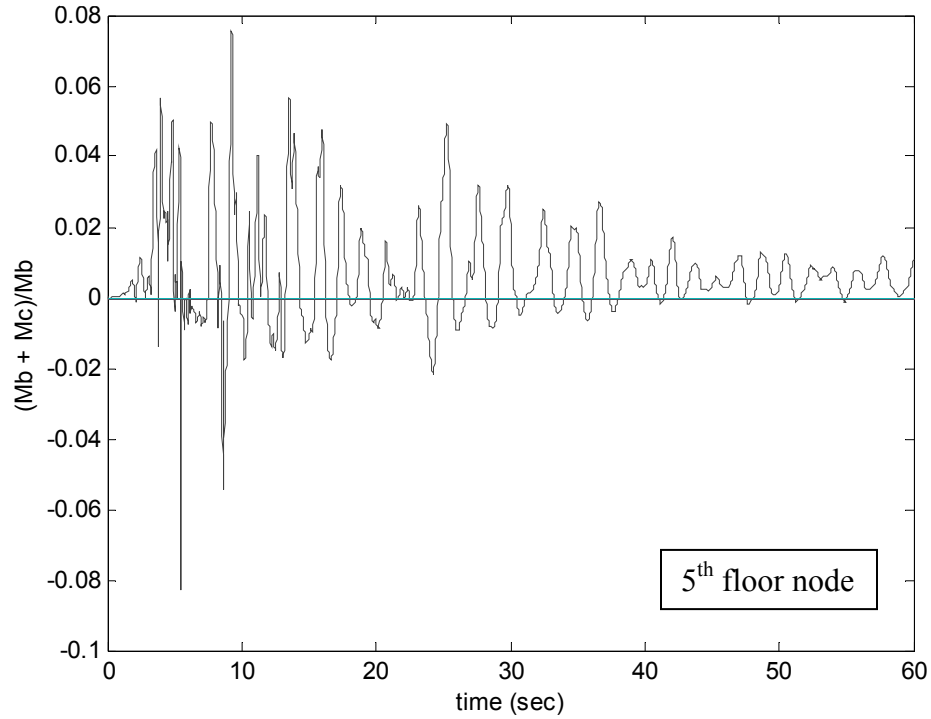
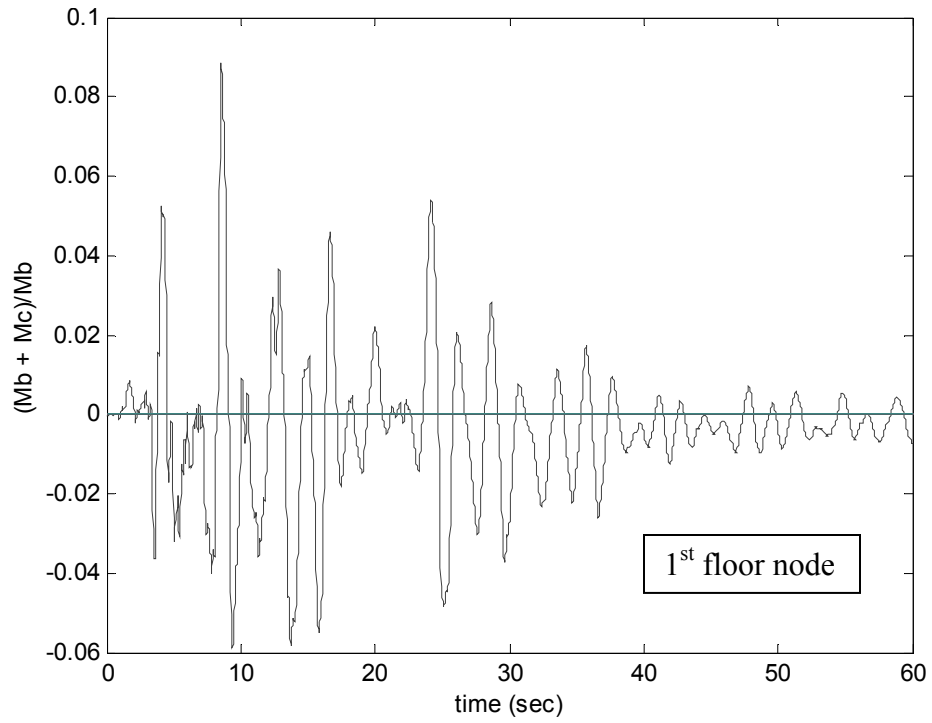


Figure 5.14 Typical Spurious Moments in Rotational Degrees of Freedom due to Damping

5.3.3 Equivalent Viscous Damping

Gulkan and Sozen (1974) idealized the behavior of an inelastic structure as an elastic substitute structure with a lower effective stiffness and higher effective damping, which accounts for hysteretic energy dissipation and initial viscous damping.

Using a single degree of freedom substitute structure and the measured acceleration time history at roof of the case study building during the San Fernando earthquake, Hart (1975) computed the effective viscous damping levels for the case study building. He found that the damping varied between 9.7% and 16.4%. Several researchers have computed the effective damping for similar older reinforced structures and found a similar range of effective damping values (Chopra, 2000).

To compare these values with the total damping induced through hysteretic and viscous damping in the current model, a multi-degree of freedom substitute structure model of the structure was developed to best fit the response predicted by the baseline model. The substitute structure is a model of the building with elastic, effective stiffness elements. The effective stiffness of the substitute model was defined to match the first mode period of the baseline model. The best fit model minimized the sum of the differences of the story displacements at the point of maximum roof displacement. The effective viscous damping was found to be 14.5 %.

CHAPTER 6

INFLUENCE OF MODELING PARAMETERS

Simulating the earthquake response of reinforced concrete structures using nonlinear hysteretic models has been the focus of many previous research efforts; recent examples include Pincheria and Jirsa (1992), Li (1996), Lepage (1997), Hueste and Wight (1997). The results of these studies show that in developing a model an analyst must choose between many plausible options, and, as a result, it is possible to have wide dispersion in simulation data. This chapter investigates the influence of modeling parameters and assumptions on simulated building response. A preliminary investigation considered multiple model parameters and the effect of these parameters on predicted response to pushover and dynamic loading under the Northridge earthquake ground motion. The results of this preliminary study indicated six parameters that have the most significant effect on building response. A second investigation was considered in which the variation in predicted response due to varying these six parameters was compared with the variation in response due to ground motion input. Here only 6 ground motion records, representing three hazard levels, were considered. Finally, a third investigation was conducted to evaluate the effect of column shear strength on predicted response. In this study 30 ground motion records representing 3 hazard levels were considered.

6.1 Study Number One

The properties of the baseline model used in the investigation are tabulated in Table 6.1. The different parameter models considered for preliminary investigation and their properties (compared to the baseline model) are tabulated in Table 6.2. The different parameter models considered are named M1, M2, etc. and are tabulated in the first column of Table 6.2.

Table 6.1 Properties of the Base model

| Modeling Parameters | Baseline Model Property |
|----------------------------|--------------------------------|
| Element formulation | Beam with hinges |
| Failure model | Splice-UCSD |
| Damping | 5% |
| P-delta effects | No |
| Global solution tolerance | 1.00e-08 |
| Hinge length | Frame member depth |
| Effective slab width | 0.5 |
| Joint type | Rigid |
| Steel type | Menegotto-Pinto model |
| Concrete strength | Actual strength |
| Crushing strength factor | 0.8 |
| Foundation | Rigid |

Table 6.2 Properties of the Different Parameter models Considered

| Model type | | Parameter model property differs from baseline model as follows | Baseline model property |
|---------------------------|--------------------------|------------------------------------------------------------------------|-----------------------------------------------------------|
| Global Parameters | $\xi = 2\%$ (M1) | Damping = 2% | Damping = 5% |
| | $\xi = 10\%$ (M2) | Damping = 8% | Damping = 5% |
| | p-delta (M3) | Including P-delta effects | Excluding P-delta effects |
| | $\delta = 10^{-10}$ (M4) | Global solution Tolerance = 1.00e-10 | Global solution tolerance = 1.00e-08 |
| Element Level Parameters | nlbc (M5) | Element formulation = non linear beam column | Element formulation = beam-with-hinges |
| | $l_p = 0.5d$ (M6) | Hinge length = 0.5* frame member depth | Hinge length = frame member depth |
| | $\alpha = 0.22$ (M7) | Effective slab width = 0.11 | Effective slab width = 0.5 |
| | flexible (M8) | Joint type = flexible | Joint type = rigid |
| Failure Models | M9 | No-splice-no-shear | Splice-UCSD |
| | M10 | Splice-no-shear | Splice-UCSD |
| | M11 | Splice-ACI | Splice-UCSD |
| | M12 | Splice-FEMA356 | Splice-UCSD |
| Material level Parameters | Steel (M13) | Bilinear steel model | Menegotto-Pinto model |
| | Design (M14) | Design concrete strength | Increased strength |
| | $\beta = 0.2$ (M15) | Crushing strength factor = 0.2 | Crushing strength factor = 0.8 |
| Reduced shear strength | reduced (M16) | Shear strength capacity reduced by 20% | Shear strength capacity defined by UCSD model (Chapter 3) |
| Increased shear strength | increased (M17) | Shear strength capacity increased by 20% | Shear strength capacity defined by UCSD model (Chapter 3) |

6.1.1 Global Level Parameters

The global level model parameters characterize the global model analysis procedures. In the current study: the level of viscous damping (ξ), convergence of global solution algorithm, and the way in which p-delta effects are simulated.

Viscous Damping (ξ)

The level of viscous damping is a very important parameter in any dynamic analysis. In the past researchers have used viscous damping values between 2% and 5% of critical damping in their nonlinear models of the case study building. But no criterion has been established regarding the correct damping value for buildings. The baseline model employs a viscous damping of 5%. Two models were chosen to study the effect of damping on predicted response, one had a lower level of damping than the baseline model ($\xi = 2\%$, (M1)) and the other had a higher level of damping ($\xi = 8\%$, (M2)).

P-Delta Effects

The base model (as tabulated in Table 6.1) did not consider the effect of P-delta effects in calculating the building response. A parameter model (pdelta, M3) was chosen which included the P-delta effects in simulating the building response.

Global Solution Tolerance (δ)

The baseline model had a global solution tolerance on the normal displacement increment of, $\delta = 10^{-8}$. A parameter model with the global solution tolerance, $\delta = 10^{-10}$ ($\delta = 10^{-10}$, M4) was chosen to study the effect that the global solution tolerance had on building response.

Results

Pushover and dynamic analyses (using the Northridge earthquake) were done for these four global parameter models and the results were compared with those of the baseline model. Figure 6.1a and Figure 6.1b show the effect that these global level

parameters have on the base shear of the building and the maximum inter-story drifts. Model M1 and M2 did not have any effect on the pushover analysis and hence are not included in Figure 6.1a.

Pushover Analyses

The results of the pushover analyses (Figure 6.1a) show a similar nonlinear mechanisms and failure mechanisms for all of the global level parameter models as observed in the baseline model (discussed in Chapter 5). However, the displacement demand at which these mechanisms develop differs for the various models. It was observed that if p-delta effects are included, the propagation of failure in the fourth and fifth story is slowed and the building maintains load carrying capacity to significantly larger roof displacement levels (1.79% roof drift) than is observed for the baseline model (1.29% roof drift). For model M4 however, the first shear failure in the ground story column at 2.9 inches (0.37% roof drift) was followed by another ground story column failing in shear at 4.8 inches (0.41% roof drift) at which point the majority of the beams on the fourth and fifth floor showed flexure failure, which led to a reduced strength of the building (Figure 6.1a). This was followed by the shear failure in the columns on the fourth and fifth floor which eventually led to the building collapse at around 13 inches (1.65% roof drift) of roof displacement.

Dynamic Analyses

For the dynamic analyses, it can be seen from Figure 6.1b that damping is the parameter that affects the building response the most. For the model with $\xi = 2\%$ (M1), the building experienced a shear failure in all the columns on the fifth floor and showed a maximum roof displacement of about 22.65 inches (2.87% roof drift) while for the baseline model, with $\xi = 5\%$ roof displacement was observed to be 8.82 inches (1.12% roof drift) under the Northridge earthquake. For model with $\xi = 8\%$ (M2), the maximum roof displacement was predicted to be 7.95 inches (1% roof drift). Including p-delta effects (M3) and reducing the global solution tolerance (M4) did not have a significant

effect on the observed maximum roof displacement, although, reducing the global solution tolerance shifted the maximum inter-story drift from the 4th story to the 3rd story.

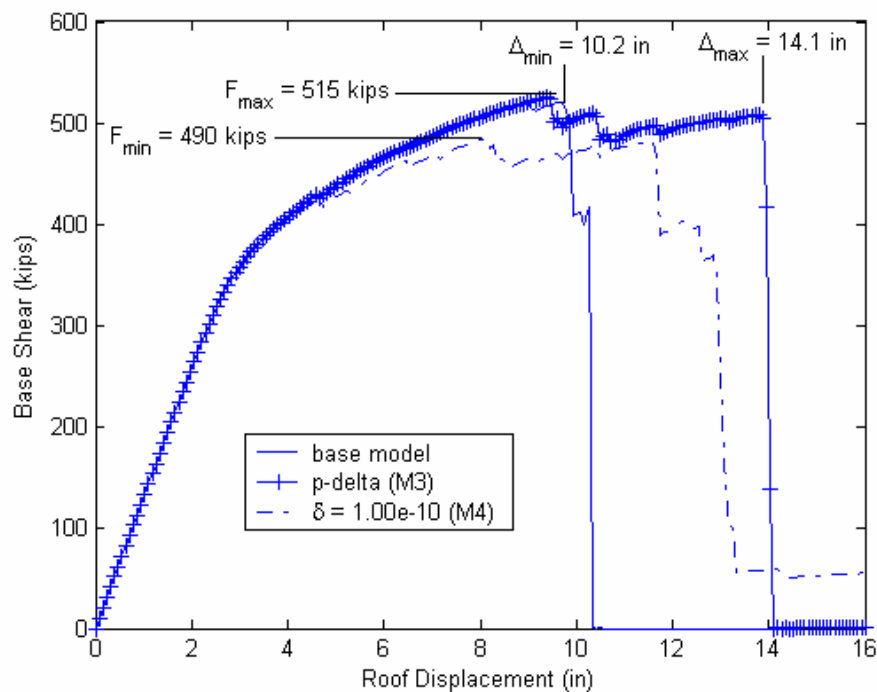


Figure 6.1a Pushover Analysis - Effect of **Global Level Parameters**

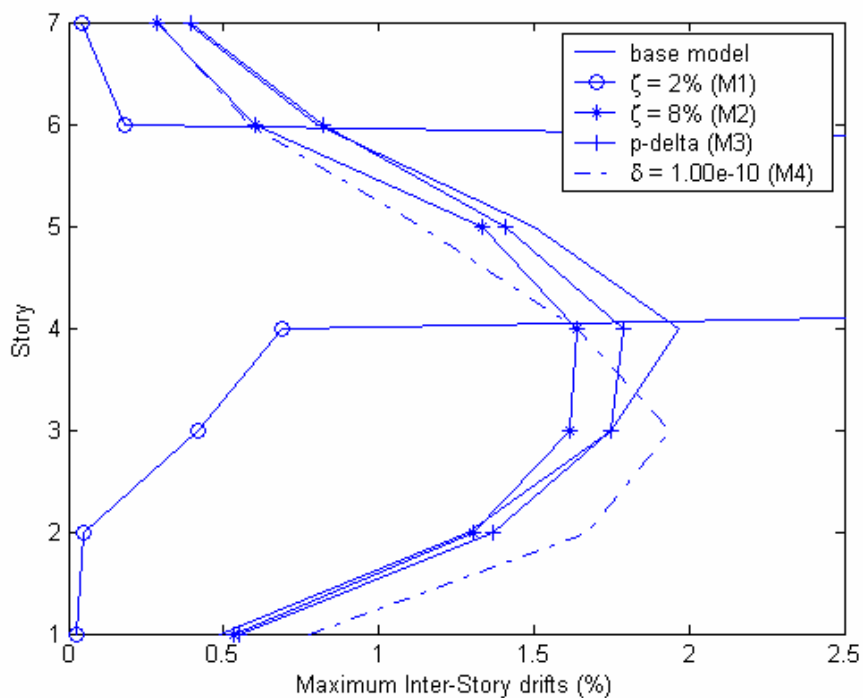


Figure 6.1b Dynamic Analysis - Effect of **Global Level Parameters**

6.1.2 Element Level Parameters

The sensitivity of building response to variation in four parameters that determine how the behavior is modeled at the element level was investigated. The parameters considered included the nonlinear beam column element (nlbc, (M5)), the plastic hinge length (l_p , (M6)) used in the beam-with-hinges element formulation, effective slab width (α , (M7)) and the joint type used.

Element Formulation – Nonlinear Beam Column

The baseline model of the case study building uses a force-based, lumped-plasticity element formulation. To study the effect that element formulation has on the simulated response of the building, a model that uses the OpenSees nonlinear beam-column element formulation (nlbc, (M5)) was created. The nonlinear beam column element formulation considers the spread of plasticity through out its length (discussed in Chapter 3). The number of integration points for nonlinear beam-column model was set as four for the beams and five for the columns.

Hinge length

The baseline model uses a beam-with-hinges element formulation. This element formulation requires the user to choose an appropriate hinge length. In the base model, this length is chosen to be equal to the element depth. However, many researchers have proposed many different equations for defining the plastic hinge length. Park and Paulay (1975), proposed that hinge length be defined as

$$l_p = 0.5d + 0.05z \quad (\text{Eq. 6.1})$$

Where, l_p is the plastic hinge at the end, d is the effective depth of the cross-section and z is the distance from the critical section to the point of contra-flexure. Using Eq. 6.1, the length of the plastic hinge for a typical exterior beam is 24 in. ($\approx d = 24$ in.).

riestley, Seible and Calvi suggested the following equation for the hinge length.

$$l_p = 0.08L + 0.15f_{ye}d_{bl} \geq 0.3f_{ye}d_{bl} \quad (\text{Eq 6.2})$$

Where, L is the distance from the critical section of the plastic hinge to the point of contra-flexure, d_{bl} is the diameter of the longitudinal reinforcement and f_{ye} is the design yield strength for longitudinal reinforcement in plastic hinge. Using Eq. 6.2, the length of the plastic hinge for a typical exterior beam is 28.2 in. ($\approx d = 24$ in.).

To study the effect that varying the hinge length parameter would have on the building response, a model was chosen ($l_p = 0.5d$, (M6)) with hinge length equal to the half the depth of the member.

Slab Width

The baseline model has an effective slab width ratio, $\alpha = 0.5$ (Chapter 3). A model with this parameter equal to 0.22 (Pan and Moehle, 1988) has been chosen ($\alpha = 0.11$, (M7)) to study the effect of slab width on building response under dynamic and static pushover loading.

Joint Type

At the element level one more parameter model with flexible joint (flexible, (M8)) was chosen. The flexible joint model is the model with the center line dimensions of the beam column and with no joint in between them unlike the rigid joint model which has a rigid offset of finite dimension at the beam-column intersection.

Pushover Analyses

Figure 6.2a shows the results of the pushover analyses. The data in Figure 6.2a shows that reduction in the plastic hinge length chosen for the beam-with-hinges element formulation ($l_p = 0.5d$, M6) results in increased stiffness and reduced displacement capacity of the structure. This would be expected since reducing the plastic hinge length increases length of the element that is assumed to respond elastically and reduces the length along which the element is assumed to respond inelastically and thereby increasing stiffness. Also, since the plastic hinge rotation is defined equal to the curvature of the section multiplied by the 50% hinge length; reducing the hinge length reduces plastic rotation by 50%. Thus if curvature ductility controls response, as is the case for non-shear

critical columns and beams, reducing the hinge length reduces also the displacement capacity of the structure. Also, the parameter model with non linear beam column element formulation, M5, and the parameter model with effective slab with $= 0.11$, M7, showed a decrease in the initial stiffness but model with reduced hinge length, M6, showed an increased initial stiffness. The failure mechanisms in pushover analysis for the element level parameter models were similar to the baseline model with a few exceptions. The reduced hinge length model, M6, like the baseline model, showed a shear failure in a ground story exterior column at 2.9 inches (0.37% roof drift) roof displacement but at around 6 inches (0.76% roof drift) there was a shear failure observed in two of the fourth story exterior columns and one ground story exterior column, which significantly reduced the load carrying capacity of the building and eventually led to a total collapse at 11.7 inches (1.48% roof drift). The propagation of shear failures in the columns of the 4th and 5th story for the model with no joint in between the beam-column elements, model M8, was not as drastic as it was for the base model and hence model M8 showed a much larger roof displacement (12 in.) at failure compared to the base model.

Dynamic Analyses

Figures 6.2b shows the results of the dynamic analyses for these different element level parameter models. The model with non linear beam column element formulation, M5, which showed a lesser stiffness in the pushover analysis, showed a correspondingly increased roof displacement under the Northridge earthquake, compared to the baseline model. Similarly the model with reduced hinge length showed a lesser roof displacement compared to the baseline model due to an increased stiffness. Model M7 showed a reduced stiffness due to the reduction in the effective slab width compared to the baseline model and hence showed a larger roof displacement compared to the baseline model. The parameter model with no joint in between the beam-column elements, M8, did not have much effect on the dynamic analysis response.

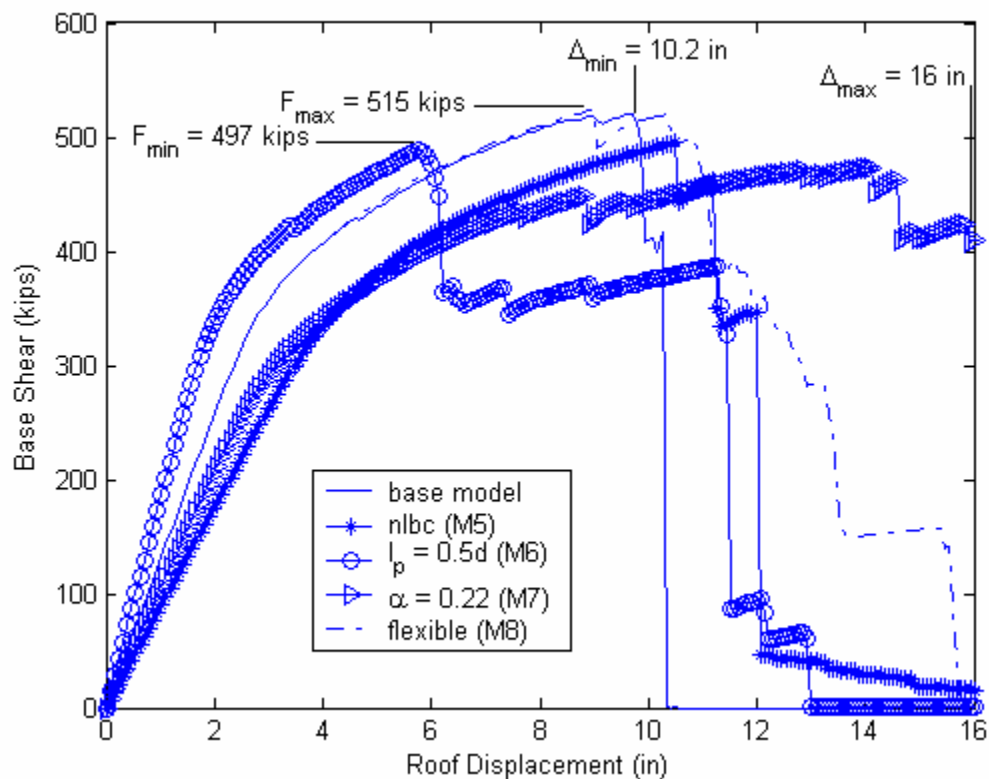


Figure 6.2a Pushover Analysis - Effect of Element Level Parameters

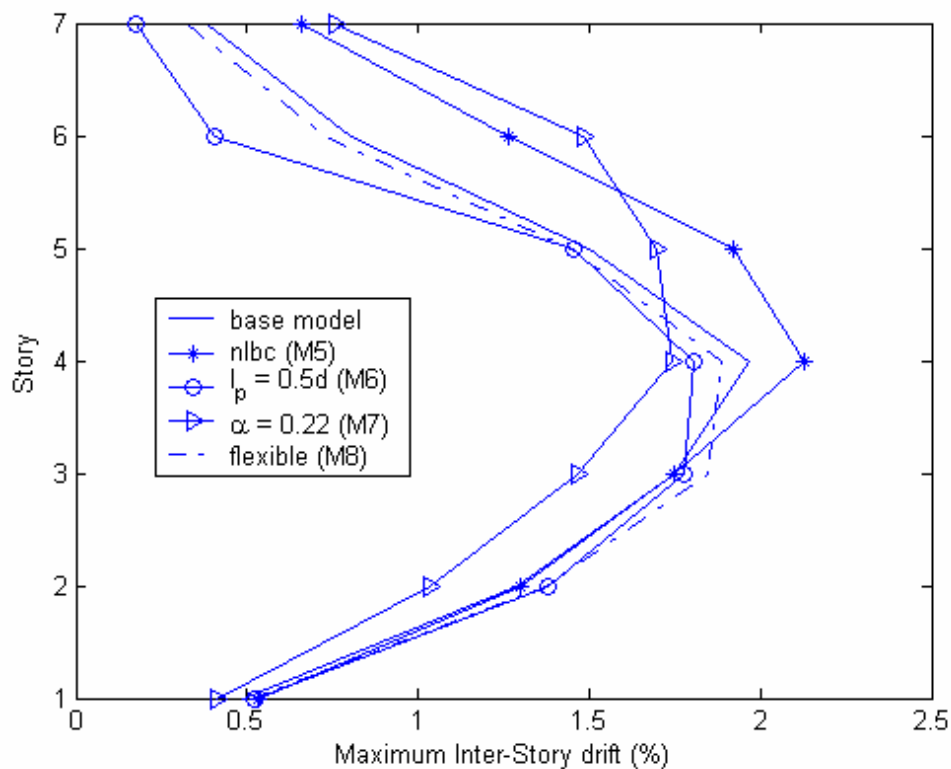


Figure 6.2b Dynamic Analysis - Effect of **Element Level Parameters**

6.1.3 Failure Models

Five different column failure models were considered. The different structural models generated using these different failure models are named: no-splice-no-shear (M9), splice-no-shear (M10), splice-ACI (M11), splice-FEMA356 (M12). The naming scheme reflects the columns failure model employed with the no-splice-no-shear representing neither a failure of the column splices nor shear failure of the columns and with splice-FEMA356 representing column splice failure using the steel model discussed in Section 3.5.1 and the FEMA 356 model for the shear strength discussed in Section 3.5.2. The impact of the failure models on the simulated building response is discussed in this section.

Pushover Analyses

Figure 6.3a shows the results obtained from the pushover analyses performed on the five failure models. Model M9 predicts the maximum base shear for the building and no loss of load carrying capacity until a roof displacement of 39 inches (4.94% roof drift) at which the ground story exterior columns fail in flexure. Models M10 and M11 showed failure mechanism which were similar to each other; splice failure in all the exterior columns of the first story. Both the models predict similar base shear versus roof displacement histories, with a maximum base shear capacity of approximately 550 kips and loss of load carrying capacity occurring at a roof displacement of 11.8 inches (1.5% roof drift). For Model M12, which is the most conservative of all failure models, showed the first shear failure in the ground story column at a roof displacement of 2.6 inches (0.33% roof drift) which was subsequently followed by two more columns, one on the fourth floor and one on the fifth floor failing in shear. Model M12 shows a much higher ductility compared to the baseline model with loss of load carrying capacity occurring at a roof displacement of 16 inches (2.1% roof drift) due to the failure of all the exterior columns on the fourth and fifth story. Model M12 predicts the base shear strength capacity of the building that is substantially less than that predicted by other models (430

kips), this is because the FEMA 356 recommendations used to define the shear failure model for model M12 are very conservative (Section 3.5.2)

Dynamic Analyses

Figure 6.3b shows the results obtained from the dynamic analyses performed using the five different structural models. For the non-linear dynamic analysis using Northridge earthquake there was not much difference in the roof displacement observed for the different models. Model M9 was the one to predict the smallest roof displacement of 8.41 in. (1.07% roof drift). This is because there was not any damage done to any of the column elements of model M9 and hence the impact of the earthquake on it was less and since the earthquake intensity wasn't too big to induce shear/splice failures in majority of the columns, there is not a noticeable difference observed between the models in terms of the roof displacement (coefficient of variation = 0.018).

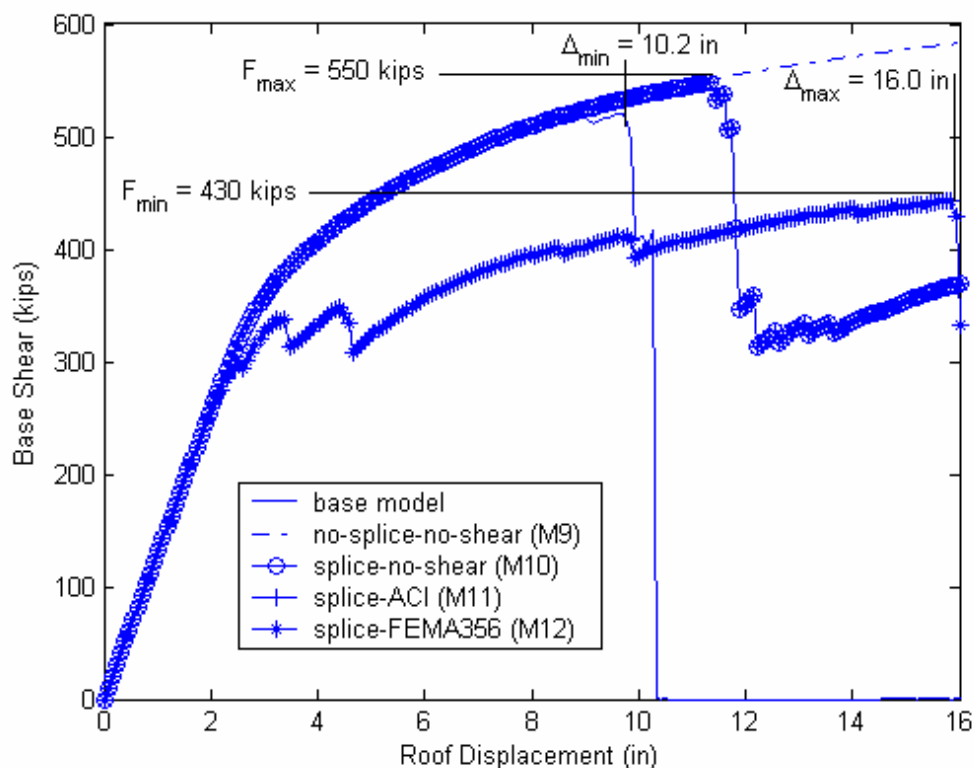


Figure 6.3a Pushover Analysis - Effect of Failure Models

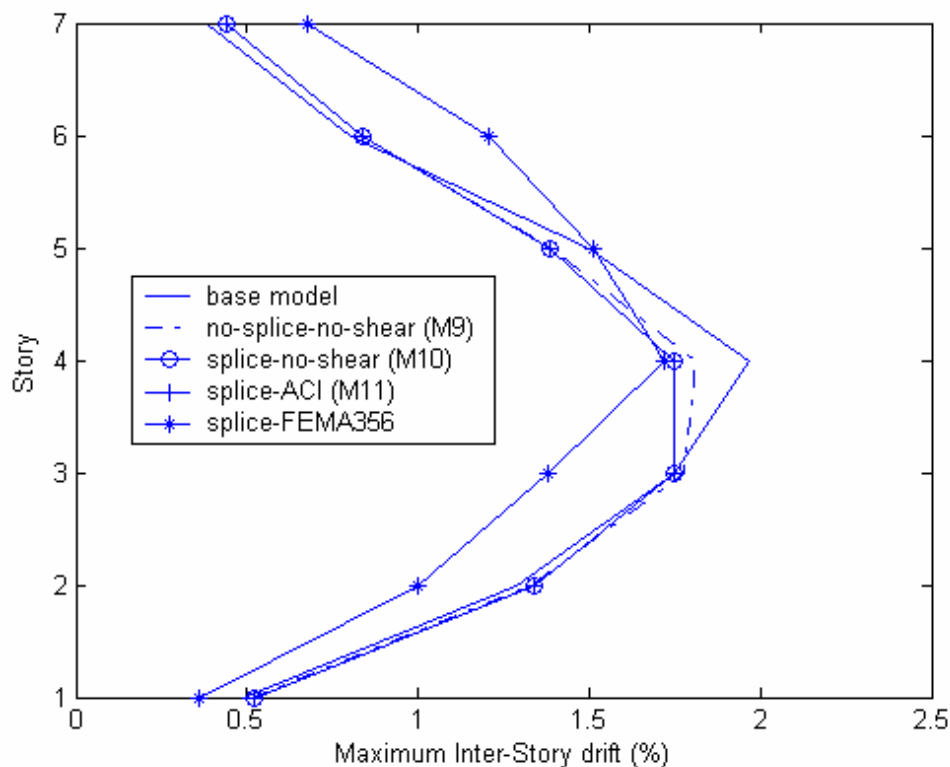


Figure 6.3b Dynamic Analysis - Effect of Failure Models

6.1.4 Material Level Parameters

The material level parameters determine the way in which material stress-strain response is simulated. Parameters considered in the study include: stress-strain response for steel, concrete strength and concrete crushing strength factor.

Steel01

The baseline model uses the OpenSees *Steel02* model which simulates the Bauschinger effect using the Menegotto-Pinto curves (Section 3.4.2). A model is developed (steel, M13) using the OpenSees *Steel01* model; this model is a simple bilinear model and does not represent Bauschinger effect.

Concrete Strength

The baseline model uses the recommendations of FEMA 356 to account for the typical over strength observed in concrete due to age and over strength at the time of casting. The base model employs over strength factors to represent these typical over strengths observed (discussed in Chapter 3). To see the impact of these over strength factors on the simulated building response, a parameter model (design, M14) was chosen which did not account for these over strengths.

Crushing Strength

The residual strength of concrete after crushing of concrete has taken place is defined by the crushing strength factor. Crushing strength factor is the ratio of the residual strength of concrete to the peak concrete compressive strength. The baseline model considered has a crushing strength factor of 0.8. To see the impact of residual concrete strength on the simulated building response a parameter model was chosen with a lower crushing strength factor ($\beta = 0.22$, M15).

Pushover Analyses

Figure 6.4a shows the effect that these material level parameters have on the base shear. The parameter model with lower concrete strength, M14, was found to affect the simulated building response the most. As expected the decrease in strength is depicted in the pushover curve where the pushover curve for model M14 shows a smaller stiffness than the baseline model due to reduced strength of its materials. The parameter model with decreased crushing strength factor, M15, because of its lower ultimate concrete strength than the baseline model showed a smaller base shear. The failure mechanisms observed were similar for all the material level parameter models.

Dynamic Analyses

Figure 6.4b shows the results of the dynamic analyses of the material level parameter models. Significant variation was not observed in the simulated response of the

building due to material level parameter variation. The coefficient of variation in the maximum roof displacement was found to be 0.055.

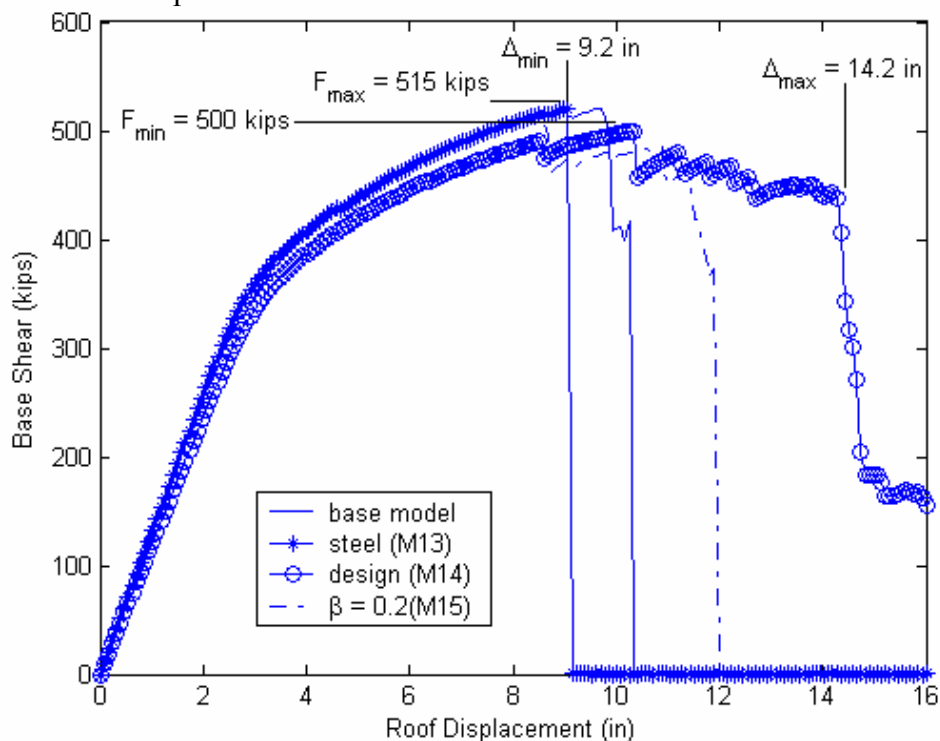


Figure 6.4a Pushover Analysis - Effect of Material Level Parameters

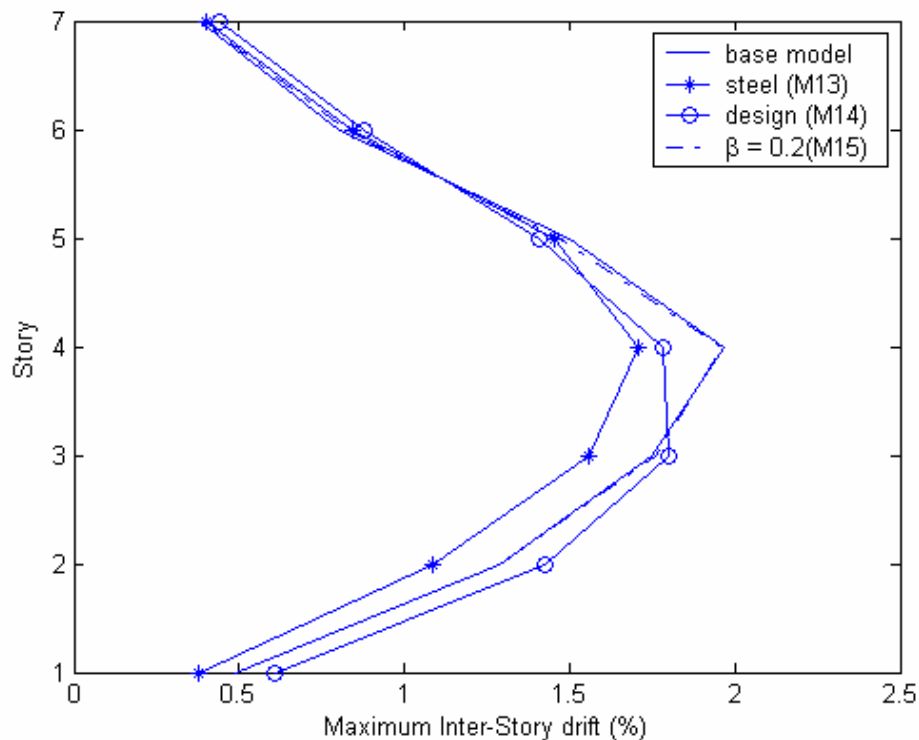


Figure 6.4b Dynamic Analysis - Effect of Material Level Parameters

6.5 Statistics of the Preliminary Parameter Study

Table 6.3 shows the statistics of the preliminary parameter study using the pushover analysis. It was found that, for all the parameter models considered, the mean base shear was 505 kips and the mean roof displacement at collapse was 12.56 in. There was very little variation observed in the maximum base shear across different parameter models but the displacement at collapse had a variation of around 19%.

Table 6.3 Parameter Study – Pushover Analyses

| Model Type | | Base Shear (kips) | Roof Displacement at Collapse (inches) |
|---------------------------------|--------------------------|----------------------|-------------------------------------------|
| Base model | | 515 | 10.2 |
| Global Level Parameters | Pdelta, M3 | 515 | 14.1 |
| | $\delta = 10^{-10}$, M4 | 490 | 13.0 |
| Element Level Parameters | nlbc, M5 | 497 | 12.1 |
| | $l_p = 0.5d$, M6 | 490 | 11.7 |
| | $\alpha = 0.11$, M7 | 497 | 16.0 |
| | Flexible, M8 | 515 | 15.8 |
| Failure Models | nosplicenoshear, M9 | 660 | 39.0 |
| | splicenoshear, M10 | 550 | 11.9 |
| | splice-ACI, M11 | 550 | 11.9 |
| | splice-FEMA356, M12 | 430 | 18.5 |
| Material level Parameters | steel, M13 | 515 | 9.2 |
| | Design, M14 | 500 | 14.2 |
| | $\beta = 0.2$, M15 | 500 | 12.1 |
| Mean* | | 505 | 13.13 |
| C.O.V* | | 0.06 | 0.19 |

* The outlier, model M9 was not taken into account in calculation of the mean and C.O.V. in Tale 6.3.

Table 6.4 shows the statistics of the preliminary parameter study for the dynamic analyses using the Northridge earthquake. The outlier for these analyses was the model which had a damping of 2%, which is not taken into account in the calculation of the mean and the coefficient of variation for the maximum inter-story drifts and maximum roof displacement. It was found that for some of the parameter models considered the fundamental period of vibration was different from that of the base model. No scaling of the ground motion record (Northridge earthquake) has been done to account for this change in fundamental period of vibration. Hence some of the variability observed across different parameter models is attributed to this change in fundamental period of vibration.

Table 6.4 Parameter study – **Dynamic analyses** (Northridge earthquake)

| Model Type | T_A sec | S_A (g) | Maximum inter-story drifts (%) | | | | | | | Roof disp.(in) |
|--------------------------|--------------|--------------|--------------------------------|-------------|-------------|-------------|--------------|-------------|-------------|-------------------|
| | | | 1 | 2 | 3 | 4 | 5 | 6 | 7 | |
| Baseline | 1.56 | 0.41 | 0.48 | 1.28 | 1.75 | 1.97 | 1.50 | 0.81 | 0.38 | 8.82 |
| $\xi = 2\%$, M1 | 1.56 | 0.41 | 0.03 | 0.05 | 0.42 | 0.69 | 20.7 | 0.18 | 0.04 | 22.66 |
| $\xi = 10\%$, M2 | 1.56 | 0.41 | 0.54 | 1.30 | 1.61 | 1.64 | 1.33 | 0.60 | 0.28 | 7.95 |
| pdelta, M3 | 1.56 | 0.41 | 0.55 | 1.37 | 1.75 | 1.78 | 1.41 | 0.82 | 0.39 | 8.75 |
| $\delta = 10^{-10}$, M4 | 1.56 | 0.41 | 0.77 | 1.67 | 1.94 | 1.64 | 1.14 | 0.58 | 0.29 | 8.85 |
| nlbc, M5 | 1.94 | 0.25 | 0.53 | 1.30 | 1.75 | 2.13 | 1.92 | 1.26 | 0.66 | 10.29 |
| $l_p = 0.5d$, M6 | 1.30 | 0.41 | 0.52 | 1.38 | 1.78 | 1.80 | 1.45 | 0.41 | 0.17 | 8.16 |
| $\alpha = 0.11$, M7 | 1.62 | 0.38 | 0.41 | 1.03 | 1.46 | 1.74 | 1.69 | 1.48 | 0.76 | 9.20 |
| flexible, M8 | 1.56 | 0.41 | 0.51 | 1.37 | 1.85 | 1.89 | 1.45 | 0.73 | 0.32 | 8.78 |
| nosplicenoshear, M9 | 1.56 | 0.41 | 0.51 | 1.33 | 1.78 | 1.81 | 1.39 | 0.84 | 0.44 | 8.76 |
| splicenoshear, M10 | 1.56 | 0.41 | 0.52 | 1.34 | 1.75 | 1.75 | 1.39 | 0.84 | 0.44 | 8.69 |
| splice-ACI, M11 | 1.56 | 0.41 | 0.52 | 1.34 | 1.75 | 1.75 | 1.39 | 0.84 | 0.44 | 8.69 |
| splice-FEMA356, M12 | 1.56 | 0.41 | 0.36 | 0.99 | 1.38 | 1.72 | 1.51 | 1.21 | 0.68 | 8.41 |
| steel, M13 | 1.56 | 0.41 | 0.37 | 1.09 | 1.56 | 1.71 | 1.45 | 0.84 | 0.40 | 7.98 |
| design, M14 | 1.63 | 0.38 | 0.61 | 1.43 | 1.80 | 1.78 | 1.41 | 0.88 | 0.44 | 9.07 |
| $\beta = 0.22$, M15 | 1.56 | 0.41 | 0.49 | 1.28 | 1.76 | 1.96 | 1.47 | 0.83 | 0.39 | 8.83 |
| Mean* | | | 0.51 | 1.30 | 1.71 | 1.81 | 1.46 | 0.86 | 0.43 | 8.75 |
| C.O.V* | | | 0.19 | 0.13 | 0.09 | 0.07 | 0.12 | 0.22 | 0.37 | 0.064 |
| Mean† | | | 0.51 | 1.30 | 1.71 | 1.78 | 1.40 | 0.81 | 0.40 | 8.59 |
| C.O.V† | | | 0.21 | 0.13 | 0.09 | 0.06 | 0.073 | 0.20 | 0.27 | 0.04 |

Substantial variation was not observed in the maximum roof displacement predicted using the different parameter models. Maximum inter-story drifts varied more significantly, with the coefficient of variation ranging from 7% to 37%. All except two parameter models predicted the fourth story having the greatest inter-story drift with a mean value of 1.81%. The parameters that were found to have maximum impact on the

* The outlier for these analyses was the model with $\xi = 2\%$ which is not taken into account in the calculation of the mean and C.O.V.

† These are the means and the C.O.V's for the models with $T_A = 1.56$ sec.

simulated building response are damping (coefficient of variations of 61% and 7.34% in simulated maximum roof displacement under Northridge earthquake ground motion for $\xi = 2\%$ and $\xi = 8\%$ respectively), non linear beam column element formulation (coefficient of variation of 10.9% in simulated roof displacement under Northridge earthquake ground motion, coefficient of variation of 2.5% for base shear under pushover type loading and 12% variation in displacement at failure under pushover loading), effective slab width (coefficient of variation of 3% in simulated roof displacement under Northridge earthquake ground motion, coefficient of variation of 2.5% for base shear under pushover type loading and 31.3% variation in displacement at failure under pushover loading), hinge length (coefficient of variation of 5.5% in simulated roof displacement under Northridge earthquake ground motion, coefficient of variation of 3.5% for base shear under pushover type loading and 9.7% variation in displacement at failure under pushover loading), strength of concrete (coefficient of variation of 2% in simulated roof displacement under Northridge earthquake ground motion, coefficient of variation of 2.1% for base shear under pushover type loading and 23.2% variation in displacement at failure under pushover loading).

6.2 Study Number Two

The results of dynamic analyses using different parameter models and the Northridge earthquake ground motion suggest that model parameters have very little effect on predicted response. However, the Northridge earthquake ground motion record corresponds to an earthquake hazard level of approximately 50% probability in 50 years for the case study building. Thus it is conceivable that variation of model parameters will have a more significant effect at higher ground motion intensity levels. To test this hypothesis, dynamic analyses were done using six ground motion records, representing 3 hazard levels, using the six models that showed the most variation for the baseline model under pushover type loading.

Also, to study the impact that these parameters had on a brittle model (baseline model) compared with a flexure model (no-splice-no-shear), these analyses were performed on a flexure as well as a brittle model. In addition to the above chosen parameters, the shear strength of the brittle model too was considered as a parameter to see the effect that it has on the building response. Two models were chosen one which had a 20% reduction in shear strength capacity (reduced, M16) and the other which had a 20% increase in shear strength capacity (increased, M17) compared to the baseline-brittle model. The six ground motions chosen were: *02in50_NR_rosc*, *02in50_NR_vnuy*, *10in50_NR_vnsc*, *10in50_SF_461*, *50in50_SF_466*, *50in50_SF_vnuy* (<http://www.peertestbeds.net>). A detailed discussion of the ground motions is provided in Appendix B.

Figures 6.5 to 6.10 show the results of the parameter study. The figures show the effect of different parameters on the brittle and flexure model for the six ground motions selected for the parameter study. Inter-story drift ratios greater than 10% have been excluded as it is not practical to get drift ratios greater than 10%. Hence, drift ratios greater than 10% are considered to be equal to 10%.

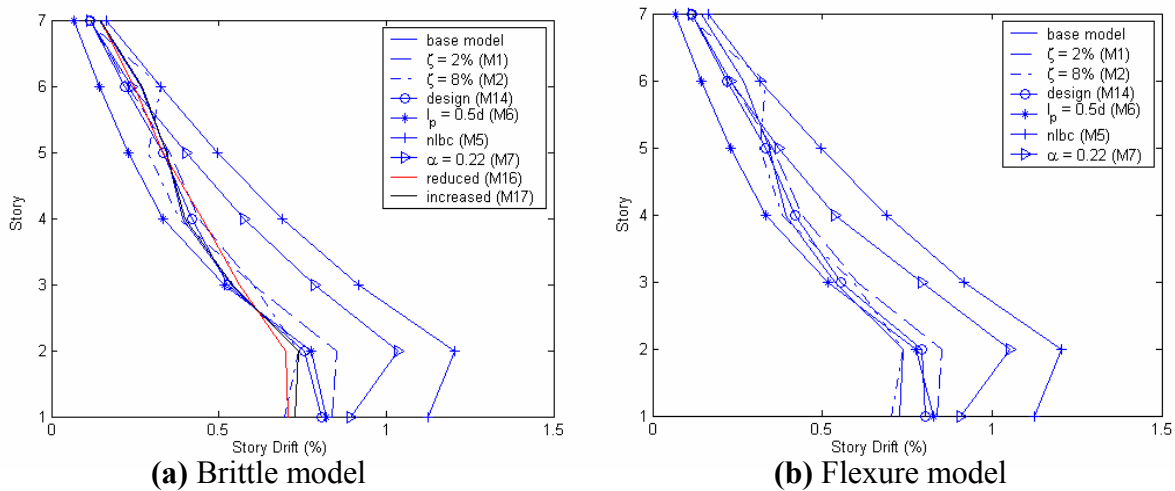


Figure 6.5 Plot of Story drifts for 50in50_SF_vnuy for Different Parameters

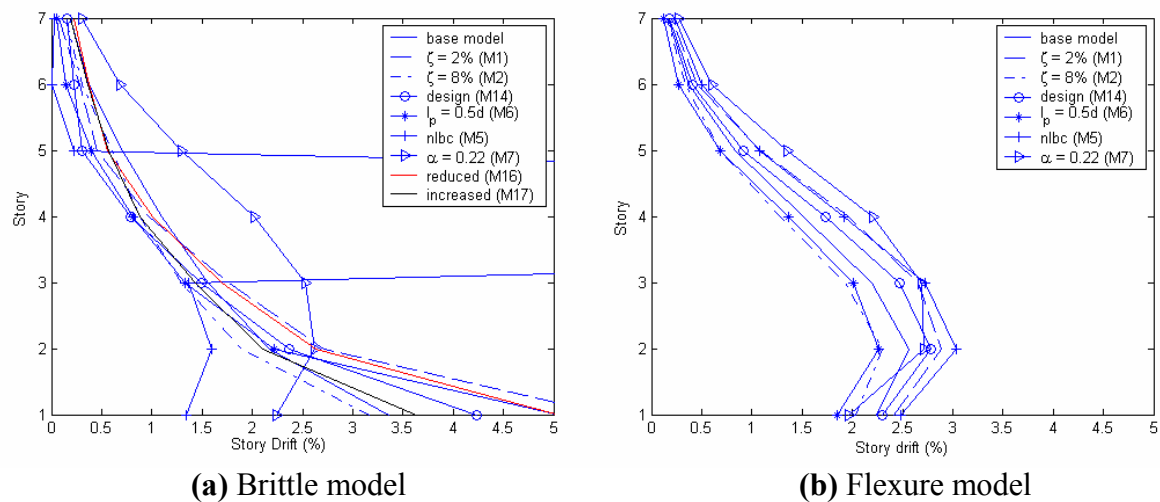


Figure 6.6 Plot of Story drifts for 50in50_SF_466 for Different Parameters

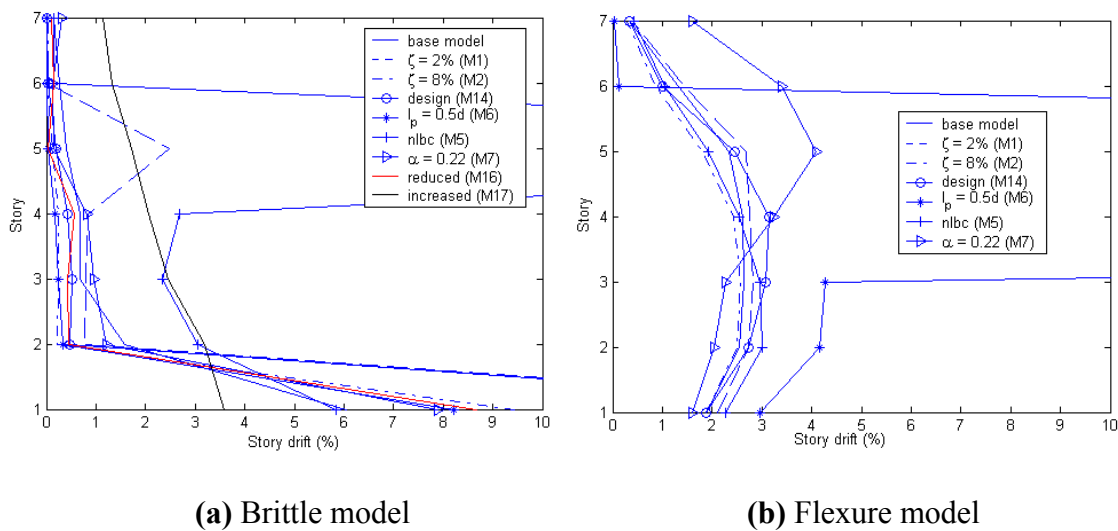


Figure 6.7 Plot of Story drifts for 10in50_NR_vnsc for Different Parameters

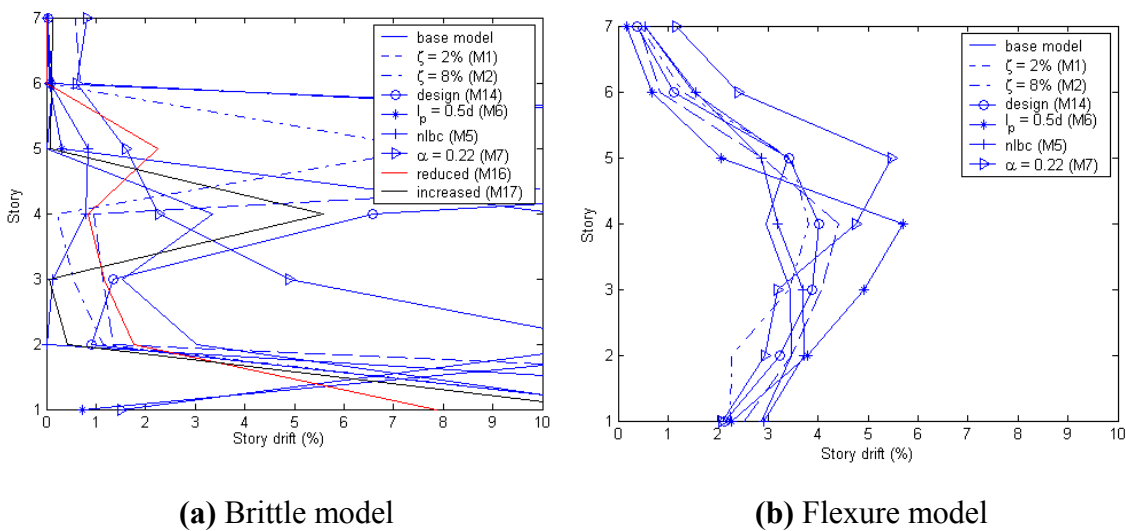
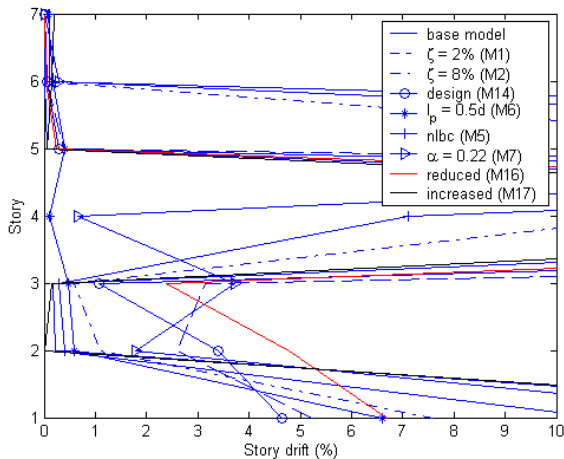
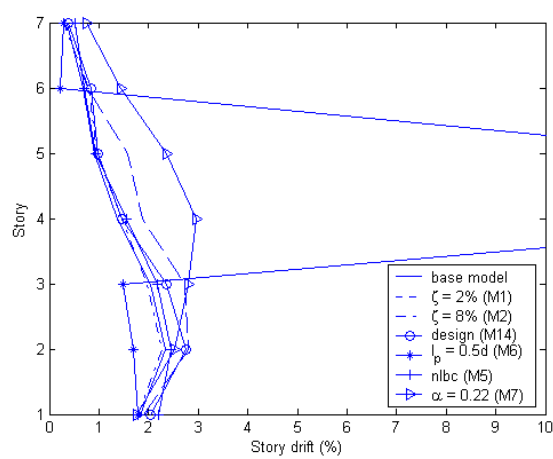


Figure 6.8 Plot of Story drifts for 10in50_SF_461 for Different Parameters

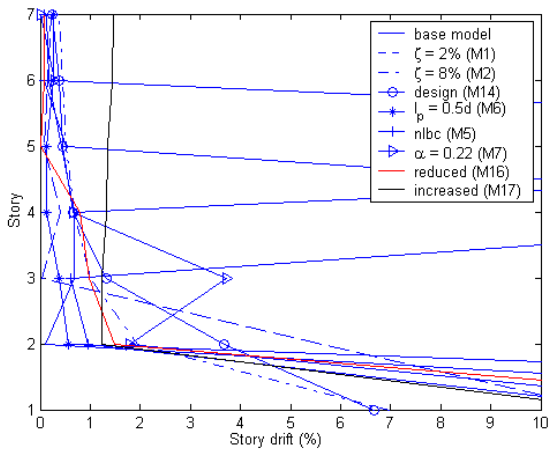


(a) Brittle model

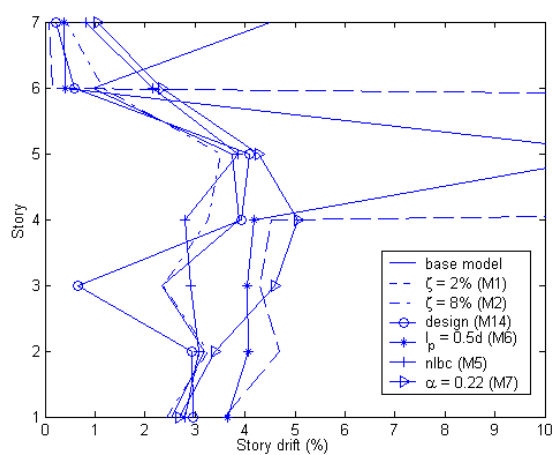


(b) Flexure model

Figure 6.9: Plot of Story Drifts for 02in50_NR_vnuy for Different Parameters



(a) Brittle model



(b) Flexure model

Figure 6.10: Plot of Story Drifts for 02in50_NR_rose for Different Parameters

6.2.1 Variability in Maximum Inter-Story Drifts

Maximum inter-story drift is one simple measure of earthquake response. Table 6.5 and Table 6.6 show the variation in the maximum inter-story drifts for the brittle model and the flexure model respectively for the six ground motions. The first two rows are for the 2% probability of occurrence in 50 years the next two for 10% and the last two for 50% probability of occurrence in 50 years.

Table 6.5 Brittle model - Variation of Maximum Inter-Story Drift (%)

| Ground motion | Base | M1 | M2 | M5 | M6 | M7 | M14 | M16 | M17 | Mean | C.O.V |
|----------------------|-------------|-----------|-----------|-----------|-----------|-----------|------------|------------|------------|-------------|--------------|
| 02 in 50 NR_rose | 10 | 10 | 6.97 | 10 | 10 | 10 | 6.66 | 10 | 10 | 9.29 | 0.15 |
| 02in50 NR_vnuy | 10 | 10 | 10 | 10 | 6.60 | 10 | 10 | 10 | 10 | 9.62 | 0.12 |
| 10in50 NR_vnsc | 6.0 | 10 | 9.44 | 10 | 8.21 | 7.90 | 10 | 8.68 | 3.58 | 8.20 | 0.26 |
| 10in50 SF_461 | 10 | 10 | 7.69 | 10 | 10 | 10 | 10 | 7.86 | 10 | 9.51 | 0.10 |
| 50in50 SF_466 | 3.36 | 5.52 | 1.89 | 10 | 5.06 | 2.62 | 4.23 | 5.03 | 3.63 | 4.60 | 0.51 |
| 50in50 SF_vnuy | 0.73 | 0.85 | 0.73 | 1.2 | 0.82 | 1.03 | 0.81 | 0.71 | 0.73 | 0.85 | 0.20 |

Table 6.6 Flexure model - Variation of Maximum Inter-Story Drift (%)

| Ground Motion | Base | M1 | M2 | M5 | M6 | M7 | M14 | Mean | C.O.V |
|----------------------|-------------|-----------|-----------|-----------|-------------|-----------|------------|-------------|--------------|
| 02in50 NR_osc | 4.51 | 4.70 | 3.52 | 3.85 | 10 | 5.05 | 4.08 | 5.10 | 0.43 |
| 02in50 NR_vnuy | 2.34 | 2.79 | 2.27 | 2.45 | 10 | 2.96 | 2.75 | 3.65 | 0.77 |
| 10in50 SF_461 | 2.63 | 2.83 | 2.58 | 3.00 | 10 | 4.08 | 3.15 | 4.04 | 0.66 |
| 10in50 SF_461 | 3.46 | 4.42 | 3.82 | 3.71 | 5.71 | 5.48 | 4.03 | 4.37 | 0.21 |
| 50in50 SF_466 | 2.56 | 2.89 | 2.30 | 3.04 | 2.26 | 2.71 | 2.78 | 2.64 | 0.11 |
| 50in50 SF_vnuy | 0.72 | 0.85 | 0.73 | 1.20 | 0.82 | 1.05 | 0.80 | 0.88 | 0.20 |

The following can be observed from Table 6.5 and Table 6.6:

1. The maximum inter story drifts are large for the brittle model compared to the flexure model. This is because in the brittle model the shear strength of the columns are reduced and hence failure occurs much before it occurs in flexure model which results in higher drift ratios.
2. For the flexure model, hinge length (model M6) has a very significant impact on the maximum inter story drift ratio. Other than the hinge length the rest of the parameter models do not significantly affect the maximum inter-story drift ratio in the flexure model.

6.2.2 Impact of Ground Motion Variability

To study the impact of ground motion variability on the building response of brittle and flexure model, an exhaustive analyses of the two baseline models (brittle and flexure baseline models) subjected to a series of 30 ground motions, 10 from each hazard level (2%, 10% and 50% probability of occurrence in 50 years) was done. Figure 6.11 to Figure 6.13 show the results of this exhaustive ground motion analysis for 2%, 10% and 50% probability of occurrence in 50 years ground motions. Table 6.7 summarizes the results (variation of maximum inter-story drift) of the analyses of the brittle and flexure model using the thirty ground motions.

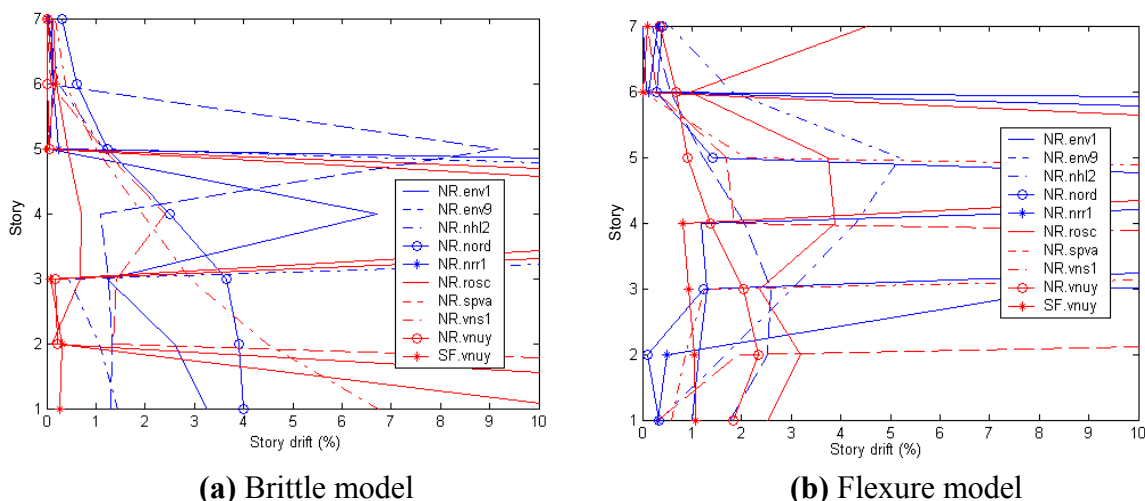


Figure 6.11 Effect of Ground motion Variability on Building Response (02% in 50years)

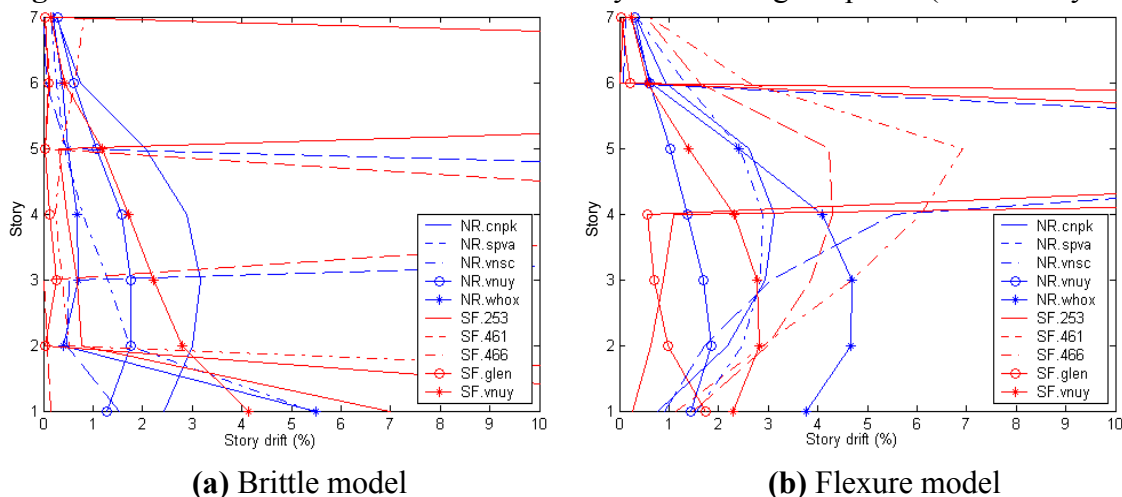
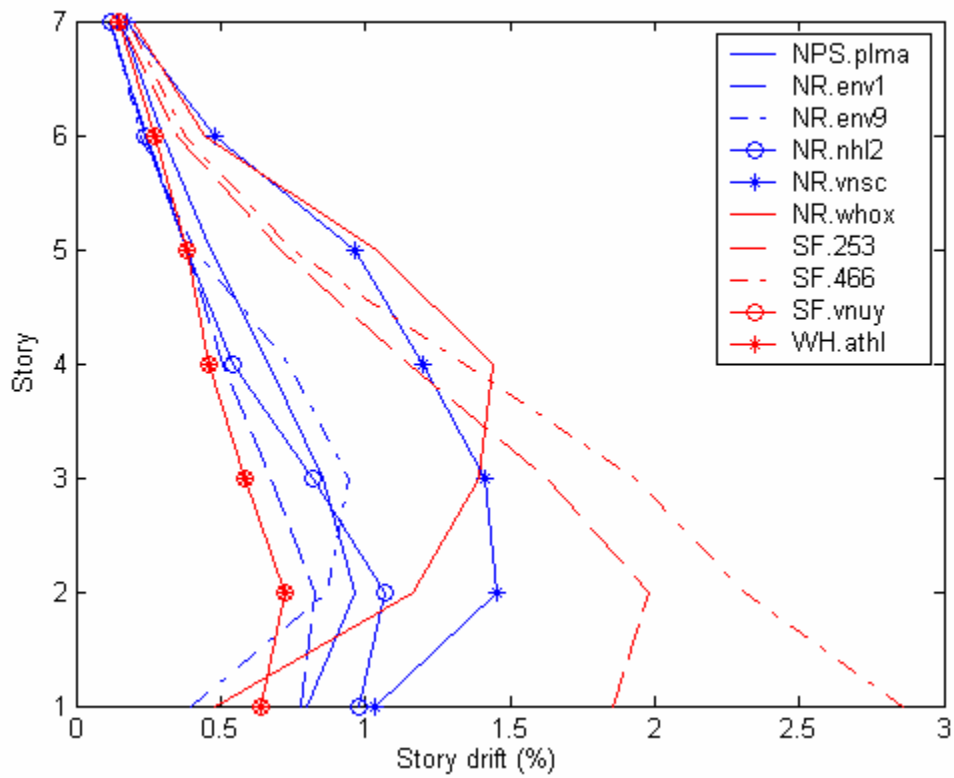
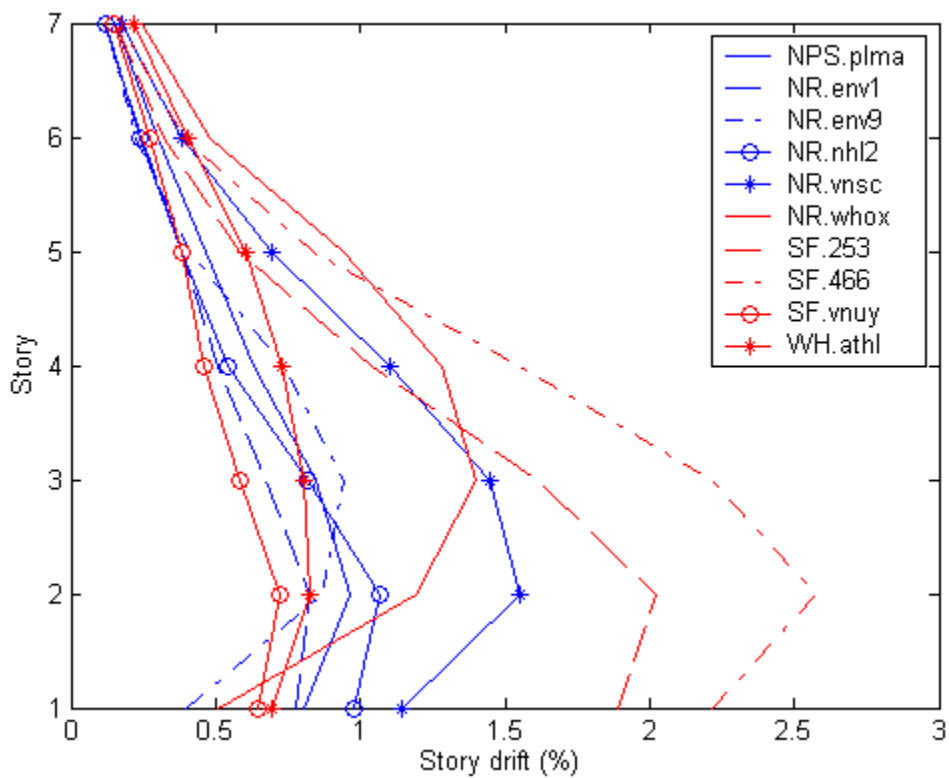


Figure 6.12 Effect of Ground motion Variability on Building Response (10% in 50years)



(a) Brittle model



(b) Flexure model

Figure 6.13 Effect of Ground motion Variability on Building Response (50% in 50years)

Table 6.7 Effect of Variability in Ground motion on Maximum Inter-Story Drift

| Ground motion | | Brittle Model (%) | Flexure Model (%) |
|------------------------|----------|--------------------------|--------------------------|
| 02 in 50 | NR_env1 | 6.73 | 10 |
| | NR_env9 | 9.16 | 2.59 |
| | NR_nhl2 | 10 | 5.21 |
| | NR_nord | 3.99 | 10 |
| | NR_nrr1 | 10 | 10 |
| | NR_rosc | 10 | 4.52 |
| | NR_spva | 10 | 10 |
| | NR_vns1 | 6.74 | 10 |
| | NR_vnuy | 10 | 2.35 |
| | SF_vnuy | 10 | 10 |
| Mean | | 8.66 | 7.47 |
| C.O.V | | 0.24 | 0.45 |
| No. of failures | | 6 | 6 |
| 10 in 50 | NR_cnpk | 3.16 | 3.12 |
| | NR_spva | 10 | 10 |
| | NR_vnsc | 6.04 | 2.63 |
| | NR_vnuy | 1.77 | 1.85 |
| | NR_whox | 5.49 | 4.70 |
| | SF_253 | 6.99 | 10 |
| | SF_461 | 10 | 3.46 |
| | SF_466 | 10 | 6.93 |
| | SF_glen | 10 | 10 |
| | SF_vnuy | 4.13 | 2.83 |
| Mean | | 6.76 | 5.55 |
| C.O.V | | 0.47 | 0.61 |
| No. of failures | | 4 | 3 |
| 50 in 50 | NPS_plma | 0.96 | 0.97 |
| | NR_env1 | 0.83 | 0.83 |
| | NR_env9 | 0.94 | 0.94 |
| | NR_nhl2 | 1.07 | 1.07 |
| | NR_vnsc | 1.45 | 1.55 |
| | NR_whox | 1.44 | 1.40 |
| | SF_253 | 1.98 | 2.02 |
| | SF_466 | 2.57 | 2.57 |
| | SF_vnuy | 0.73 | 0.73 |
| | WH_athl | 0.78 | 0.83 |
| Mean | | 1.28 | 1.29 |
| C.O.V | | 0.47 | 0.47 |
| No. of failures | | 0 | 0 |

The following can be observed from Table 6.7:

- It was found that for only lower intensity earthquakes collapse did not occur. For medium and higher intensity earthquakes the building collapsed irrespective of whether it is a brittle or a flexure model.
- For the 50% probability of occurrence in 50 years earthquake hazard level, it was found that the brittle model and the flexure model behaved identically. This is because for lower intensity earthquakes the shear demand in the columns for the brittle model did not exceed the shear capacity and hence the brittle and the flexure model behaved in a similar manner.
- In most cases the brittle model led to larger drifts than did the ductile model because the brittle model had shear strength capacities much lower than the flexure model and hence failure would be initiated much earlier in the brittle model than in the flexure model which would lead to larger drift values for the brittle model.
- In four cases the ductile model suffered failure (drift > 10%) while the brittle model did not. The reason might be that the initiation of failure in both models were different for these particular ground motions. The propagation of failure after the initiation of first failure in the flexure model might be more significant than for the brittle model.

6.3 Study Number Three

Analyses was also done for the shear strength parameter using the thirty ground motions to see the effect that increasing/decreasing (model M16 and model M17) the shear strength has on building response in combination with the variation in the ground motions. Figure 6.14 to 6.16 shows the mean inter story drifts for the baseline model, the reduced shear strength model and the increased shear strength model.

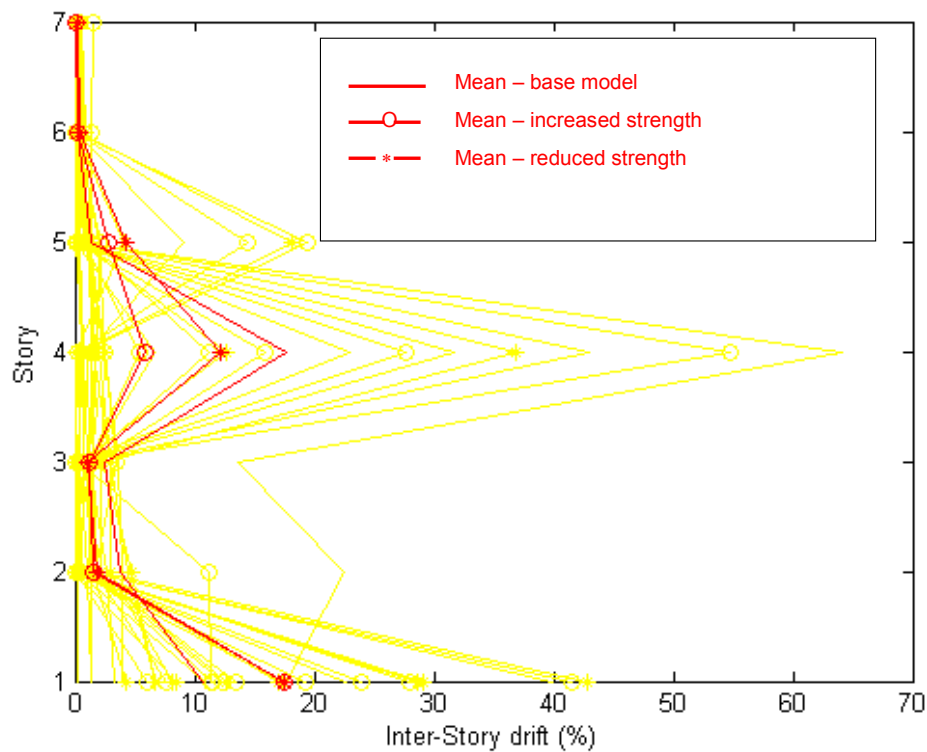


Figure 6.14 Shear Strength Capacity Variability - 2% in 50 years

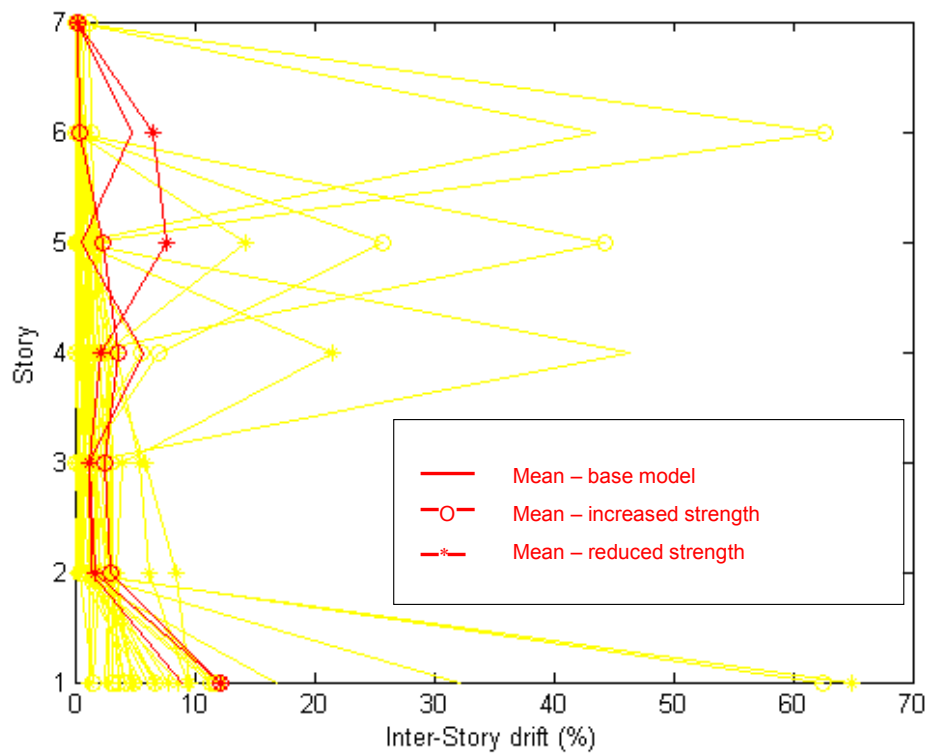


Figure 6.15 Shear Strength Capacity Variability - 10% in 50 years

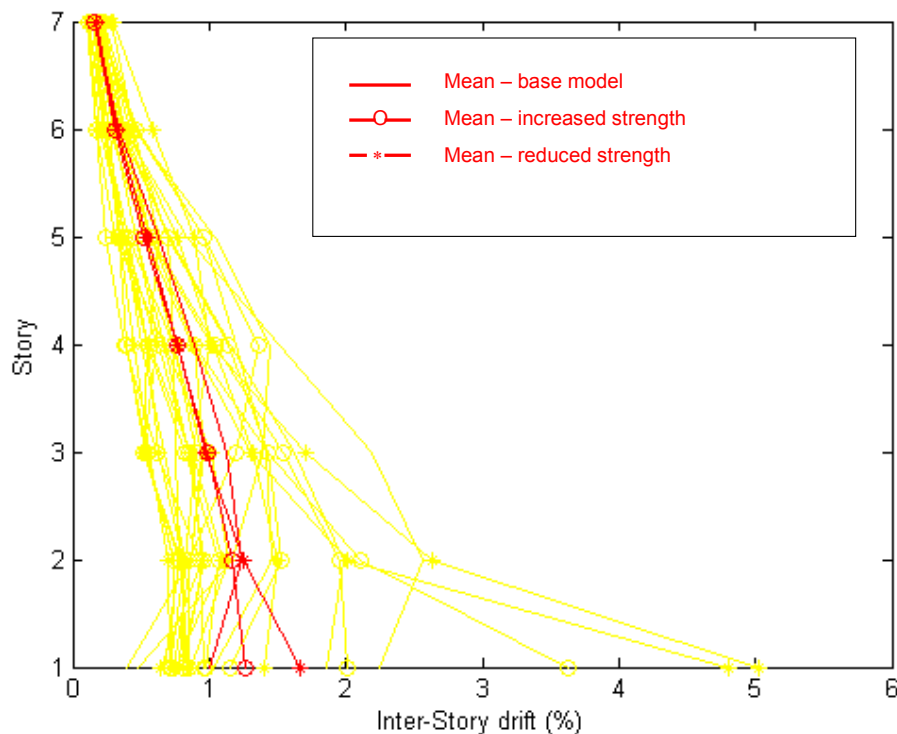


Figure 6.16 Shear Strength Capacity Variability - 50% in 50 years

Table 6.8 summarizes the results of the variation between the two models in terms of the maximum inter-story drifts. Values of maximum inter-story drifts greater than 10% have been set as 10% as it is not practical to observe drift demands greater than 10%. The following can be observed from Table 6.8:

- It was found that reducing the shear strength capacity had more impact on the building response than increase in shear strength. This would suggest that for most cases when the shear demand on the columns exceeded the shear capacity of the baseline model columns, it also exceeded the shear capacity which is 20% higher than the baseline model and hence a similar inter story drifts were observed for the baseline model and the model with increased shear strength capacity.
- It was also found that ground motion variation had more impact on the response of the building than shear strength variation.

Table 6.8 Maximum Inter-Story Drift for three Models with Varying Shear Strengths

| Ground motion | | Base model | Reduced strength | Increased strength | Mean (%) | C.O.V |
|---------------|----------|------------|------------------|--------------------|-------------|-------------|
| 02 in 50 | NR_env1 | 6.73 | 8.45 | 6.05 | 7.07 | 0.17 |
| | NR_env9 | 9.16 | 10 | 10 | 9.72 | 0.05 |
| | NR_nhl2 | 10 | 10 | 10 | 10 | 0.00 |
| | NR_nord | 3.99 | 8.11 | 7.71 | 6.60 | 0.34 |
| | NR_nrr1 | 10 | 10 | 10 | 10 | 0.00 |
| | NR_rosc | 10 | 10 | 10 | 10 | 0.00 |
| | NR_spva | 10 | 10 | 10 | 10 | 0.0 |
| | NR_vns1 | 6.74 | 10 | 10 | 8.91 | 0.21 |
| | NR_vnuy | 10 | 10 | 10 | 10 | 0.00 |
| | SF_vnuy | 10 | 10 | 10 | 10 | 0.00 |
| Mean | | 8.66 | 9.66 | 9.37 | 9.23 | 0.05 |
| C.O.V | | 0.24 | 0.07 | 0.15 | 0.15 | |
| 10 in 50 | NR_cnpk | 3.16 | 2.83 | 3.18 | 3.06 | 0.06 |
| | NR_spva | 10 | 10 | 10 | 10 | 0.00 |
| | NR_vnsc | 6.04 | 8.68 | 3.58 | 6.10 | 0.42 |
| | NR_vnuy | 1.77 | 1.35 | 2.00 | 1.71 | 0.19 |
| | NR_whox | 5.49 | 6.76 | 6.69 | 6.31 | 0.11 |
| | SF_253 | 10 | 10 | 10 | 10 | 0.00 |
| | SF_461 | 10 | 7.86 | 10 | 9.29 | 0.13 |
| | SF_466 | 10 | 9.43 | 10 | 9.81 | 0.03 |
| | SF_glen | 10 | 10 | 10 | 10 | 0.00 |
| | SF_vnuy | 4.13 | 4.99 | 4.88 | 4.67 | 0.10 |
| Mean | | 7.06 | 7.19 | 7.03 | 7.09 | 0.01 |
| C.O.V | | 0.47 | 0.44 | 0.47 | 0.46 | |
| 50 in 50 | NPS_plma | 0.96 | 0.95 | 0.95 | 0.96 | 0.00 |
| | NR_env1 | 0.83 | 0.81 | 0.96 | 0.87 | 0.09 |
| | NR_env9 | 0.94 | 0.84 | 0.85 | 0.88 | 0.06 |
| | NR_nhl2 | 1.07 | 1.13 | 1.07 | 1.09 | 0.04 |
| | NR_vnsc | 1.45 | 1.09 | 1.53 | 1.36 | 0.17 |
| | NR_whox | 1.44 | 1.50 | 1.36 | 1.43 | 0.05 |
| | SF_253 | 1.98 | 4.80 | 2.01 | 2.93 | 0.55 |
| | SF_466 | 2.57 | 5.03 | 3.63 | 3.74 | 0.33 |
| | SF_vnuy | 0.73 | 0.71 | 0.74 | 0.72 | 0.02 |
| | WH_athl | 0.79 | 0.95 | 0.91 | 0.88 | 0.09 |
| Mean | | 1.28 | 1.78 | 1.4 | 1.49 | 0.17 |
| C.O.V | | 0.47 | 0.93 | 0.62 | 0.67 | |

CHAPTER 7

SUMMARY AND CONCLUSIONS

7.1 Summary

The objectives of this study were to evaluate the accuracy with which the applied nonlinear modeling procedures predict building response and capture the inelastic failure modes of an older reinforced concrete frame building. This was done by evaluating the results of nonlinear analysis of an older reinforced concrete frame building and comparing the simulated and observed response of the building subjected to ground motions recorded during the 1994 Northridge earthquake. Additionally, the influence of selected modeling parameters and assumptions on the calculated response of the building was evaluated.

The OpenSees analysis platform was used to compute the fundamental period of vibration of the building, and to compute the nonlinear static and dynamic response of the study building. Inelastic pushover analyses were performed to estimate the lateral strength, deformation capacity and failure mechanisms of the building. Inelastic time history analyses were conducted to evaluate the accuracy of the modeling procedures to compute the seismic response and failure modes of the building during the 1994 Northridge earthquake. Several parameter studies were done to investigate the impact of different modeling assumptions on the building response.

7.2 Conclusions

The results of this study support the following:

- **Pushover Analysis**

1. The results of the pushover analyses show that variation in model parameters results in very little variation (6%) in base shear demand and significant variation (19%) in the displacement at which failure occurs.
 2. The results of the pushover analysis indicated that this analysis method may be used to predict the mechanism that determines earthquake response of a non-ductile reinforced concrete frame. Using the base line model, a pushover analysis predicted that response of the building was determined by shear damage of the 4th and 5th story columns. Damage of these columns was observed after the Northridge earthquake.
 3. The results of the pushover analyses using the baseline model suggest that the predicted failure mechanism is relatively insensitive to the load distribution. A similar failure mechanism was observed for different load distributions (uniform, triangular and FEMA 356).
- **Dynamic Analysis**
 1. Dynamic analyses using the baseline model predicted peak displacement with a high level of accuracy.
 2. Dynamic analysis did not predict the displacement history accurately; the time at which peak displacement occurred and the direction in which it occurred were not predicted by the model.
 3. It was observed that the exterior frame was more severely damaged than the interior frame. Shear failures were captured on the fourth and fifth story columns of the exterior frame which was observed during the Northridge earthquake. The model however did not predict splice failures which were observed in some of the ground story columns under the Northridge earthquake.

- **Parameter Study**

1. It was found that none of the parameter models had significant impact on the response of the building under the Northridge earthquake.
2. With the exception of hinge length, the variation in response due to parameter variation for the brittle model was found to be more significant than the variation in response of the flexure model. It was found that for higher intensity earthquakes there was less variation compared to the lower and moderate intensity earthquakes because the building was failing irrespective of the modeling assumptions.
3. It was found that at any earthquake hazard level, variability in earthquake ground motion had more effect on the variability of maximum inter story than did variability in shear strength.

7.3 Recommendations for Future Research

The following topics are suggested for future research efforts:

1. The columns on the ground story are fixed to the ground and it has been assumed that the ground is rigid and has no deformation which might be one reason for not predicting the splice failure in some of the ground story columns. Hence, allowing for ground movement by using springs to model the ground would be a better model to predict the earthquake response.
2. The beam-column joint has been assumed to be rigid in the baseline model thus disallowing any deformation that might be occurring in the joint. A better joint representation (eg: rotational joint) is recommended for better prediction of the response.
3. The flexure model considered has a displacement ductility capacity of around 4 which is considered low according to the current design standards. Hence

redefining the flexure model with higher displacement ductility would be helpful in understanding the differences between the flexure and the brittle model response better.

4. The splice failures occurring in some of the ground story columns during the Northridge earthquake were not captured by the model. A 3D model with ground motions applied to both the longitudinal and the transverse direction might be a better model to predict the splice failure that was observed during the Northridge earthquake.

REFERENCES

Alice Rissman (1965), *“Drawings of Holiday Inn Building”*, Rissman & Rismann Associated Ltd.

American Society of Civil Engineers (2000) *“FEMA356: Pre standard and commentary for the seismic rehabilitation of building.”* Washington D.C.: Federal Emergency Management Agency

Anil K. Chopra (2000), *“Dynamics of Structures: Theory and applications to earthquake engineering.”* Upper Saddle River, NJ: Prentice Hall

Barin B., Pincheria J.A., (2002), *“Influence of modeling parameters and assumptions on the seismic response of an existing RC building.”*

Bernal D., (1994). *“Viscous damping in inelastic structural response”*, *Journal of structural Engineering* 120 (4)

Browning J., Li Y.R., Lynn A., Moehle J.P. (2000). *“Performance assessment for a reinforced concrete frame building.”* *Earthquake Spectra* 16 (3): 541-555

Crisfield, M.A. *“Snap-Through and Snap-Back Response in Concrete Structures and the Dangers of Under Integration.”* *International Journal of Numerical Methods in Engineering* 22 (1986): 751-756

Dotiwala, F.S. (1998), *“A nonlinear flexure-shear model for R.C columns subjected to earthquake loads”*, M.S., Advanced Independent Study Report, University of Wisconsin-Madison

EERI Special Earthquake Report – December 1999.

Frankel, A., et al., 1996. “*USGS National Seismic maps: Documentation.*” USGS Open File Report 96-532.

Gary C. Hart (1975), “*Earthquake design of buildings: damping.*” *Journal of the Structural Division, ACSE.*

Gulkan, P. and M.A. Sozen, “*Inelastic Response of Reinforced Concrete Structures to Earthquake Motions*”. *Journal of ACI*, vol. 71, No. 12, Dec. 1974.

Helmut Krawlinker and G.D.P.K. Seneviratna (1998), “*Pros and Cons of a Pushover Analysis of Seismic Performance evaluation*”

Islam S. (1996). “*Analysis of the Northridge earthquake response of a damaged non-ductile concrete frame building*” *The Structural Design of Tall Buildings* 5(3): 151-182

John A. Blume & Associates, Engineers (1997). “*Holiday Inn (29)*”

Kant, D., (1999), “*Inelastic modeling and analyses of a RC building subjected to earthquake loads*”, M.S. Thesis, University of Wisconsin-Madison.

Kowalsky MJ, Priestley MJN (2000): “*Improved analytical model for shear strength of circular reinforced concrete columns in seismic regions.*” *ACI Structural Journal* 97 (3): 388-396

Luo, Y.H. and Durrani, A.J., (1995), “*Experimental beam model for flat-slab buildings – Part I; Interior connections*”, *ACI Structural Journal*, 92(2) March-April 1995, pp 250-257

M.D. Trifunac, S.S. Ivanovic and M.I. Todorovska (1999), “*Instrumented 7-Story Reinforced Concrete Building in Van Nuys, California: Description of Damage from the*

1994 Northridge Earthquake and Strong motion Data”, Report CE 99-02, Los Angeles, California, July 1999.

M.D. Trifunac, S.S. Ivanovic and M.I. Todorovska (2001), “*Apparent period of buildings*”, *Journal of structural engineering*, 127 (5), May 2001

Megegotto, M., P. Pinto (1973), “*Method of analysis of cyclically loaded reinforced concrete plane frames including changes in geometry and inelastic behavior of elements under combined normal geometry and inelastic behavior of elements under combined normal force and bending*”, Proceedings of the IABSE Symposium on the Resistance and Ultimate Deformability of Structures Acted on by Well-Defined Repeated Loads. Lisbon

M.H. Scott, “*A Software Architecture for Finite Element Material Models*”. Master’s thesis, University of California, Berkeley, April 2001

M.J.N Priestley, F. Seible and G.M. Calvi, “*Seismic Design and Retrofit of Brdges*”, John Wiley and Sons, New York (1996).

Naeim F., (1998), “*Performance of 20 extensively-instrumented buildings during the 1994 Northridge earthquake*”, *The structural design of tall buildings* 7. 179-194 (1998)

Newmark N.M., Hall W.J. (1982), “*Earthquake monographs on earthquake criteria, structural design, and strong motion records v. 3*, Berkeley: Earthquake Engineering Research Institute.

Pacific Earthquake Engineering Research Center Test Beds website,
<http://www.peertestbeds.net>

Pan, A. and Moehle, J.P., (1988) “*Reinforced concrete flat plates under lateral loading: An experimental study including biaxial effects*”. Report No. UCB/EERC88/16, College of Engineering, University of California at Berkeley.

Pecknold, D.A. (1975), “*Slab width for equivalent frame analysis*”, *ACI journal*, Proceedings 72 (4), April 1975, pp. 135-137

R. Park and T. Paulay (1975), “*Reinforced Concrete Structure*”, John Wiley and Sons, New York

Somerville P., Collins N., URS Corporation (2002), “*Ground motion time histories for the Van Nuys building.*”

APPENDIX A: DETAILS OF THE TCL SCRIPTS

Appendix A provides a detailed discussion and excerpts from the *tcl* scripts which have been developed to set, define and analyze the model in OpenSees. As discussed in Chapter 4, the main function to be ‘sourced in’ in order to analyze the Van Nuys building model is the *VanNuysAnalysis.tcl*.

- **VanNuysAnalysis.tcl**

The *VanNuysAnalysis.tcl* ‘sources in’ the following *tcl* files as discussed in Chapter 4.

source selfrun.tcl

source units.tcl

source setAnalysisParameters.tcl

source setFrameGeometry.tcl

source setMaterialProperties.tcl

source defineElasticElementProperties.tcl

source setFrameMemberSectionProperties.tcl

source defineStructuralMaterials.tcl

source defineSections.tcl

source setNodalMass.tcl

source defineNodes.tcl

source defineElements.tcl

source defineBoundaryConditions.tcl

source analyze.tcl

- **selfrun.tcl**

This script automates the analyses process which is very useful for parameter study. Three variables, *controller*, *control* and *groundmotions* are defined. The *controller* is the list of parameters that are to be analyzed and the *control* is a list of values for the parameters that have been defined in *controller*.

```
Set Controller [list "Damping" "Hingelength" "FiberDim" "Slabwidth"];
```

```
Set Control [list "2%" "0.5" "1" "0.22"];
```

```
Set groundmotions [list "50in50_SF_vnuuy" "10in50_NR_nord" "02in50_SF_466"];
```

The script has been set up so as to loop through all the parameters with different control values and then loop through all the ground motions defined in the *groundmotions list*. After the analyses has been done the results are saved in separate files named after the type of ground motion used, the parameter being studied and the value of the parameter.

- **setAnalysisParameters.tcl**

This script defines the parameters that control the analysis. Modification of the analysis (pushover vs. dynamic, variation in the input motion, etc., requires only modification of the parameters in this file. The analysis parameter used in a particular analysis is defined, other options, are listed in parentheses.

```
Set ColumnElementType = "elastic" ("fiber-hinge", "fiber", "elastick", "displacement-based")
```

```
set BeamElementType = "elastic" ("fiber-hinge", "fiber", "elastick", "displacement-based")
```

“elastic” – beam and column elements are defined by gross section properties. Concrete elastic modulus and *beamGrossSectionStiffnessParameters* (column** and slab**). *BeamGrossSectionStiffnessParameters* may be used to reduce gross-section stiffness.

“elastick” – The modulus of elasticity is reduced to take into account the effect due to the damage done to the building.

“fiber” – nonlinear beam column element based on non-iterative force formulation and considers spread of plasticity along the element. The integration algorithm used is Gauss-Lobatto quadrature rule.

“fiber-hinge” – beam and column elements with hinges which are based upon non-iterative flexibility formulation and considers plasticity to be concentrated over specified hinge lengths at the element ends. The remaining beam is considered to be as linear elastic.

“displacement-based” – beam and column elements with distributed plasticity. The integration is based upon the Gauss-Legendre quadrature rule.

```

If ColumnElementType == "elastic" || BeamElementType == "elastic"
(***)GrossSectionStiffnessFactor are used to reduce gross-section stiffness)
set BeamGrossSectionStiffnessFactor = 1.0
set ColumnGrossSectionStiffnessFactor = 1.0
set SlabGrossSectionStiffnessFactor = 1.0

```

```

if ColumnElementType == "fiber" || "displacement-based"
(define number of integration points (i.e., sections) along element length)
set NumColIntPoints = 5

```

```

if BeamElementType == "fiber" || "displacement-based"
(define number of integration points (i.e., sections) along element length)
set NumBeamIntPoints = 4

```

```

set ConcreteMaterialType = "elastic" ("Concrete01", "Concrete02", "Concrete03")

```

“elastic” – uniaxial material with elastic modulus, E

“Concrete01” – uniaxial concrete model with degraded unloading and reloading stiffness based on work of Karsan and Jirsa. The model does not account for Concrete Tensile Strength. The Compressive envelope is based on the model proposed by Kent-Scott-Park.

“Concrete02” – uniaxial concrete model with tensile strength and linear tension softening.

Set SteelMaterialType = “elastic” (“Steel01”, “Steel02”)

“elastic” – uniaxial material with elastic modulus, E

“Steel01” – uniaxial bilinear steel model with kinematic hardening and optional isotropic hardening. Kinematic hardening is linear while Isotropic Hardening is described in terms of nonlinear evolution equations :- one for tension and other for compression.

“Steel02” – uniaxial Menegotto-Pinto steel model with isotropic strain hardening.

Set MaxFiberDim = 0.5 in

(defines maximum size of the fiber)

set FcStrengthFactor = 1

(defines strength factor for concrete)

set ColumnStripWidthFactor = 1

(defines strength factor for concrete)

set CoverBeamColumn = 2 in

(defines the cover for beams and columns)

set ConcreteAgeFactor = 1.50 (from FEMA 356)

(defines the increase in concrete strength over time)

set BeamStiffnessReductionFactorFlex 0.5

```
set BeamStiffnessReductionFactorAxial 1
set BeamStiffnessReductionFactorShear 0.4
set BeamStiffnessReductionFactorTorsion 1
set ColumnStiffnessReductionFactorFlex 0.5
set ColumnStiffnessReductionFactorAxial 1
set ColumnStiffnessReductionFactorShear 0.4
set ColumnStiffnessReductionFactorTorsion 1
set SlabStiffnessReductionFactorFlex 0.5
set SlabStiffnessReductionFactorAxial 1
set SlabStiffnessReductionFactorShear 0.4
set SlabStiffnessReductionFactorTorsion 1
```

(defines the effective stiffness of the building due to damage)

```
set ConfinedConcreteStrengthFactor = 1.00
```

(defines the increase in concrete strength due to confinement)

```
set CrushingStrengthFactor = 0.1
```

(defines the ratio of the crushing strength of concrete to the ultimate strength)

```
set SlabCover = 3/4 in
```

(defines the cover for slabs)

```
set 2Dvs3Dmodel = "2D" ("3D")
```

(defines the type of model to be used for the analysis)

```
set AnalysisType = "gravity" ("eigenvalue", "dynamic", "pushover")
```

(defines the type of analysis to be performed on the model)

```
if AnalysisType == "dynamic"
set groundMotionFileList = "groundMotionFileList.tcl"
```

(defines the name of the tcl script that lists ground motion files)

set gamma = 0.5

set beta = 0.25

(defines the parameters for newmark-beta integration)

set alphaM = 0

set betaK = 0

set betaKcomm = 0.02

set betaKinit = 0

(defines the mass and stiffness proportional damping for Rayleigh Damping)

if AnalysisType == "pushover"

set PUSHOVER = "DispControl" ("LoadControl")

(defines the type of displacement or load type of control used pushover analysis)

set TypicalColumnDepth = 18 in

set TypicalBeamDepth = 24 in

set AvgStoryheight = 10 ft

set AvgBayWidth = 225 in

(variables required for defining the hinge length ratio for beams and columns)

set ColumnHingeLengthRatio = TypicalColumnDepth/ AvgStoryheight

set BeamHingeLengthRatio = TypicalBeamDepth/ AvgBayWidth

- **setFrameGeometry.tcl**

This script defines the building geometry or basically the geometry of the frame members.

set nBaysNSFrame = 3

(defines the number of NS Frame Bays)

set nBaysEWFrame = 9

(defines the number of EW Frame Bays)

set nStories = 7

(defines the number of Stories)

set iBayWidthNSFrame

(defines the list of width of NS Frames)

set iBayWidthEWFrame

(defines the list of width of EW Frames)

set iStoryHeight

(defines the list of story heights)

set iNSFrames = (1 2 3 4 5 6 7 8 9)

(defines the list of NS Frame numbers)

set iEWFrames = (A B C D)

(defines the list of EW Frame numbers)

set iStory = (1 2 3 4 5 6 7)

set iStoryAll = (1 2 3 4 5 6)

(defines the list of Story numbers)

set aSlabThickness(Story)

(defines the Slab Thickness of each Story)

set aBeamNSGeoProp(Story, "height")

(defines the height of NS Beam for each Story)

set aBeamNSGeoProp(Story, "width")

(defines the width of NS Beam for each Story)

set aBeamEWGeoProp(Story, "height")

(defines the height of EW Beam for each Story)

set aBeamEWGeoProp(Story, "width")

(defines the width of EW Beam for each Story)

set aColumnGeoProp(NSFrame,EWFrame,Story, "NS")

(defines the NS dimension of the column for each NSFrame, EWFrame, Story)

set aColumnGeoProp(NSFrame,EWFrame,Story, "EW")

(defines the EW dimension of the column for each NSFrame, EWFrame, Story)

*set ColumnStripWidth = 9 ft 9.5 in * ColumnStripWidthFactor*

(defines the Column Strip width)

- **setMaterialProperties.tcl**

This script defines the material properties for concrete and steel.

Source setSteelProperties.tcl

source setConcreteProperties.tcl

- **setSteelProperties.tcl**

This script defines the material properties for steel. Local variables are set to define steel material parameters (e.g. Yield strength, yield strain, end of yield plateau stress and strain, ultimate strength and strain, hardening ratio for bilinear model). They are then updated into a list which is lastly defined as a Global variable.

set Es

(defines the Young's Modulus for Steel)

set iGR40SteelData

(defines the list of Grade 40 steel data containing young's modulus for steel, strength and strain values at yield and end of yield plateau and also the hardening ratio for the bilinear model.)

set iGR60SteelData

(defines the list of Grade 60 steel data containing young's modulus for steel, strength and strain values at yield and end of yield plateau and also the hardening ratio for the bilinear model.)

- **setConcreteProperties.tcl**

This script defines the material properties for concrete. Local variables are set to define concrete material parameters which are later defined as a global variable.

Set iColumnConcTypes (“fcColumnG”, “fcColumn2”, “fcColumnO”)

(defines the concrete types of the column at different story levels. *** these are later set as global.)

set iBeamConcTypes (“fcBeamI”, “fcBeamO”)

(defines the concrete types of the beams at different story levels. *** these are later set as global.)

set aFC (Concrete Type)

(defines the compressive strength of concrete.)

set aFC (Concrete Type, Elastic, confined)

(defines the list of parameters required to define a Confined Elastic Material Model.)

set aFC (Concrete Type, Elastic, unconfined)

(defines the list of parameters required to define a UnConfined Elastic Material Model.)

set aFC (Concrete Type, Concrete01, confined)

(defines the list of parameters required to define a Confined Concrete01 Material Model.)

set aFC (Concrete Type, Concrete01, unconfined)

(defines the list of parameters required to define a UnConfined Concrete01 Material Model.)

set aFC (Concrete Type, Concrete02, confined)

(defines the list of parameters required to define a Confined Concrete02 Material Model.)

set aFC (Concrete Type, Concrete02, unconfined)

(defines the list of parameters required to define a UnConfined Concrete02 Material Model.)

set aFC (Concrete Type, Concrete03, confined)

(defines the list of parameters required to define a Confined Concrete03 Material Model.)

set aFC (Concrete Type, Concrete03, unconfined)

(defines the list of parameters required to define an unconfined Concrete03 Material Model.)

Where Concrete Type represents all values in iColumnConcTypes and iBeamConcTypes.

All Lists of variable aFC are set as Global.

- **defineElasticElementProperties.cl**

This script defines the elastic properties for the beam and column

source setConcreteProperties.tcl

set aElasticElementProperties(\$NSFrame,\$EWFrame,\$Story,Ec)

(defines the modulus of elasticity for each floor)

set aElasticElementProperties(\$NSFrame,\$EWFrame,\$Story,ColumnArea)

(defines the column area)

set aElasticElementProperties(\$NSFrame,\$EWFrame,\$Story,BeamArea)

(defines the beam area)

set aElasticElementProperties(\$NSFrame,\$EWFrame,\$Story,Gc)

(defines the shear modulus)

set aElasticElementProperties(\$NSFrame,\$EWFrame,\$Story,ColumnJ)

(defines the column torsion rigidity)

set aElasticElementProperties(\$NSFrame,\$EWFrame,\$Story,BeamJ)

(defines the beam torsion rigidity)

set aElasticElementProperties(\$NSFrame,\$EWFrame,\$Story,ColumnIy)

(defines the moment of inertia of the column along the weak axis)

set aElasticElementProperties(\$NSFrame,\$EWFrame,\$Story,BeamIy)

(defines the moment of inertia of the beam along the weak axis)

set aElasticElementProperties(\$NSFrame,\$EWFrame,\$Story,ColumnIz)

(defines the moment of inertia of the column along the strong axis)

set aElasticElementProperties(\$NSFrame,\$EWFrame,\$Story,BeamIz)

(defines the moment of inertia of the beam along the strong axis)

- **setFrameMemberSectionProperties.tcl**

This script defines the section properties for the frame members.

source setColumnSectionProperties.tcl

source setBeamSectionProperties.tcl

source setSlabSectionProperties.tcl

- **setColumnSectionProperties.tcl**

This script defines the section properties for column.

Source procDefineLongSteelProperties.tcl

set aColumnSectionProperties(NSFrame,EWFrame,Story,"concrete")

(defines the value representing Concrete Type from the list of iColumnConcType List.)

Call procDefineLongSteelProperties

(A procedure that takes in a string for definition of steel)

set aColumnSectionProperties(NSFrame,EWFrame,Story,"numLongBars")

(defines the value representing number of longitudinal bars in the column (obtained from the above procedure call).)

set aColumnSectionProperties(NSFrame,EWFrame,Story,"longBarArea")

(defines the value representing number of area of longitudinal bars in the column (obtained from the above procedure call).)

- **setBeamSectionProperties.tcl**

This script defines the section properties for beam.

source NSBeamSectionPropertiesO.tcl

source NSBeamSectionProperties2.tcl

source EWBeamSectionPropertiesO.tcl

source EWBeamSectionProperties2.tcl

We obtain the following values from the above sourced files:

set aNSBeamSectionProperties2(Story,NSFrame,EW1,EW2,"topbars1")

(defines the value representing total area of top-bars from EW1 to EW2 corresponding to a NS Beam of Story 2.)

set aNSBeamSectionProperties2(Story,NSFrame,EW1,EW2,"topbars2")

(defines the value representing total area of top-bars from EW2 to EW1 corresponding to a NS Beam of Story 2.)

set aNSBeamSectionProperties2(Story,NSFrame,EW1,EW2,"bottombars")

(defines the value representing total area of bottom-bars in between EW1 and EW2 corresponding to a NS Beam of Story 2.)

set aNSBeamSectionPropertiesO(Story,NSFrame,EW1,EW2,"topbars1")

(defines the value representing total area of top-bars from EW1 to EW2 corresponding to a NS Beam of Stories other than 2.)

set aNSBeamSectionPropertiesO(Story,NSFrame,EW1,EW2,"topbars2")

(defines the value representing total area of top-bars from EW2 to EW1 corresponding to a NS Beam of Stories other than 2.)

set aNSBeamSectionPropertiesO(Story,NSFrame,EW1,EW2,"bottombars")

(defines the value representing total area of bottom-bars in between EW1 and EW2 corresponding to a NS Beam of Stories other than 2.)

set aEWBeamSectionProperties2(Story,EWFrame,NS1,NS2,"topbars1")

(defines the value representing total area of top-bars from NS1 to NS2 corresponding to a EW Beam of Story 2.)

set aEWBeamSectionProperties2(Story,EWFrame,NS1,NS2,"topbars2")

(defines the value representing total area of top-bars from NS2 to NS1 corresponding to a EW Beam of Story 2.)

set aEWBeamSectionProperties2(Story,EWFrame,NS1,NS2,"bottombars")

(defines the value representing total area of bottom-bars in between NS1 and NS2 corresponding to a EW Beam of Story 2.)

set aEWBeamSectionPropertiesO(Story,EWFrame,NS1,NS2,"topbars1")

(defines the value representing total area of top-bars from NS1 to NS2 corresponding to a EW Beam of Stories other than 2.)

set aEWBeamSectionPropertiesO(Story,EWFrame,NS1,NS2,"topbars2")

(defines the value representing total area of top-bars from NS2 to NS1 corresponding to a EW Beam of Stories other than 2.)

set aEWBeamSectionPropertiesO(Story,EWFrame,NS1,NS2,"bottombars")

(defines the value representing total area of bottom-bars in between NS1 and NS2 corresponding to a EW Beam of Stories other than 2.)

- **setSlabSectionProperties.tcl**

This script defines the section properties for a slab.

Set aNSSlabsectionproperties(Story,"concrete")

(defines the Concrete Type of the NS beam in each story.)

set aEWSlabsectionproperties(Story,"concrete")

(defines the Concrete Type of the EW beam in each story.)

set aNSSlabsectionproperties(NSFrame,Story,EW1,EW2,"topbars1")

(defines the value representing total area of top-bars from EW1 to EW2 by the column strip width area corresponding to a NS Beam of each story.)

set aNSSlabsectionproperties(NSFrame,Story,EW1,EW2,"topbars2")

(defines the value representing total area of top-bars from EW2 to EW1 by the column strip width area corresponding to a NS Beam of each story.)

set aNSSlabsectionproperties(NSFrame,Story,EW1,EW2,"bottombars")

(defines the value representing total area of bottom-bars from EW1 to EW2 by the column strip width area corresponding to a NS Beam of each story.)

set aEWSlabsectionproperties(EWFrame,Story,NS1,NS2,"topbars1")

(defines the value representing total area of top-bars from NS1 to NS2 by the column strip width area corresponding to a EW Beam of each story.)

set aEWSlabsectionproperties(EWFrame,Story,NS1,NS2,"topbars2")

(defines the value representing total area of top-bars from NS2 to NS1 by the column strip width area corresponding to a EW Beam of each story.)

set aEWSlabsectionproperties(EWFrame,Story,NS1,NS2,"bottombars")

(defines the value representing total area of bottom-bars from NS1 to NS2 by the column strip width area corresponding to a EW Beam of each story.)

- **defineStructuralMaterials.tcl**

This script defines the section tags and also activates the *uniaxialMaterial* command of OpenSees to generate the specific material.

source procDefineSteelMaterials.tcl

source procDefineConcreteMaterials.tcl

call procDefineSteelMaterials

(a procedure that activates and thereby defines the material type in OpenSees based upon the user specified option of Steel Material Type.)

set aSteelTag(Steel Material type) = SteelID

(defines the steel Tag Value corresponding to the steel type as provided by the user.)

call procDefineConcreteMaterials

(a procedure that activates and thereby defines the material type in OpenSees based upon the user specified option of Concrete Material Type, for both columns and beams.)

set aConcreteTag(Concrete Material type) = ConcreteID

(defines the concrete Tag Value corresponding to the concrete type as provided by the user, for both columns and beams.)

- **defineSections.tcl**

This script defines the aggregate and the torsion tags for column and beam sections and also generates the section using OpenSees commands.

```
source procColumnSection.tcl
```

```
source procBeamSection.tcl
```

```
set aColumnSectionProperties(NSFrame,EWFrame,Story,"AggSectionTag")
```

(defines the aggregate section tag value for columns corresponding to a *NSFrame*, *EWFrame* and *Story*.)

```
set aColumnSectionProperties(NSFrame,EWFrame,Story,"TorsionTag")
```

(defines the torsion tag value for columns corresponding to a *NSFrame*, *EWFrame* and *Story*.)

```
call procColumnSection
```

(a procedure that generates the section and attaches suitable tags to it based upon the Column Element Type specified by the user. This procedure in turn calls another procedure named *procRCRectangularSection*.)

```
call procRCRectangularSection
```

(a procedure that generates a rectangular reinforced concrete column section with confined and unconfined concrete and reinforcement distributed around the perimeter.)

```
set aEWBeamSectionProperties(NSFrame,EWFrame,Story,"AggSectionTag")
```

(defines the aggregate section tag value for EW beams corresponding to a *NSFrame*, *EWFrame* (only C and D) and *Story*.)

set aEWBeamSectionProperties(NSFrame,EWFrame,Story,"TorsionTag")

(defines the torsion tag value for EW beams corresponding to a *NSFrame*, *EWFrame* (only C and D) and *Story*.)

call procBeamSection

(a procedure that generates the section and attaches suitable tags to it based upon the Beam Element Type specified by the user, and the EW Frame (for *EWFrame* C it calls *procCBeamSection*, or for EW Frame D it calls *procTBeamSection*.)

call procCBeamSection

(a procedure that generates a C shaped rectangular reinforced concrete beam section with confined and unconfined concrete and distributed reinforcements.)

call procTBeamSection

(a procedure that generates a T shaped rectangular reinforced concrete beam section with confined and unconfined concrete and distributed reinforcements.)

- **setNodalMass.tcl**

This script defines the nodal masses for the entire structure.

set aNodalMass(NSFrame,EWFrame,Story)

(defines the nodal mass associated with the *NSFrame*, *EWFrame* and *Story*.)

- **defineNodes.tcl**

This script generates the nodes for the entire structure.

set aNode(NSFrame,EWFrame,Story)

(defines the nodal numbering for based on *NSFrame*, *EWFrame* and *Story*.)

Activates the Node command of Opensees to generate the nodes of the structure and if the element is *elastic/elastic* then sets up corresponding mass to each of the nodes.

- **defineElements.tcl**

This script generates the elements for the entire structure.

set ColumnGeoTransformation

(defines the Linear Geometric Transformation object tag

geomTransLinear ColumnGeoTransformation 0 1 0

(constructs a Linear Geometric Transformation object with tag *ColumnGeoTransformation* and a local vector in xz plane which lies along the global vector <0 1 0>)

set BeamGeoTransformation

(defines the Linear Geometric Transformation object tag)

geomTransLinear BeamGeoTransformation 0 0 1

(constructs a Linear Geometric Transformation object with tag *BeamGeoTransformation* and a local vector in xz plane which lies along the global vector <0 0 1>)

set MassDensity(\$story,massdensity)

(defines the *massdensity* for each of the elements. Sets it to zero if the element is *elastic/elastic*)

call procDefineFrameElements

(a procedure that generates the element based upon the *ColumnElementType* and *BeamElementType* specified by the user. This procedure is activated for each *EWFrame*, *NSFrame* and Story and thereby defines all the element in the structure.)

- **defineBoundaryConditions.tcl**

This script generates the boundary conditions for the entire structure. The bases at the columns are fixed and equal degree of freedom is provided to the adjacent C and D Frame nodes.

- **analyze.tcl**

Script to perform analysis taking into consideration the *AnalysisType* specified by the user.

APPENDIX B: GROUND MOTIONS FOR THE VANNUYS BUILDING

Uniform hazard spectra for the site were derived from the USGS probabilistic ground motion maps for rock site conditions (Frankel et al., 1996; 2001). Modification to account for near fault rupture directivity effects, and the use of separate response spectra for the fault normal and fault parallel components of ground motion, was not required (Somerville, Collins 2002).

Although the site is located near active faults in map view, none of the faults that dominate the seismic hazard at the site are oriented in such a way that the site will experience strong rupture directivity effects. For each set of recordings, a scaling factor was found by matching the east component time history to the longitudinal uniform hazard spectra of 1.5 sec. This scaling factor was then applied to all three components of the recording. This scaling procedure preserves the relative scaling between the three components of the recording (Somerville, Collins 2002).

The time histories used to represent the 50%, 10% and 2% probability of occurrence in 50 years ground motions are listed in Tables B-1, B-2 and B-3 respectively. These time histories are derived from 1971 San Fernando, 1986 North Palm Springs, 1987 Whittier Narrows, and 1994 Northridge earthquakes.

The variability in the ground motion recordings for each component for each ground motion level is shown in Figure B-1 for the horizontal components. These figures show the median and plus and minus one standard deviation level for each set of ten recordings. The scaling causes the variability to go to zero for the longitudinal component at 1.5 sec.

Table B-1: Time Histories Representing 50% in 50 years hazard level at the Van Nuys Building (Somerville and Collins, 2002)

| Earthquake | Mw, Strike (°E of N) | Station | Distance | Site | Scale | PGA (cm/sec/sec) | Reference |
|-----------------------------------|----------------------------|---------|----------|------|-------|---------------------|--------------------------------|
| North Palm Springs 1986.7.8 | 6.0 287 | Plma | 9.6 | Soil | 2.392 | 478 | Hartzell (1989) |
| Northridge 1994.1.17 | 6.7 122 | env1 | 17.7 | Soil | 0.433 | 213.8 | Wald et al. (1996) |
| | | env9 | 17.9 | Soil | 0.519 | 125.6 | |
| | | nhl2 | 18.4 | Soil | 0.691 | 125.5 | |
| | | vnsc | 12.8 | Soil | 1.173 | 545.2 | |
| | | whox | 20.0 | Soil | 0.761 | 237.4 | |
| San Fernando 1971.2.9 | 6.6 290 | 253 | 16.3 | Soil | 1.754 | 349.7 | Heaton (1982) |
| | | 466 | 16.4 | Soil | 1.62 | 260.0 | |
| | | vnuy | .5 | Soil | 0.736 | 97.1 | |
| Whittier Narrows 1987.10.1 | 6.0 280 | athl | 16.6 | Soil | 3.885 | 566.9 | Hartzell and Iida (1990) |

Table B-2 Time Histories Representing 10% in 50 years hazard level at the Van Nuys Building (Somerville and Collins, 2002)

| Earthquake | Mw, Strike (°E of N) | Station | Distance | Site | Scale | PGA (cm/sec/sec) | Reference |
|-----------------------------|-------------------------|---------|----------|------|-------|---------------------|-----------------------|
| Northridge 1994.1.17 | 6.7 | cnpk | 17.7 | Soil | 2.081 | 882.3 | Wald et al. (1996) |
| | | spva | 9.2 | Soil | 1.227 | 1130.7 | |
| | | vnsc | 12.8 | Soil | 2961 | 1375.9 | |
| | 122 | vnuy | 11.3 | Soil | 1.043 | 878.5 | |
| | | whox | 20.0 | Soil | 1.922 | 599.0 | |
| San Fernando 1971.2.9 | 6.6 290 | 253 | 16.3 | Soil | 4.427 | 882.5 | Heaton (1982) |
| | | 461 | 16.2 | Soil | 4.370 | 648.3 | |
| | | 466 | 16.4 | Soil | 4.087 | 656.2 | |
| | | glen | 18.8 | Soil | 3.853 | 858.3 | |
| | | vnuy | 9.5 | Soil | 1.858 | 244.9 | |

Table B-3 Time Histories Representing 2% in 50 years hazard level at the Van Nuys Building (Somerville and Collins, 2002)

| Earthquake | Mw, Strike (°E of N) | Station | Distance | Site | Scale | PGA (cm/sec/sec) | Reference |
|-----------------------------|-------------------------|---------|----------|------|-------|---------------------|-----------------------|
| Northridge 1994.1.17 | 6.7 | env1 | 17.7 | Soil | 2.001 | 574.2 | Wald et al. (1996) |
| | | env9 | 17.9 | Soil | 2.396 | 1020.5 | |
| | | nhl2 | 18.4 | Soil | 3.193 | 1006.4 | |
| | | nord | 9.4 | Soil | 3.601 | 1088.1 | |
| | | nrr1 | 13.7 | Soil | 3.298 | 1346.0 | |
| | 122 | rosc | 10.8 | Soil | 2.901 | 861.8 | |
| | | spva | 9.2 | Soil | 2.246 | 1657.9 | |
| | | vns1 | 12.8 | Soil | 3.246 | 868.7 | |
| | | vnuy | 11.3 | Soil | 1.909 | 770.2 | |
| San Fernando 1971.2.9 | 6.7 290 | vnuy | 9.5 | | 3.401 | 849.3 | Heaton (1982) |

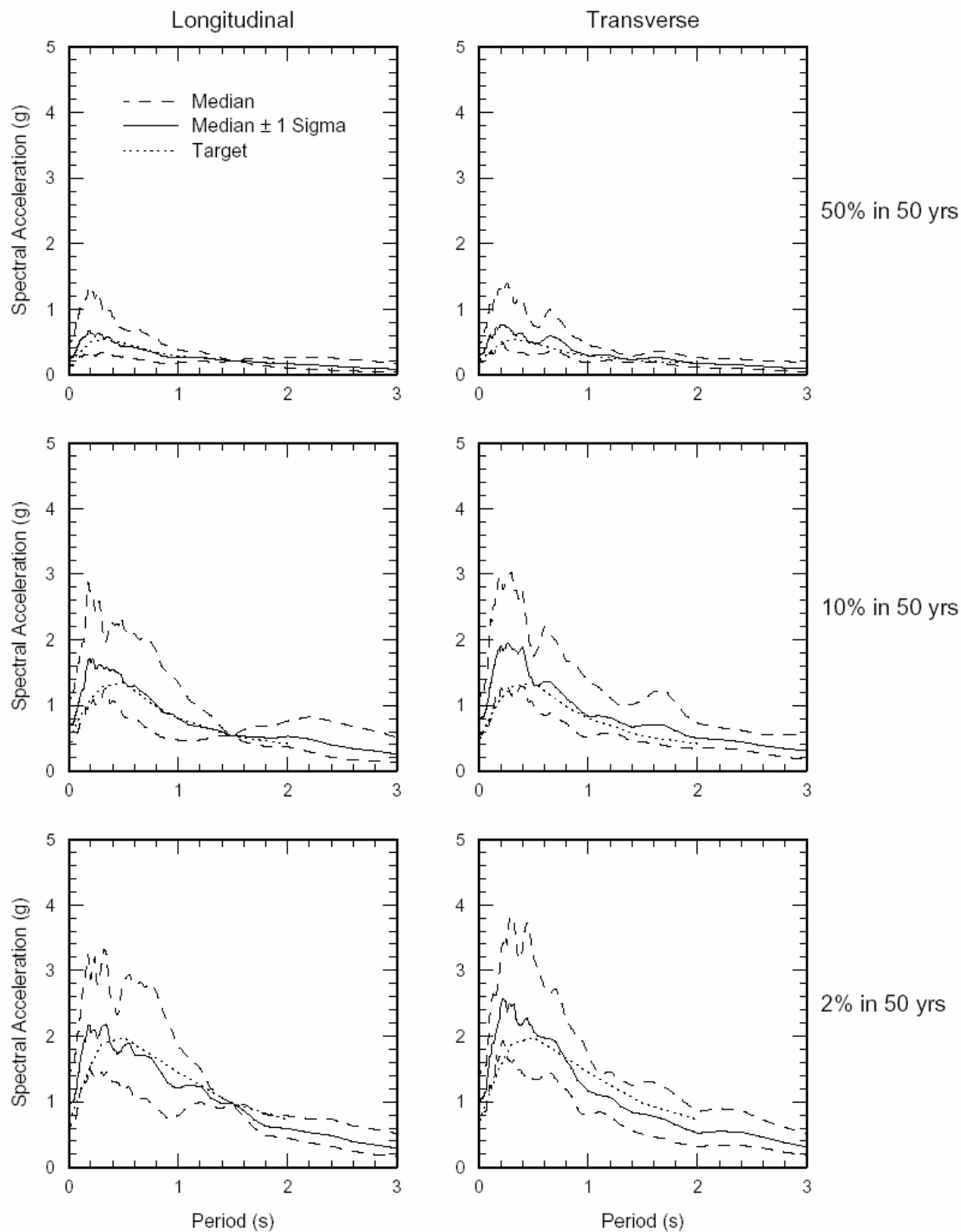


Figure B-1 Variability in the Ground motions of each set of ten Scaled Recordings for the Longitudinal and Transverse Components for each of Three Ground motion Levels (Somerville and Collins, 2002)